

HIGH ORDER SPLITTING METHODS FOR SDES SATISFYING A COMMUTATIVITY CONDITION*

JAMES FOSTER [†], GONALO DOS REIS [‡], AND CALUM STRANGE [§]

Abstract. In this paper, we introduce a new simple approach to developing and establishing the convergence of splitting methods for a large class of stochastic differential equations (SDEs), including additive, diagonal and scalar noise types. The central idea is to view the splitting method as a replacement of the driving signal of an SDE, namely Brownian motion and time, with a piecewise linear path that yields a sequence of ODEs – which can be discretised to produce a numerical scheme. This new way of understanding splitting methods is inspired by, but does not use, rough path theory. We show that when the driving piecewise linear path matches certain iterated stochastic integrals of Brownian motion, then a high order splitting method can be obtained. We propose a general proof methodology for establishing the strong convergence of these approximations that is akin to the general framework of Milstein and Tretyakov. That is, once local error estimates are obtained for the splitting method, then a global rate of convergence follows. This approach can then be readily applied in future research on SDE splitting methods. By incorporating recently developed approximations for iterated integrals of Brownian motion into these piecewise linear paths, we propose several high order splitting methods for SDEs satisfying a certain commutativity condition. In our experiments, which include the Cox-Ingersoll-Ross model and additive noise SDEs (noisy anharmonic oscillator, stochastic FitzHugh-Nagumo model, underdamped Langevin dynamics), the new splitting methods exhibit convergence rates of $O(h^{3/2})$ and outperform schemes previously proposed in the literature.

Key words. Numerical methods for SDEs, high order strong convergence, operator splitting

AMS subject classifications. 60H35, 60J65, 60L90, 65C30

1. Introduction. Stochastic differential equations (SDEs) are commonly used for modelling random continuous-time phenomena, with applications ranging from finance [7, 59] and statistical physics [51, 61] to machine learning [45, 46, 77, 82, 85]. In such applications, SDE solutions can rarely be obtained exactly or in closed-form, and so numerical methods and Monte Carlo simulation are often employed in practice.

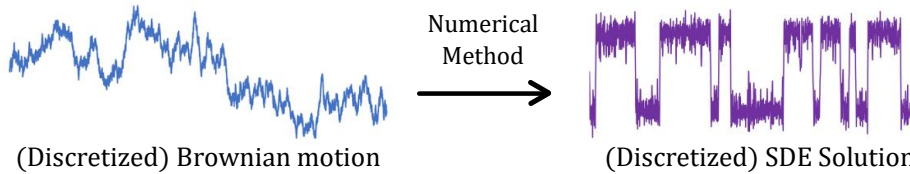


FIG. 1. In the Monte Carlo paradigm, information about the Brownian motion is generated and then mapped to a numerical solution of the SDE. Typically, only Brownian increments are sampled.

In this paper, we present a study of high order splitting-based numerical methods for Stratonovich SDEs of the form

$$(1.1) \quad dy_t = f(y_t)dt + g(y_t) \circ dW_t, \quad y_0 \in L^2(\mathbb{R}^e),$$

* **Funding:** The first author was supported by the Department of Mathematical Sciences at the University of Bath as well as the DataSig programme under the EPSRC grant EP/S026347/1. The second author acknowledges support from the *Fundaao para a Ciencia e a Tecnologia* (Portuguese Foundation for Science and Technology) through the projects UIDB/00297/2020 and UIDP/00297/2020 (Center for Mathematics and Applications, CMA/FCT/UNL).

[†] University of Bath, Department of Mathematical Sciences. jmf68@bath.ac.uk.

[‡] University of Edinburgh, School of Mathematics. G.dosReis@ed.ac.uk.

[§] University of Edinburgh, School of Mathematics. c.strange-1@ed.ac.uk.

where $W = (W^1, \dots, W^d) = \{W_t\}_{t \in [0, T]}$ denotes a d -dimensional Brownian motion, $L^2(\mathbb{R}^e)$ is the space of \mathbb{R}^e -valued square-integrable random variables, the vector fields are given by $f \in \mathcal{C}^2(\mathbb{R}^e, \mathbb{R}^e)$ and $g = (g_1, \dots, g_d) \in \mathcal{C}^3(\mathbb{R}^e, \mathbb{R}^{e \times d})$ where we understand $g(y_t) \circ dW_t = \sum_{i=1}^d g_i(y_t) \circ dW_t^i$. The columns $\{g_i\}_{1 \leq i \leq d}$ of g can each be viewed as a vector field on \mathbb{R}^e and are assumed to satisfy the following commutativity condition:

$$(1.2) \quad g'_i(y)g_j(y) = g'_j(y)g_i(y), \quad \forall y \in \mathbb{R}^e.$$

We also assume g_i are globally Lipschitz continuous with globally Lipschitz derivatives.

Without the condition (1.2), high order numerical methods for SDEs require the use, or approximation, of second iterated integrals of the Brownian motion [73]. Generating both the increments and iterated integrals, or equivalently Lévy areas, of Brownian motion is a difficult problem [16, 23] and beyond the scope of this paper. We refer the reader to [20, 26, 27, 33, 66, 83] for studies on Lévy area approximation. Nevertheless, there is a large variety of SDEs used in applications that satisfy (1.2), such as SDEs with scalar, diagonal or additive noise types. While we focus on schemes for SDEs satisfying the commutativity condition (1.2), the error analysis that we introduce for establishing convergence is generic and does not rely on this condition.

Inspired by rough path theory [32], which views SDEs as functions that map Brownian motion to continuous paths (see Figure 1), we propose an approximation $y^\gamma = \{y_r^\gamma\}_{r \in [0, 1]}$ for (1.1) that comes from the controlled differential equation (CDE),

$$(1.3) \quad dy_r^\gamma = f(y_r^\gamma) d\gamma^\tau(r) + g(y_r^\gamma) d\gamma^\omega(r), \quad y_0^\gamma = y_0,$$

or equivalently

$$y_r^\gamma = y_0 + \int_0^r f(y_u^\gamma) d\gamma^\tau(u) + \int_0^r g(y_u^\gamma) d\gamma^\omega(u),$$

where $\gamma = (\gamma^\tau, \gamma^\omega)^\top : [0, 1] \rightarrow \mathbb{R}^{1+d}$ is a parameterised (continuous) piecewise linear path designed to match certain iterated integrals of the “space-time” Brownian motion $\{(t, W_t)\}_{t \in [0, T]}$. Since the path γ is piecewise linear, it immediately follows that $d\gamma(r) = \frac{1}{r_{i+1} - r_i} \gamma_{r_i, r_{i+1}} dr$ for $r \in [r_i, r_{i+1}]$, where $r_i \in [0, 1]$ is the parameter value at the start of the i -th piece of γ and $\gamma_{r_i, r_{i+1}}$ is the increment of the linear piece. Therefore the CDE (1.3) reduces to a sequence of ODEs, corresponding to each piece of γ , which can be discretised by a suitable ODE solver, such a Runge-Kutta method. Furthermore, we will see that this approach can be interpreted as a splitting method. We refer the reader to Section 3 of [8] for an overview of splitting methods for SDEs.

More generally, CDEs are one of the key objects in rough path theory [31, 32, 57] (often referred to as “rough” differential equations). However, we emphasise that this manuscript is *not a rough paths paper* – and no p -variation or lift maps are used. Instead, we will heavily draw upon ideas and interpretations from rough path theory. Similarly, we point towards [11, 29, 44, 47, 58, 64, 65, 70] as works presenting results for stochastic processes or continuous data streams, without “rough path” statements, but making use of the machinery and insights that are provided by rough path theory.

Perhaps the simplest example of an approximation with the form of the CDE (1.3) is the Wong-Zakai approximation [70, 76, 84] where γ is the standard piecewise linear discretisation of space-time Brownian motion. However, the Wong-Zakai approach only uses the increments of the Brownian motion, and is thus constrained to a first order convergence rate for SDEs satisfying the commutativity condition (1.2) [16]. We will show that by generating both increments and “space-time” Lévy areas of the Brownian path, we can construct paths γ yielding order 3/2 strong convergence rates.

DEFINITION 1.1. The rescaled **space-time Lévy area** of a Brownian motion W over an interval $[s, t]$ corresponds to the signed area of the associated bridge process.

$$H_{s,t} := \frac{1}{h} \int_s^t \left(W_{s,u} - \frac{u-s}{h} W_{s,t} \right) du,$$

where $h := t - s$ and $W_{s,u} := W_u - W_s$ for $u \in [s, t]$.

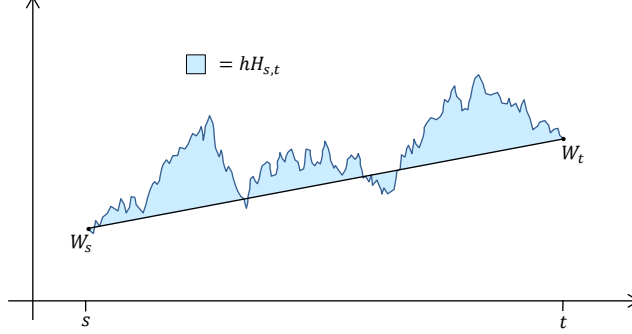


FIG. 2. Space-time Lévy area gives the area between a Brownian path and its linear approximant.

Remark 1.2. It was shown in [29] that $H_{s,t} \sim \mathcal{N}(0, \frac{1}{12}h)$ is independent of $W_{s,t}$ when $d = 1$. Since the coordinate processes of a Brownian motion are independent, it therefore follows that $W_{s,t} \sim \mathcal{N}(0, hI_d)$ and $H_{s,t} \sim \mathcal{N}(0, \frac{1}{12}hI_d)$ are independent.

Using the increment $W_{s,t}$ and space-time Lévy area $H_{s,t}$ of the Brownian motion, we give an example of a path γ and its associated 3/2 strong order spitting method.

EXAMPLE 1.3. Let $\gamma = (\gamma^\tau, \gamma^\omega)^\top : [0, 1] \rightarrow \mathbb{R}^{1+d}$ denote a piecewise linear path where the vertices between pieces are at $r_i := \frac{i}{5}$ for $0 \leq i \leq 5$ and the increments are

$$\gamma_{r_i, r_{i+1}} = \begin{cases} \left(\frac{3-\sqrt{3}}{6}h, 0 \right), & \text{if } i = 0 \\ \left(0, \frac{1}{2}W_{s,t} + \sqrt{3}H_{s,t} \right), & \text{if } i = 1 \\ \left(\frac{\sqrt{3}}{3}h, 0 \right), & \text{if } i = 2 \\ \left(0, \frac{1}{2}W_{s,t} - \sqrt{3}H_{s,t} \right), & \text{if } i = 3 \\ \left(\frac{3-\sqrt{3}}{6}h, 0 \right), & \text{if } i = 4. \end{cases}$$

(diagram not drawn accurately; the “vertical” pieces are only the same in distribution)

Therefore, by replacing the driving signal $t \mapsto (t, W_t)$ in the SDE (1.1) with the parameterisation $r \mapsto \gamma_r$, the approximating CDE (1.3) reduces to the splitting (formulated in a more classical way):

$$y_1^\gamma = \exp\left(\frac{3-\sqrt{3}}{6}f(\cdot)h\right) \exp\left(g(\cdot)\left(\frac{1}{2}W_{s,t} - \sqrt{3}H_{s,t}\right)\right) \\ \exp\left(\frac{\sqrt{3}}{3}f(\cdot)h\right) \exp\left(g(\cdot)\left(\frac{1}{2}W_{s,t} + \sqrt{3}H_{s,t}\right)\right) \exp\left(\frac{3-\sqrt{3}}{6}f(\cdot)h\right) y_0^\gamma,$$

where $\exp(V)x$ denotes the solution z_1 at time $u = 1$ of the ODE $z' = V(z)$, $z(0) = x$.

The main result of this paper will allow us to establish the high order strong convergence of (1.3) primarily by checking that the path γ has the following properties:

$$(1.4) \quad \gamma^\omega(1) - \gamma^\omega(0) = W_{s,t}, \quad \int_0^1 (\gamma^\omega(r) - \gamma^\omega(0)) d\gamma^\tau(r) = \int_s^t W_{s,u} du,$$

$$(1.5) \quad \mathbb{E} \left[\int_0^1 (\gamma^\omega(r) - \gamma^\omega(0))^{\otimes 2} d\gamma^\tau(r) \right] = \mathbb{E} \left[\int_s^t W_{s,u}^{\otimes 2} du \right] = \frac{1}{2} h^2 I_d.$$

These quantities correspond to terms in the Taylor expansions of the SDE (1.1) and its CDE approximation (1.3). Provided γ satisfies mild regularity conditions, ensuring that the integrals in (1.4) and expected integrals in (1.5) coincide allows the Taylor expansions (and hence solutions) of (1.1) and (1.3) to be close in an $L^2(\mathbb{P})$ sense. Moreover, we will see that the conditions (1.4) and (1.5) imposed on γ are a specific instance of a more general framework, which we shall make rigorous in Theorem 3.8. In terms of proof methodologies for the error analysis, it is worth noting that ours differs from previous works on splitting methods for SDEs [8, 28, 41, 51, 62, 68, 69, 81], which are either extensions of the Strang splitting [79] or use the Baker-Campbell-Hausdorff formula for expanding the compositions of ODEs (see [62] for the latter). That said, our approach does draw inspiration from ‘‘Cubature on Wiener Space’’ [58] where (deterministic) piecewise linear paths are used to weakly approximate SDEs. For some perspective, we present an informal version of our main result, Theorem 3.8, which describes our approach to high order splitting methods for commutative SDEs.

THEOREM 1.4 (Convergence of path-based splitting for SDEs (informal version)). *Given a fixed number of steps N , we will define a numerical solution $Y = \{Y_k\}_{0 \leq k \leq N}$ for the SDE (1.1) over the finite time horizon $[0, T]$ as follows,*

$$Y_{k+1} := \left(\text{Solution at time } r = 1 \text{ of CDE (1.3) driven by } \gamma_k : [0, 1] \rightarrow \mathbb{R}^{1+d} \right) (Y_k),$$

where each piecewise linear path γ_k is constructed from $\{W_t : t \in [\frac{kT}{N}, \frac{(k+1)T}{N}]\}$, is sufficiently regular (see Assumption A1), and for some fixed $p \in \{\frac{m}{2}\}_{m \in \mathbb{N}}$ satisfies

1. the iterated integrals of γ_k and (t, W_t) with order less than $p - \frac{1}{2}$ coincide,
2. the iterated integrals of γ_k and (t, W_t) with order p match in expectation.

Then, there exists a constant $C > 0$, such that for sufficiently small $h = \frac{T}{N}$, we have

$$(1.6) \quad \mathbb{E} \left[\|Y_k - y_{kh}\|^2 \right]^{\frac{1}{2}} \leq Ch^{p-\frac{1}{2}}.$$

for $k \in \{1, \dots, N\}$. If $p = 2$, and the SDE satisfies the commutativity condition (1.2), then the estimate (1.6) holds under the assumption that each γ_k is sufficiently regular and has coordinate processes $\{\gamma_k^{\omega,i}\}_{1 \leq i \leq d}$ that are independent, symmetric and satisfy

$$(1.7) \quad \gamma_k^{\omega,i}(1) - \gamma_k^{\omega,i}(0) = W_{kh, (k+1)h}^i, \quad \gamma_k^\tau(1) - \gamma_k^\tau(0) = h,$$

$$(1.8) \quad \int_0^1 (\gamma_k^{\omega,i}(r) - \gamma_k^{\omega,i}(0)) d\gamma_k^\tau(r) = \int_{kh}^{(k+1)h} W_{kh,u}^i du,$$

$$(1.9) \quad \mathbb{E} \left[\int_0^1 (\gamma_k^{\omega,i}(r) - \gamma_k^{\omega,i}(0))^2 d\gamma_k^\tau(r) \right] = \frac{1}{2} h^2.$$

The paper is outlined as follows. In Section 2, we impose regularity conditions on the path γ and establish a (fourth) moment bound for the solution of the CDE (1.3).

In Section 3, we will present Taylor expansions for both the SDE (1.1) and CDE (1.3). Since the error analysis of stochastic Taylor approximations is well known, our focus is to obtain $L^2(\mathbb{P})$ estimates for the remainder terms in the CDE Taylor expansion. We end Section 3.3 with our main result, Theorem 3.8, which establishes convergence rates for SDE splitting methods corresponding to the CDE (1.3) driven by a path γ . To establish 3/2 strong convergence rates in the setting where the SDE satisfies the commutativity condition (1.2), we simplify certain terms in the Taylor expansions of (1.1) and (1.3). This is the focus of Section 3.4, with technical details in Appendix A.

In Section 4, we provide several examples of piecewise linear paths that correspond to high order splitting methods. Two of the paths will be constructed using a recently developed approximation [26, Theorem 5.1.2] for the stochastic integral $\int_s^t W_{s,u}^2 du$. Building upon the approach of [29], this integral estimator can be obtained as a certain conditional expectation of the iterated integral and is thus optimal in an $L^2(\mathbb{P})$ sense. However, unlike in [29], we shall generate an additional Rademacher random variable to improve the approximation to aid in the construction of the piecewise linear paths. To keep this article self-contained, this integral estimator is derived in Appendix B. We also note that [26] is the doctoral thesis of the first author and [26, Chapter 5] has several ‘‘rough path inspired’’ ideas that are refined and analysed in this article.

In Section 5, we test the proposed splitting methods on some well-known SDEs, including the Cox-Ingersoll-Ross [2, 17] and stochastic FitzHugh-Nagumo [8] models. Due to the analytic tractability of these SDEs, our high order splitting schemes will produce ODEs that can be either solved exactly or further split into ‘‘solvable’’ ODEs. We also discuss the setting of additive noise SDEs, where the drift vector field may not give analytically tractable ODEs. For these problems, we propose applying a certain second order Runge-Kutta method (Ralston’s method) to the ‘‘non-diffusion’’ ODE. Furthermore, we show that the Taylor expansion of the resulting stochastic Ralston method contains the high order terms needed to obtain order 3/2 strong convergence.

In the specific application to underdamped Langevin dynamics [51], we briefly discuss the choice of splitting path and Runge-Kutta method which can lead to a third order strong convergence rate to the SDE solution (see [30] for further details). Finally, we demonstrate the improved accuracy of the stochastic Ralston method when compared to the SRA1 scheme in [73], for simulating a simple anharmonic oscillator. Moreover, as both methods require two drift evaluations per step, we would expect stochastic Ralston to be state-of-the-art for additive noise SDEs with expensive drifts. At the same time, we also show that a simple splitting-based adjustment can improve the accuracy of the standard Euler-Maruyama method for SDEs with additive noise.

1.1. Notation. In this section, we summarise some of the notation in the paper. Given vectors $a \in \mathbb{R}^n$ and $b \in \mathbb{R}^m$, we shall denote their tensor product $a \otimes b \in \mathbb{R}^{nm}$ by $a \otimes b := \{a_i b_j\}_{i=1, j=1}^{n, m}$. We define iterated integrals of W and $\gamma : [0, 1] \rightarrow \mathbb{R}^n$ as

$$(1.10) \quad I_\alpha(F) := \int_0^h \int_0^{r_n} \cdots \int_0^{r_2} F(y_{r_1}) dB_{r_1}^{\alpha_1} \cdots dB_{r_n}^{\alpha_n},$$

$$(1.11) \quad I_\alpha^\gamma(F) := \int_0^1 \int_0^{r_n} \cdots \int_0^{r_2} F(y_{r_1}^\gamma) d\gamma^{\alpha_1}(r_1) \cdots d\gamma^{\alpha_n}(r_n),$$

where y and y^γ are the solutions of the SDE (1.1) and its CDE approximation (1.3) (constructed using a step size $h > 0$), $F : \mathbb{R}^e \rightarrow \mathbb{R}^e$, $\alpha = (\alpha_1, \dots, \alpha_n) \in \{\tau, \omega\}^n$ denotes a multi-index, $dB_r^\tau = dr$ and $dB_r^\omega = \otimes \circ dW_r$. The CDE approximation will

be defined with the same initial condition as the SDE throughout (that is, $y_0^\gamma := y_0$). We denote the set of multi-indices by $\mathcal{A} = \cup_{n \geq 0} \{\tau, \omega\}^n$. We also define the integrals,

$$(1.12) \quad J_\alpha(F) := I_\alpha(F) - F(y_0)I_\alpha(1), \quad J_\alpha^\gamma(F) := I_\alpha^\gamma(F) - F(y_0^\gamma)I_\alpha^\gamma(1),$$

where we understand $I_\alpha(1)$ and $I_\alpha^\gamma(1)$ as defined in (1.10) and (1.11), but with $F(y)$ replaced by the scalar 1. For a given multi-index $\alpha = (\alpha_i)_{1 \leq i \leq n}$, we will define its order by $\text{ord}(\alpha) := |\alpha|_\tau + \frac{1}{2}|\alpha|_\omega$, where $|\alpha|_\tau := \sum_{i=1}^n \mathbf{1}_{\alpha_i = \tau}$ and $|\alpha|_\omega := \sum_{i=1}^n \mathbf{1}_{\alpha_i = \omega}$.

Given normed vector spaces U and V , $\mathcal{C}_{\text{Lip}}^p(U, V)$ will be the subspace of $\mathcal{C}^p(U, V)$ containing globally Lipschitz continuous functions with their p derivatives globally Lipschitz continuous. We write the Lipschitz constant of a function F as $\|F\|_{\text{Lip-1}}$. The above notation shall be employed in the study of Taylor expansions in Section 3.

Throughout, $\|\cdot\|$ will denote the standard Euclidean norm on \mathbb{R}^n and $L^p(\mathbb{R}^n)$ is the space of \mathbb{R}^n -valued random variables with finite p -th moments (i.e. $\mathbb{E}[\|X\|^p] < \infty$). Given a continuous path $\gamma : [0, 1] \rightarrow \mathbb{R}^n$, we will denote its length using the notation,

$$\|\gamma\|_{1\text{-var}, [0,1]} = \int_0^1 |d\gamma(r)| := \sup_{\substack{0=r_0 < r_1 < \dots < r_N=1, \\ N \geq 1}} \left(\sum_{i=0}^{N-1} \|\gamma(r_{i+1}) - \gamma(r_i)\| \right).$$

When defining numerical methods, we shall often use W_k as shorthand for $W_{t_k, t_{k+1}}$, (and similarly H_k and n_k instead of $H_{t_k, t_{k+1}}$ and $n_{t_k, t_{k+1}}$).

2. Main assumption and preliminary results. Before we prove the strong convergence of the CDE (1.3), we will first establish a moment bound for its solution. As discussed previously, this requires us to make certain assumptions on the path γ . Our main assumption (given below) ensures the path γ scales like Brownian motion.

ASSUMPTION A1 (Brownian-like scaling). *Let $\gamma = (\gamma^\tau, \gamma^\omega)^\top : [0, 1] \rightarrow \mathbb{R}^{1+d}$ be a piecewise linear path with $m \in \mathbb{N}$ components that have, almost surely, finite length. For $i \geq 0$, we denote the increment of the i -th piece of γ by $\gamma_{r_i, r_{i+1}}$ and assume that*

1. $\gamma_{r_i, r_{i+1}}^\tau$, the increment in the time component of γ , is deterministic.
2. $\gamma_{r_i, r_{i+1}}^\tau$ scales with the step size h and the increment in the space component, $\gamma_{r_i, r_{i+1}}^\omega$, has finite even moments scaling with h . Concretely, we have

$$\gamma_{r_i, r_{i+1}}^\tau = O(h), \quad \text{and} \quad \mathbb{E}[|(\gamma_{r_i, r_{i+1}}^\omega)_j|^{2k}] = O(h^k),$$

for every $j \in \{1, \dots, d\}$.

3. When a CDE driven by γ is considered, y_0^γ and γ are assumed independent.

Remark 2.1 (Comment on Assumption A1). We impose that γ^τ is deterministic for convenience and, inspecting the proof, one may be able to lift this constraint. Moreover, we expect our methodology can accommodate for randomised algorithms (see [6, 39, 49, 50, 75] for examples of SDE solvers with a randomised time component).

We now present the main result of this section – a moment bound for the CDE, which will be used to control remainder terms of the Taylor expansion discussed later. Following the approach of [32, Theorem 3.7], we obtain our main result, Theorem 2.2.

THEOREM 2.2 (Fourth moment bound for CDEs). *Let γ satisfy Assumption A1 and let y^γ denote the solution to (1.3) with $y_0^\gamma \in L^4(\mathbb{R}^e)$. Suppose that f and g satisfy*

$$(2.1) \quad \|f(y)\| \leq C(1 + \|y\|), \quad \text{and} \quad \|g(y)\| \leq C(1 + \|y\|),$$

with $\mathbb{E}[\exp(16C \int_0^1 |d\gamma(u)|)] < \infty$. Then there exists a positive constant $\tilde{C} > 0$, depending only on the path γ and growth constant C in (2.1), such that for $r \in [0, 1]$,

$$(2.2) \quad \mathbb{E}[\|y_r^\gamma - y_0^\gamma\|^4] \leq \tilde{C}h^2(1 + \mathbb{E}[\|y_0^\gamma\|^4]).$$

Proof. Let $G : \mathbb{R}^e \rightarrow \mathbb{R}^{e \times (d+1)}$ have first column given by $f : \mathbb{R}^e \rightarrow \mathbb{R}^e$ and the rest of the matrix given by $g : \mathbb{R}^e \rightarrow \mathbb{R}^{e \times d}$. Then the growth assumption (2.1) implies that $\|G(y)\| \leq C(1 + \|y\|)$. Thus, by direct application of [32, Theorem 3.7], we have

$$\|y_r^\gamma - y_0^\gamma\| \leq C(1 + \|y_0^\gamma\|) \exp\left(2C \int_0^r |d\gamma(u)|\right) \int_0^r |d\gamma(u)|,$$

for $r \in [0, 1]$. Since y_0^γ is independent of γ , we can estimate the fourth moment as

$$\begin{aligned} \mathbb{E}[\|y_r^\gamma - y_0^\gamma\|^4] &\leq C^4 \mathbb{E}\left[(1 + \|y_0^\gamma\|)^4 \exp\left(8C \int_0^r |d\gamma(u)|\right) \left(\int_0^r |d\gamma(u)|\right)^4\right] \\ &\leq C^4 (1 + \mathbb{E}[\|y_0^\gamma\|^4]) \mathbb{E}\left[\exp\left(16C \int_0^r |d\gamma(u)|\right)\right]^{\frac{1}{2}} \mathbb{E}\left[\left(\int_0^r |d\gamma(u)|\right)^8\right]^{\frac{1}{2}}, \end{aligned}$$

by the Cauchy-Schwarz inequality. We now assume for a contradiction that there exists $0 = s_0 < s_1 < \dots < s_M = 1$ such that $\sum_{i=0}^{m-1} \|\gamma_{r_i, r_{i+1}}\| < \sum_{j=0}^{M-1} \|\gamma_{s_j, s_{j+1}}\|$. As each piece $\{\gamma(t) : t \in [r_i, r_{i+1}]\}$ is linear, adding points does not change the sum:

$$\sum_{i=0}^{m-1} \|\gamma_{r_i, r_{i+1}}\| = \sum_{k=0}^{N-1} \|\gamma_{t_k, t_{k+1}}\|, \quad \text{where } \{t_k\} := \{r_j\} \cup \{s_i\}.$$

We also note that each increment $\gamma_{s_j, s_{j+1}}$ can be expressed as a sum of increments from $\{\gamma_{t_k, t_{k+1}} : s_j \leq t_k < s_{j+1}\}$. Therefore, by the triangle inequality, it follows that $\sum_{j=0}^{M-1} \|\gamma_{s_j, s_{j+1}}\| \leq \sum_{k=0}^{N-1} \|\gamma_{t_k, t_{k+1}}\| \implies \sum_{j=0}^{M-1} \|\gamma_{s_j, s_{j+1}}\| \leq \sum_{i=0}^{m-1} \|\gamma_{r_i, r_{i+1}}\|$. From this contradiction, we have $\|\gamma\|_{1\text{-var}, [0,1]} = \int_0^1 |d\gamma(u)| = \sum_{i=0}^{m-1} \|\gamma_{r_i, r_{i+1}}\|$ and so

$$\begin{aligned} \mathbb{E}\left[\left(\int_0^r |d\gamma(u)|\right)^8\right] &\leq \mathbb{E}\left[\left(\int_0^1 |d\gamma(u)|\right)^8\right] = \mathbb{E}\left[\left(\sum_{i=0}^{m-1} \|\gamma_{r_i, r_{i+1}}\|\right)^8\right] \\ &\leq m^7 \sum_{i=0}^{m-1} \mathbb{E}\left[\|\gamma_{r_i, r_{i+1}}\|^8\right] = O(h^4), \end{aligned}$$

using Jensen's inequality and Assumption A1. Since $\mathbb{E}[\exp(16C \int_0^1 |d\gamma(u)|)] < \infty$, it now follows that there exists $\tilde{C} > 0$, not depending on y_0^γ , such that for $r \in [0, 1]$,

$$\mathbb{E}[\|y_r^\gamma - y_0^\gamma\|^4] \leq \tilde{C}h^2(1 + \mathbb{E}[\|y_0^\gamma\|^4]). \quad \square$$

3. Taylor expansions and error analysis. We consider the Taylor expansions of both the Stratonovich SDE (1.1) and the CDE (1.3) driven by a splitting path γ . By matching the lower order terms in the Taylor expansions and showing that the remainder terms are higher order, we can bound local errors for our splitting schemes. We then apply Milstein and Tretyakov's framework for mean-square error analysis [61] to obtain a global strong convergence rate – which is our main result in Theorem 3.8.

3.1. Stratonovich Taylor expansion. Letting y denote the solution to (1.1), we have the usual chain rule (see [48, Theorem 5.6.1] with $\mathcal{A} = \{\emptyset\}$) for $F \in \mathcal{C}^1(\mathbb{R}^e)$,

$$(3.1) \quad F(y_r) = F(y_0) + \int_0^r F'(y_s) \circ dy_s.$$

By expanding “ dy_s ” and iteratively applying (3.1), we obtain the Taylor expansion.

PROPOSITION 3.1 (Stochastic Taylor expansion of the Stratonovich SDE (1.1) [5, Proposition 1.1], [48, Theorem 5.6.1]). *Let $p \in \{\frac{k}{2}\}_{k \in \mathbb{N}}$, $f \in \mathcal{C}_{\text{Lip}}^{[p-1]}(\mathbb{R}^e, \mathbb{R}^e)$ and $g \in \mathcal{C}_{\text{Lip}}^{2p-1}(\mathbb{R}^e, \mathbb{R}^{e \times d})$. The Stratonovich Taylor expansion of (1.1), up to order p , is*

$$(3.2) \quad y_h = y_0 + \sum_{\substack{\alpha \in \mathcal{A}, \\ \text{ord}(\alpha) \leq p}} V(\alpha)(y_0) I_\alpha(1) + R_p(h, y_0),$$

where, we recall the definition of $\text{ord}(\alpha) := |\alpha|_\tau + \frac{1}{2}|\alpha|_\omega$ after equation (1.12), and

$$(3.3) \quad R_p(h, y_0) := \sum_{\substack{\alpha \in \mathcal{A}, \\ \text{ord}(\alpha) = p}} J_\alpha(V(\alpha)),$$

with the vector field derivatives $V(\alpha) : \mathbb{R}^e \rightarrow L((\mathbb{R}^d)^{\otimes |\alpha|_\omega}, \mathbb{R}^e)$ defined for multi-indices recursively by $V(\tau)(y) := f(y)$, $V(\omega)(y) := g(y)$ and

$$V(l\beta)(y) = V(\beta)'V(l)(y),$$

where $l \in \{\tau, \omega\}$ and $l\beta := (l, \beta_1, \dots, \beta_n)$ denotes concatenation. Moreover, we have

$$(3.4) \quad \mathbb{E}[\|R_p(h, y_0)\|^2]^{1/2} = O(h^{p+\frac{1}{2}}).$$

3.2. Controlled Taylor expansion. We now present a CDE Taylor expansion. Just as with the Stratonovich SDE, we have the following chain rule for $F \in \mathcal{C}^1(\mathbb{R}^e)$,

$$(3.5) \quad F(y_r^\gamma) = F(y_0^\gamma) + \int_0^r F'(y_s^\gamma) dy_s^\gamma, \quad r \in [0, 1],$$

where y^γ denotes the solution to the CDE (1.3). Again, just as in the SDE setting, by expanding “ dy_s^γ ” and iteratively applying (3.5), we can obtain a Taylor expansion.

PROPOSITION 3.2. *Let $p \in \{\frac{k}{2}\}_{k \in \mathbb{N}}$, $f \in \mathcal{C}_{\text{Lip}}^{[p-1]}(\mathbb{R}^e, \mathbb{R}^e)$ and $g \in \mathcal{C}_{\text{Lip}}^{2p-1}(\mathbb{R}^e, \mathbb{R}^{e \times d})$. Then the (controlled) Taylor expansion of the CDE (1.3) up to order p is given by*

$$(3.6) \quad y_1^\gamma = y_0^\gamma + \sum_{\substack{\alpha \in \mathcal{A}, \\ \text{ord}(\alpha) \leq p}} V(\alpha)(y_0^\gamma) I_\alpha^\gamma(1) + R_p^\gamma(h, y_0^\gamma),$$

where, using the same notation for vector field derivatives as Proposition 3.1, we have

$$(3.7) \quad R_p^\gamma(h, y_0^\gamma) := \sum_{\substack{\alpha \in \mathcal{A}, \\ \text{ord}(\alpha) = p}} J_\alpha^\gamma(V(\alpha)).$$

Remark 3.3. We note the proof of Proposition 3.2 is essentially identical to that of the Stratonovich Taylor expansion (but with $t \mapsto (t, W_t)$ replaced by $r \mapsto (\gamma_r^\tau, \gamma_r^\omega)$). Moreover, we consider Stratonovich SDEs precisely because we can apply the “same” chain rule and integration by parts formula as for standard Riemann-Stieltjes integrals.

We now show that the size of the terms in the CDE expansion (3.6) are dictated by the order of α . This will allow us to obtain a bound on the remainder term R_p^γ which we will then use to establish the (strong) convergence rate of the CDE approximation. To begin, we shall consider the iterated integrals I_α^γ , which do not depend on f or g .

LEMMA 3.4. *Suppose the path γ satisfies Assumption A1 and let $\alpha \in \mathcal{A}$. Then*

$$\mathbb{E}[\|I_\alpha^\gamma(1)\|^2] = O(h^{2\text{ord}(\alpha)}).$$

Proof. Since γ is piecewise linear, we may split the iterated integral of γ into a finite sum of iterated integrals over intervals where the derivatives of γ are constant. This directly follows by the standard additive property of Riemann-Stieltjes integrals. We may convert these path integrals into regular (deterministic) integrals over these intervals as $d\gamma^\tau(r) = \frac{1}{r_{i+1}-r_i} \gamma_{r_i, r_{i+1}}^\tau dr$ and $d\gamma^\omega(r) = \frac{1}{r_{i+1}-r_i} \gamma_{r_i, r_{i+1}}^\omega dr$ for $r \in [r_i, r_{i+1}]$. By Assumption A1, $\gamma_{r_i, r_{i+1}}^\tau = O(h)$ is a deterministic constant and we therefore have

$$\begin{aligned} \mathbb{E}[\|I_\alpha^\gamma(1)\|^2] &\leq Ch^{2|\alpha|_\tau} \sum_{\text{intervals}} \mathbb{E} \left[\left\| \bigotimes_{j=1}^{|\alpha|_\omega} \gamma_{r_i^j, r_{i+1}^j}^\omega \right\|^2 \right], \\ &= Ch^{2|\alpha|_\tau} \sum_{\text{intervals}} \mathbb{E} \left[\sum_{i_1=1}^d \cdots \sum_{i_{|\alpha|_\omega}=1}^d (\gamma_{r_i^1, r_{i+1}^1}^\omega)_{i_1}^2 \times \cdots \times (\gamma_{r_i^{|\alpha|_\omega}, r_{i+1}^{|\alpha|_\omega}}^\omega)_{i_{|\alpha|_\omega}}^2 \right], \end{aligned}$$

where “intervals” refers to the finite collection of subdomains of the simplex with $d\gamma^\tau(r) = \frac{1}{r_{i+1}-r_i} \gamma_{r_i, r_{i+1}}^\tau dr$ and $d\gamma^\omega(r) = \frac{1}{r_{i+1}-r_i} \gamma_{r_i, r_{i+1}}^\omega dr$. We can then estimate the $\gamma_{r_i, r_{i+1}}^\omega$ terms by iteratively applying Hölder’s inequality to the expectation and applying the assumption that $\mathbb{E}[|(\gamma_{r_i, r_{i+1}}^\omega)_j|^{2k}] = O(h^k)$ for $k \in \mathbb{N}$. This implies that

$$\mathbb{E}[\|I_\alpha^\gamma(1)\|^2] \leq C_{d,m,|\alpha|} h^{2\text{ord}(\alpha)}. \quad \square$$

We now consider the J_α^γ terms, which will follow in much the same way as for I_α^γ .

LEMMA 3.5. *Suppose that the assumptions of Theorem 2.2 hold. Let $\alpha \in \mathcal{A}$ and $F : \mathbb{R}^e \rightarrow L((\mathbb{R}^d)^{\otimes b}, \mathbb{R}^e)$ be a globally Lipschitz continuous map for some $b \geq 1$, then*

$$\mathbb{E}[\|J_\alpha^\gamma(F)\|^2] = O(h^{2\text{ord}(\alpha)+1}).$$

Proof. Just as in the previous proof, we may split the iterated integral of the piecewise linear path γ into a finite sum of iterated integrals over the intervals where both $d\gamma^\tau(r) = \frac{1}{r_{i+1}-r_i} \gamma_{r_i, r_{i+1}}^\tau dr$ and $d\gamma^\omega(r) = \frac{1}{r_{i+1}-r_i} \gamma_{r_i, r_{i+1}}^\omega dr$ for all $r \in [r_i, r_{i+1}]$. Applying Jensen’s and Hölder’s inequalities to the finite sum in $\mathbb{E}[\|J_\alpha^\gamma(F)\|^2]$ yields

$$\begin{aligned} \mathbb{E}[\|J_\alpha^\gamma(F)\|^2] &\leq Ch^{2|\alpha|_\tau} \sum_{\text{intervals}} \mathbb{E} \left[\left\| \int_{0 < r_{|\alpha|} < \cdots < r_1 < 1} \cdots \int (F(y_{r_{|\alpha|}}^\gamma) - F(y_0^\gamma)) dr_{|\alpha|} \cdots dr_1 \right\|^4 \right]^{\frac{1}{2}} \\ &\quad \times \mathbb{E} \left[\left\| \bigotimes_{j=1}^{|\alpha|_\omega} \gamma_{r_i^j, r_{i+1}^j}^\omega \right\|^4 \right]^{\frac{1}{2}}. \end{aligned}$$

By applying Jensen's inequality to the uniform distribution on $[s, t]$, we have that $\|\int_s^t z_r dr\|^4 \leq (t-s)^3 \int_s^t \|z_r\|^4 dr$ for any continuous integrable process z_r . Therefore,

$$(3.8) \quad \mathbb{E}[\|J_\alpha^\gamma(F)\|^2] \leq C_1 h^{2|\alpha|_\tau} \sum_{\text{intervals}} \mathbb{E} \left[\int_{0 < r_{|\alpha|} < \dots < r_1 < 1} \|F(y_{r_{|\alpha|}}^\gamma) - F(y_0^\gamma)\|^4 dr_{|\alpha|} \dots dr_1 \right]^{\frac{1}{2}} \\ \times \mathbb{E} \left[\left\| \bigotimes_{j=1}^{|\alpha|_\omega} \gamma_{r_i^j, r_{i+1}^j}^\omega \right\|^4 \right]^{\frac{1}{2}}.$$

By repeatedly applying Hölder's inequality, we can estimate the term (3.8) as $O(h^{|\alpha|_\omega})$. Since $\text{ord}(\alpha) = |\alpha|_\tau + \frac{1}{2}|\alpha|_\omega$, it follows from the global Lipschitz continuity of F that

$$\mathbb{E}[\|J_\alpha^\gamma(F)\|^2] \leq C_2 \|F\|_{\text{Lip-1}}^2 h^{2\text{ord}(\alpha)} \\ \times \sum_{\text{intervals}} \left(\int_{0 < r_{|\alpha|} < \dots < r_1 < 1} \mathbb{E}[\|y_{r_{|\alpha|}}^\gamma - y_0^\gamma\|^4] dr_{|\alpha|} \dots dr_1 \right)^{\frac{1}{2}}.$$

By Theorem 2.2, we have $\mathbb{E}[\|y_{r_{|\alpha|}}^\gamma - y_0^\gamma\|^4] = O(h^2)$ and thus the result follows. \square

3.3. Main result. Now that we have Taylor expansions for both the CDE and the Stratonovich SDE, along with control over the size of the remainder terms in each, we can establish the strong convergence properties of path-based splitting schemes. We first obtain local strong and weak error estimates using a direct application of Lemmas 3.4 and 3.5 before applying the framework of Milstein and Tretyakov [61], which allows us to prove a global strong convergence rate for the approximating CDE.

THEOREM 3.6 (Local error estimates). *Suppose that the path $\gamma : [0, 1] \rightarrow \mathbb{R}^{1+d}$ satisfies Assumption A1 and for a fixed $p \in \{\frac{k}{2}\}_{k \in \mathbb{N}}$, let $f \in \mathcal{C}_{\text{Lip}}^{[p-1]}(\mathbb{R}^e, \mathbb{R}^e)$ and $g \in \mathcal{C}_{\text{Lip}}^{2p-1}(\mathbb{R}^e, \mathbb{R}^{e \times d})$. Suppose also that the assumptions of Theorem 2.2 hold and the integrals $I_\alpha^\gamma(1)$ and $I_\alpha(1)$ agree almost surely for $\alpha \in \mathcal{A}$ with $\text{ord}(\alpha) \leq p - \frac{1}{2}$ and in expectation for all $\alpha \in \mathcal{A}$ with $\text{ord}(\alpha) = p$. Let Y_1 denote an approximation (e.g. using an ODE solver) of the CDE solution $\{y_r^\gamma\}_{r \in [0,1]}$ driven by γ , such that $y_0^\gamma = y_0$ and*

$$(3.9) \quad \mathbb{E}[\|y_1^\gamma - Y_1\|^2]^{\frac{1}{2}} = O(h^p), \quad \text{and} \quad \|\mathbb{E}[y_1^\gamma] - \mathbb{E}[Y_1]\| = O(h^{p+\frac{1}{2}}),$$

where $y = \{y_t\}_{t \in [0,h]}$ is the solution of the SDE (1.1) and $h > 0$ is the step size. Then

$$\mathbb{E}[\|y_h - Y_1\|^2]^{\frac{1}{2}} = O(h^p), \quad \text{and} \quad \|\mathbb{E}[y_h] - \mathbb{E}[Y_1]\| = O(h^{p+\frac{1}{2}}).$$

Remark 3.7. In the above, Y_1 could represent the approximation of y_1^γ obtained by applying one step of a standard Runge-Kutta method along each linear piece of γ . This Runge-Kutta method should be of sufficiently high order so that (3.9) can hold.

Proof. We start by proving the local strong error. By the triangle inequality,

$$\mathbb{E}[\|y_h - Y_1\|^2]^{\frac{1}{2}} \leq \mathbb{E}[\|y_h - y_1^\gamma\|^2]^{\frac{1}{2}} + \mathbb{E}[\|y_1^\gamma - Y_1\|^2]^{\frac{1}{2}} = \mathbb{E}[\|y_h - y_1^\gamma\|^2]^{\frac{1}{2}} + O(h^p),$$

as the second term is the difference between the CDE solution and its approximation.

Recall the remainder terms $R_p(h, y_0)$ and $R_p^\gamma(h, y_0)$ in Propositions 3.1 and 3.2. Then, by another two applications of the triangle inequality, it directly follows that

$$\begin{aligned} \mathbb{E}[\|y_h - Y_1\|^2]^{\frac{1}{2}} &\leq \mathbb{E}[\|(y_h - R_p(h, y_0)) - (y_1^\gamma - R_p^\gamma(h, y_0))\|^2]^{\frac{1}{2}} \\ &\quad + \mathbb{E}[\|R_p(h, y_0)\|^2]^{\frac{1}{2}} + \mathbb{E}[\|R_p^\gamma(h, y_0)\|^2]^{\frac{1}{2}} + O(h^p), \end{aligned}$$

where the first term is simply the difference in the Taylor expansions, up to order p , of the SDE solution y_h and the CDE solution y_1^γ . Therefore, by the assumption that all integrals of the form $I_\alpha^\gamma(1)$ are matched almost surely for $\text{ord}(\alpha) \leq p - \frac{1}{2}$, we have

$$\mathbb{E}[\|y_h - Y_1\|^2]^{\frac{1}{2}} \leq \mathbb{E}[\|R_p(h, y_0)\|^2]^{\frac{1}{2}} + \mathbb{E}[\|R_p^\gamma(h, y_0)\|^2]^{\frac{1}{2}} + O(h^p).$$

By Proposition 3.1, the SDE remainder term will satisfy $\mathbb{E}[\|R_p(h, y_0)\|^2]^{\frac{1}{2}} = O(h^{p+\frac{1}{2}})$. On the other hand, $R_p^\gamma(h, y_0)$ is given by (3.7) and therefore, by Lemma 3.5, we have

$$\mathbb{E}[\|R_p^\gamma(h, y_0)\|^2]^{\frac{1}{2}} = O(h^{p+\frac{1}{2}}).$$

This gives the desired result for the local strong error, that $\mathbb{E}[\|y_h - Y_1\|^2]^{\frac{1}{2}} = O(h^p)$.

We now turn our attention to the local weak error. Using the triangle inequality and the same Taylor expansions as in the proof of local strong error, it follows that

$$\begin{aligned} \|\mathbb{E}[y_h] - \mathbb{E}[Y_1]\| &\leq \|\mathbb{E}[y_h - R_p(h, y_0)] - \mathbb{E}[y_1^\gamma - R_p^\gamma(h, y_0)]\| \\ &\quad + \|\mathbb{E}[y_1^\gamma] - \mathbb{E}[Y_1]\| + \|\mathbb{E}[R_p(h, y_0)]\| + \|\mathbb{E}[R_p^\gamma(h, y_0)]\|. \end{aligned}$$

From our assumption, the $I_\alpha^\gamma(1)$ terms in the SDE and CDE Taylor expansions are matched in expectation for $\text{ord}(\alpha) \leq p$ and, therefore, the first term disappears. Moreover, we assume $\|\mathbb{E}[y_1^\gamma] - \mathbb{E}[Y_1]\| = O(h^{p+\frac{1}{2}})$ and, by Jensen's inequality, we have

$$\|\mathbb{E}[R_p(h, y_0)]\| \leq \mathbb{E}[\|R_p(h, y_0)\|^2]^{\frac{1}{2}}, \quad \text{and} \quad \|\mathbb{E}[R_p^\gamma(h, y_0)]\| \leq \mathbb{E}[\|R_p^\gamma(h, y_0)\|^2]^{\frac{1}{2}}.$$

Since the above terms were previously shown to be $O(h^{p+\frac{1}{2}})$, the result follows. \square

Using the local estimates given by Theorem 3.6 and following the mean-square analysis of Milstein and Tretyakov [61, Theorem 1.1.1], we now obtain our main result.

THEOREM 3.8 (Global strong error estimate). *Given a fixed number of steps N , we define a numerical solution $\{Y_k\}_{0 \leq k \leq N}$ for the SDE (1.1) over $[0, T]$ as follows,*

$$Y_{k+1} := (\text{Solution at } r = 1 \text{ of CDE (1.3) driven by } \gamma_k : [0, 1] \rightarrow \mathbb{R}^{1+d})(Y_k) + E_k,$$

where $Y_0 := y_0$ and, for a fixed $p \in \{\frac{k}{2}\}_{k \in \mathbb{N}}$, the ‘‘CDE errors’’ $\{E_k\}$ uniformly satisfy

$$\mathbb{E}[\|E_k\|^2]^{\frac{1}{2}} = O(h^p), \quad \|\mathbb{E}[E_k]\| = O(h^{p+\frac{1}{2}}),$$

and each path $\gamma_k : [0, 1] \rightarrow \mathbb{R}^{1+d}$ is expressible as $\gamma_k = \varphi(\{(t, W_t) : t \in [\frac{kT}{N}, \frac{(k+1)T}{N}]\})$ for some fixed path-valued function φ . We will assume that the paths $\{\gamma_k\}$ uniformly satisfy Assumption A1 and that $f \in \mathcal{C}_{\text{Lip}}^{[p-1]}(\mathbb{R}^e, \mathbb{R}^e)$ and $g \in \mathcal{C}_{\text{Lip}}^{2p-1}(\mathbb{R}^e, \mathbb{R}^{e \times d})$. Suppose also that the assumptions of Theorem 2.2 hold and that the integrals $I_\alpha^{\gamma_k}(1)$ and $I_\alpha(1)$ agree almost surely for all $\alpha \in \mathcal{A}$ with $\text{ord}(\alpha) \leq p - \frac{1}{2}$ and in expectation for all $\alpha \in \mathcal{A}$ with $\text{ord}(\alpha) = p$. Then over the finite interval $[0, T]$, for $k \in \{1, 2, \dots, N\}$, we have

$$\mathbb{E}[\|y_{kh} - Y_k\|^2]^{1/2} = O(h^{p-\frac{1}{2}}).$$

Remark 3.9. Here, the ‘‘CDE errors’’ E_k represent the difference between the exact solution of the CDE and the numerical approximation obtained by discretizing each ODE in the splitting. Of course, if we can solve the ODEs exactly, then $E_k = 0$.

Remark 3.10 (Weak error estimates). . Whilst it is not the focus of this paper, global weak error estimates can also be established for path-based splitting methods. Moreover, to achieve high order weak convergence, splitting paths need only match moments of Brownian iterated integrals – just as in ‘‘Cubature on Wiener Space’’ [58]. We refer the reader to the PhD thesis of the final author [80, Section 4.3] for details.

Remark 3.11 (Infinite time horizon). The convergence results in this paper are established over a finite time horizon T . However, our framework could be employed to deal with the infinite time horizon setting under suitable conditions on the SDE. For instance, if the SDE is ergodic with an exponential contraction property then contributions of local errors to the global error are reduced (exponentially in time). An extension of the classical Milstein-Tretyakov mean-square error analysis [61] to the infinite time horizon case for such contractive SDEs is given by [54, Theorem 3.3.]. See also [25, Section 3] for similar, but employing Multilevel Monte Carlo (MLMC).

3.4. Application to commutative SDEs. Although Theorem 3.8 identifies conditions on the piecewise linear path γ to achieve a given strong convergence rate, it can be difficult to generate the required integrals (as discussed in the introduction). Fortunately, the commutativity condition (1.2) leads to certain simplifications in the Taylor expansions of the Stratonovich SDE (1.1) and its CDE approximation (1.3). This is detailed in Appendix A but, as a consequence, we have the following theorem.

THEOREM 3.12 (Global strong error estimate for SDEs with commutative noise). *Let y be the solution of SDE (1.1) whose diffusion vector fields satisfy the condition*

$$g'_i(y)g_j(y) = g'_j(y)g_i(y), \quad \forall y \in \mathbb{R}^e.$$

Suppose the assumptions of Theorem 3.8 hold for $p = 2$, but with the exception that each path γ_k now matches only the following iterated integrals of Brownian motion:

$$\begin{aligned} \gamma_k(1) - \gamma_k(0) &= (h, W_{kh, (k+1)h}), \\ \int_0^1 (\gamma_k^\omega(r) - \gamma_k^\omega(0)) d\gamma_k^\tau(r) &= \int_{kh}^{(k+1)h} W_{kh,u} du, \\ \mathbb{E} \left[\int_0^1 \left((\gamma_k^\omega)^i(r) - (\gamma_k^\omega)^i(0) \right)^2 d\gamma_k^\tau(r) \right] &= \mathbb{E} \left[\int_{kh}^{(k+1)h} W_{kh,u}^2 du \right] = \frac{1}{2} h^2, \end{aligned}$$

and for distinct $i, j, l \in \{\tau, (\omega, 1), \dots, (\omega, d)\}$ with $\tau \in \{i, j, l\}$, we have

$$\mathbb{E} \left[\int_0^1 \int_0^{r_1} \int_0^{r_2} d\gamma_k^i(r_3) d\gamma_k^j(r_2) d\gamma_k^l(r_1) \right] = 0.$$

Then on the interval $[0, T]$, for $k \in \{1, 2, \dots, N\}$, the numerical solution $\{Y_k\}$ satisfies

$$\mathbb{E}[\|y_{kh} - Y_k\|^2]^{1/2} = O(h^{\frac{3}{2}}).$$

Proof. By Theorem A.6, we see that the CDE Taylor expansion can match all the ‘‘noise only’’ terms with $\text{ord}(\alpha) \leq 2$ simply by the path γ_k having the increment

$\gamma_k^\omega(1) - \gamma_k^\omega(0) = W_{kh, (k+1)h}$. Adopting the general notation used within Appendix A, we recall Theorem A.4, which gives the following decompositions of iterated integrals:

$$(3.10) \quad I_{ij} = \frac{1}{2}I_i \cdot I_j + \frac{1}{2}I_{[i,j]},$$

$$(3.11) \quad I_{ijk} = \frac{1}{6}I_i \cdot I_j \cdot I_k + \frac{1}{4}I_i \cdot I_{[j,k]} + \frac{1}{4}I_{[i,j]} \cdot I_k + \frac{1}{6}(I_{[[i,j],k]} + I_{[i,[j,k]]}),$$

for indices $i, j, k \in \{1, \dots, d\}$. However, by identifying a coordinate of the Brownian motion with time, we see that the above would still hold when $i, j, k \in \{0, 1, \dots, d\}$. (In the following paragraph, the verb ‘‘match’’ refers to when $r \mapsto (\gamma_k^\tau, \gamma_k^\omega)(r)$ and $t \mapsto (t, W_t)$ give the same iterated integral – either almost surely or in expectation).

Thus, by virtue of matching $\{I_0, I_i, I_{i0}\}_{1 \leq i \leq d}$, γ_k matches $\{I_{[i,0]}\}$ and thus $\{I_{0i}\}$. Using integration by parts, we note the following identities for triple iterated integrals:

$$\begin{aligned} \int_0^1 \int_0^{r_1} \int_0^{r_2} d(\gamma_k^\omega)^i(r_3) d(\gamma_k^\omega)^i(r_2) d\gamma_k^\tau(r_1) &= \int_0^1 \frac{1}{2} \left((\gamma_k^\omega)^i(r) - (\gamma_k^\omega)^i(0) \right)^2 d\gamma_k^\tau(r), \\ \int_{kh}^{(k+1)h} \int_{kh}^{u_1} \int_{kh}^{u_2} \circ dW_{u_3}^i \circ dW_{u_2}^i du_1 &= \int_{kh}^{(k+1)h} \frac{1}{2} W_{kh,u}^2 du. \end{aligned}$$

Since γ_k is assumed to match $\{I_{ii0}\}$ in expectation and the lower order terms exactly, by (3.11) and the fact that $I_{[0,[i,i]]} = 0$, it will also match $\{I_{[i,[i,0]}\}$ in expectation. Hence, γ_k matches $\{I_{i0i}, I_{0ii}\}$ in expectation by (3.11) and the antisymmetry of $[\cdot, \cdot]$. By assumption, the remaining integrals $\{I_{ij0}, I_{i0j}, I_{0ij}\}$ are matched in expectation.

From the above, we see the Taylor expansions of the SDE (1.1) and CDE (1.3) coincide up to order $p = 2$, as required by Theorem 3.8. The result now follows. \square

Remark 3.13. Just as in Theorem 3.8, we account for the fact that the CDE (1.3), or rather the resulting sequence of ODEs, may be approximated using an ODE solver. However, obtaining the required estimates for these additional ‘‘CDE errors’’ $\{E_k\}$ may be non-trivial and thus, we leave such an error analysis as a topic of future work. That said, to achieve strong order 3/2 convergence, we expect that a single step of a second order ODE solver would be sufficient to discretise ODEs depending on just f and a single step of a fourth order solver (such as RK4) to suffice for the other ODEs. The intuition is that γ has Brownian-like scaling and so vector fields are either $O(h)$ or $O(h^{\frac{1}{2}})$. Hence, we expect the local errors to be $O(h^3)$ or $O(h^{\frac{5}{2}})$ in these two cases.

4. Paths. In this section, we present a variety of piecewise linear paths which fall into the proposed framework for developing SDE splitting methods (Theorem 3.8). These ‘‘splitting paths’’ correspond to both well-known numerical methods (such as Lie-Trotter and Strang splitting [79]) as well as the new high order splitting methods, which can exploit the optimal integral estimators that are derived in Appendix B. Furthermore, we illustrate both the Strang and high order splitting paths in Figure 3. Throughout, we use the notation in Example 1.3 and define paths by their increments.

EXAMPLE 4.1 (Lie-Trotter). *A Lie-Trotter splitting can be defined by one of two possible two-piece paths $\gamma^{LT1}, \gamma^{LT2} : [0, 1] \rightarrow \mathbb{R}^{1+d}$ given by $\gamma^{LT}(z) = (\gamma^\tau, \gamma^\omega)(z)$ with*

$$(4.1) \quad \gamma_{r_i, r_{i+1}}^{LT1} := \begin{cases} (h, 0), & \text{if } i = 0 \\ (0, W_{s,t}), & \text{if } i = 1, \end{cases} \quad \gamma_{r_i, r_{i+1}}^{LT2} := \begin{cases} (0, W_{s,t}), & \text{if } i = 0 \\ (h, 0), & \text{if } i = 1. \end{cases}$$

EXAMPLE 4.2 (Strang splitting). *The Strang splitting, see Figure 3, can be defined as a three-piece path $\gamma^S : [0, 1] \rightarrow \mathbb{R}^{1+d}$ given by $\gamma^S(z) = (\gamma^\tau, \gamma^\omega)(z)$ with the pieces:*

$$(4.2) \quad \gamma_{r_i, r_{i+1}}^S := \begin{cases} (\frac{1}{2}h, 0), & \text{if } i = 0, 2 \\ (0, W_{s,t}), & \text{if } i = 1. \end{cases}$$

Remark 4.3. Using Theorem 3.8, it is straightforward to show that these splitting paths produce approximations with order 1 strong convergence for commutative SDEs. However, since the Strang splitting path satisfies the conditions of Theorem 3.12, except $\int_0^1 ((\gamma_k^{S,\omega})^i(r) - (\gamma_k^{S,\omega})^i(0)) d\gamma_k^{S,\tau}(r) = \frac{1}{2} W_{kh, (k+2)h} h$, it achieves a second order weak convergence rate for commutative SDE. To achieve high order weak convergence more generally, additional random variables representing Lévy area are required [42, 68].

We now proceed to “higher order” piecewise linear paths that are constructed to match the increment $W_{s,t}$ and space-time Lévy area $H_{s,t}$ of the Brownian motion. Unless stated otherwise, these paths will correspond to splitting methods that achieve order 3/2 strong convergence. We note that for these paths to match the necessary higher order iterated integrals in expectation, at least three pieces will be required. The inability of paths with two pieces to match the conditions (1.8) and (1.9) required for high order strong convergence was explicitly shown in [26, p97 and Appendix A]. We begin by presenting paths (4.3) and (4.4), which each have a total of five pieces (vertical and horizontal), and can thus be seen as extensions of the Strang splitting.

EXAMPLE 4.4 (High order Strang splitting (linear version)). *A high order Strang splitting, see Figure 3, can be defined using a five-piece path $\gamma^{HS1} : [0, 1] \rightarrow \mathbb{R}^{1+d}$, which is linear in the Brownian motion and has the pieces:*

$$(4.3) \quad \gamma_{r_i, r_{i+1}}^{HS1} := \begin{cases} (\frac{3-\sqrt{3}}{6}h, 0), & \text{if } i = 0, 4 \\ (0, \frac{1}{2}W_{s,t} + (2-i)\sqrt{3}H_{s,t}), & \text{if } i = 1, 3 \\ (\frac{\sqrt{3}}{3}h, 0), & \text{if } i = 2. \end{cases}$$

The next splitting path that we define will be a non-linear function of $W_{s,t}$ and $H_{s,t}$. However, in addition, it will utilize the following (independent) Rademacher variables.

DEFINITION 4.5. *The space-time Lévy **swing** (side with **integral greater**) of a Brownian motion over $[s, t]$ is defined as $n_{s,t} \in \{-1, 1\}^d$ where*

$$n_{s,t}^i := \text{sgn}(H_{s, s+\frac{1}{2}h}^i - H_{s+\frac{1}{2}h, t}^i).$$

THEOREM 4.6. *$n_{s,t}$ is a Rademacher random vector, independent of $(W_{s,t}, H_{s,t})$.*

Proof. The independence is detailed in the proof of Theorem B.4 in Appendix B, where the tuple $(W_{s,t}, H_{s,t}, Z_{s,u}, N_{s,t})$ is shown to be jointly normal and uncorrelated, with $u := s + \frac{1}{2}h$, $Z_{s,u} := \frac{1}{8}(W_{s,u} - W_{u,t}) + \frac{3}{8}(H_{s,u} + H_{u,t})$ and $N_{s,t} := H_{s,u} - H_{u,t}$. \square

EXAMPLE 4.7 (High order Strang splitting (non-linear version)). *A high order Strang splitting, see Figure 3, can be defined as a five-piece path $\gamma^{HS2} : [0, 1] \rightarrow \mathbb{R}^{1+d}$, which is based on an optimal estimator for a certain Brownian integral and has pieces:*

$$(4.4) \quad \gamma_{r_i, r_{i+1}}^{HS2} := \begin{cases} (0, \frac{1}{2}W_{s,t} + (1 - \frac{1}{2}i)H_{s,t} - \frac{1}{2}C_{s,t}), & \text{if } i = 0, 4 \\ (\frac{1}{2}h, 0), & \text{if } i = 1, 3 \\ (0, C_{s,t}), & \text{if } i = 2. \end{cases}$$

where the random vector $C_{s,t}$ is defined component-wise by

$$(4.5) \quad C_{s,t}^j := \epsilon_{s,t}^j \left(\frac{1}{3} (W_{s,t}^j)^2 + \frac{4}{5} (H_{s,t}^j)^2 + \frac{4}{15} h - \frac{1}{\sqrt{6\pi}} h^{\frac{1}{2}} n_{s,t}^j W_{s,t}^j \right)^{\frac{1}{2}},$$

$$(4.6) \quad \epsilon_{s,t}^j := \operatorname{sgn} \left(W_{s,t}^j - \frac{3}{\sqrt{24\pi}} h^{\frac{1}{2}} n_{s,t}^j \right).$$

Remark 4.8. The formula (4.5) for $C_{s,t}$ is derived so that $\int_0^1 ((\gamma_r^\omega)^j - (\gamma_0^\omega)^j)^2 d\gamma_r^\tau$ is equal to the optimal estimator $\mathbb{E} \left[\int_s^t (W_{s,u}^j)^2 du \mid W_{s,t}, H_{s,t}, n_{s,t} \right]$, see Theorem B.7.

For paths with three pieces, two of which are vertical and only relate to diffusion vector field, we refer to the resulting approximation as the ‘‘Shifted ODE’’ approach. We use this terminology as, in the additive noise setting, the vertical pieces correspond to additive shifts for the numerical solution and so there is only one non-trivial ODE. As before, paths can be linear or non-linear functions of the input random variables.

EXAMPLE 4.9 (Shifted ODE splitting (high order and linear)). *We can define a high order splitting by a three-piece path $\gamma^{SO1} : [0, 1] \rightarrow \mathbb{R}^{1+d}$ with the following pieces:*

$$(4.7) \quad \gamma_{r_i, r_{i+1}}^{SO1} := \begin{cases} (0, (1-i)H_{s,t} + \frac{1}{2}\sqrt{h}n_{s,t}), & \text{if } i = 0, 2 \\ (h, W_{s,t} - \sqrt{h}n_{s,t}), & \text{if } i = 1. \end{cases}$$

EXAMPLE 4.10 (Shifted ODE splitting (high order and non-linear)). *We can define a high order splitting, see Figure 3, using a three-piece path $\gamma^{SO2} : [0, 1] \rightarrow \mathbb{R}^{1+d}$, which is based on an optimal estimator for a certain Brownian integral and has pieces:*

$$(4.8) \quad \gamma_{r_i, r_{i+1}}^{SO2} := \begin{cases} (0, \frac{1}{2}W_{s,t} + (1-i)H_{s,t} - \frac{1}{2}\tilde{C}_{s,t}), & \text{if } i = 0, 2 \\ (h, \tilde{C}_{s,t}), & \text{if } i = 1, \end{cases}$$

where the random vector $\tilde{C}_{s,t}$ is defined component-wise by

$$\begin{aligned} \tilde{C}_{s,t}^j &:= \epsilon_{s,t}^j \left((W_{s,t}^j)^2 + \frac{12}{5} (H_{s,t}^j)^2 + \frac{4}{5} h - \frac{3}{\sqrt{6\pi}} h^{\frac{1}{2}} n_{s,t}^j W_{s,t}^j \right)^{\frac{1}{2}}, \\ \epsilon_{s,t}^j &:= \operatorname{sgn} \left(W_{s,t}^j - \frac{3}{\sqrt{24\pi}} h^{\frac{1}{2}} n_{s,t}^j \right). \end{aligned}$$

Remark 4.11. Just as $C_{s,t}$ in (4.5), $\tilde{C}_{s,t}$ is derived so that $\int_0^1 ((\gamma_r^\omega)^j - (\gamma_0^\omega)^j)^2 d\gamma_r^\tau$ is equal to the optimal estimator $\mathbb{E} \left[\int_s^t (W_{s,u}^j)^2 du \mid W_{s,t}, H_{s,t}, n_{s,t} \right]$, see Theorem B.7.

The following paths do not generally result in high order approximations for SDEs satisfying the commutativity condition (1.2). However, the piecewise linear path given by (4.9) results in the ‘‘Shifted Euler’’ method for SDEs with additive noise, which we demonstrate can outperform the standard Euler-Maruyama method in Section 5.

EXAMPLE 4.12 (Shifted ODE splitting (low order; suitable for Euler’s method)). *We can define a low order splitting by a three-piece path $\gamma^{SO3} : [0, 1] \rightarrow \mathbb{R}^{1+d}$ with*

$$(4.9) \quad \gamma_{r_i, r_{i+1}}^{SO3} := \begin{cases} (0, \frac{1}{2}W_{s,t} + (1-i)H_{s,t}), & \text{if } i = 0, 2 \\ (h, 0), & \text{if } i = 1. \end{cases}$$

The path (4.10) is also not usually high order, but gives a third order approximation when applied to underdamped Langevin dynamics (ULD), given by equation (5.13). This surprising convergence rate is due to the fact that the non-Gaussian integral $\int_s^t W_{s,u}^{\otimes 2} du$ does not appear within the Taylor expansion of ULD (see [30] for details).

EXAMPLE 4.13 (Shifted ODE splitting for the underdamped Langevin diffusion [30]). We can define a splitting by a three-piece path $\gamma^{SO4} : [0, 1] \rightarrow \mathbb{R}^{1+d}$ with pieces:

$$(4.10) \quad \gamma_{r_i, r_{i+1}}^{SO4} := \begin{cases} (0, (1-i)H_{s,t} + 6K_{s,t}), & \text{if } i = 0, 2 \\ (h, W_{s,t} - 12K_{s,t}), & \text{if } i = 1. \end{cases}$$

where $K_{s,t} \sim \mathcal{N}(0, \frac{1}{720}hI_d)$ is independent of $(W_{s,t}, H_{s,t})$ and given by the integral

$$K_{s,t} := \frac{1}{h^2} \int_s^t \left(W_{s,u} - \frac{u-s}{h} W_{s,t} \right) \left(\frac{1}{2}h - (u-s) \right) du.$$

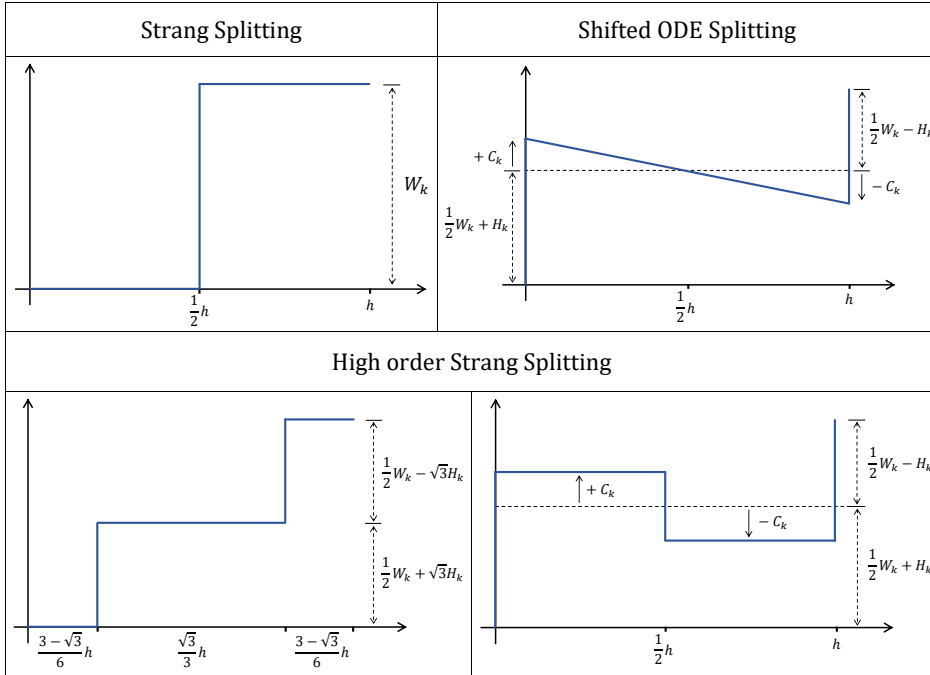


FIG. 3. Illustration of piecewise linear paths associated with various splitting methods for SDEs. (these diagrams are not drawn accurately; the “vertical” pieces are only the same in distribution)

5. Examples.

We demonstrate the proposed splitting methods on several SDEs. In each example, we consider just one high order splitting, which are chosen as follows:

- For the Cox-Ingersoll-Ross (CIR) model, we will consider the “linear” high order Strang splitting due to its provable weak approximation properties (Theorem 5.2).
- For general additive-noise SDEs, we will consider the “Shifted ODE” splittings because they only require a single non-trivial ODE to be discretised in each step. (and specifically (4.8) for a scalar oscillator as it uses optimal integral estimators).

- For the stochastic FitzHugh-Nagumo (FHN) model, we consider the “non-linear” high order Strang splitting as it uses optimal integral estimators and produces “drift ODEs” which we can be resolved using the Strang splitting technique in [8].
- For underdamped Langevin dynamics, which has special structure, we apply the Shifted ODE splitting (4.10) since it achieves third order strong convergence [30].

For the last three examples, the “non-diffusion” ODEs that come from the SDE splitting will not admit a closed-form solution and thus must be further discretised. We will show that such ODEs can be resolved by Runge-Kutta or splitting methods.

Throughout, we shall compare methods using the following strong error estimator:

DEFINITION 5.1 (Strong error estimator for SDEs). *For $N \geq 1$, let Y_N denote a numerical solution to the SDE (1.1) computed at time T with a fixed step size $h = \frac{T}{N}$. Then we define the following estimator for quantifying the strong convergence of Y_N :*

$$(5.1) \quad S_N := \sqrt{\mathbb{E} \left[(Y_N - Y_T^{fine})^2 \right]},$$

where Y_T^{fine} denotes a numerical solution to (1.1) computed with a finer step size, $h^{fine} \leq \frac{1}{10}h$, but using the same Brownian motion (so that Y_N and Y_T^{fine} are close). In our examples, the expectation in (5.1) will be estimated by standard Monte Carlo.

All the experiments were conducted on a laptop in either C++, Python or R. Associated code is available at github.com/james-m-foster/high-order-splitting and github.com/james-m-foster/high-order-langevin for the Langevin dynamics example.

5.1. Cox-Ingersoll-Ross model. The Cox-Ingersoll-Ross (or CIR) model is a popular one-factor short rate model used in mathematical finance for modelling interest rates [17] and stochastic volatility [38]. It is given by the following Itô SDE:

$$(5.2) \quad dy_t = a(b - y_t) dt + \sigma\sqrt{y_t} dW_t,$$

where the parameters $a, b, \sigma \geq 0$ describe the mean reversion speed/level and volatility. Over the years, a variety of numerical methods have been proposed for the CIR model and we refer the reader to some of these approaches [2, 3, 4, 18, 22, 26, 37, 43, 60, 69]. As we propose splitting methods, we first rewrite the SDE (5.2) in Stratonovich form:

$$dy_t = a(\tilde{b} - y_t) dt + \sigma\sqrt{y_t} \circ dW_t.$$

where $\tilde{b} := b - \frac{\sigma^2}{4a}$. To ensure non-negativity of \tilde{b} and our scheme, we assume $\sigma^2 \leq 4ab$. By driving (5.2) with the piecewise linear path (4.3), we obtain the splitting method:

$$(5.3) \quad \begin{aligned} Y_k^{(1)} &:= e^{-\frac{3-\sqrt{3}}{6}ah} Y_k + \tilde{b}(1 - e^{-\frac{3-\sqrt{3}}{6}ah}), \\ Y_k^{(2)} &:= \left(\sqrt{Y_k^{(1)}} + \frac{\sigma}{2} \left(\frac{1}{2}W_k + \sqrt{3}H_k \right) \right)^2, \\ Y_k^{(3)} &:= e^{-\frac{\sqrt{3}}{3}ah} Y_k^{(2)} + \tilde{b}(1 - e^{-\frac{\sqrt{3}}{3}ah}), \\ Y_k^{(4)} &:= \left(\sqrt{Y_k^{(3)}} + \frac{\sigma}{2} \left(\frac{1}{2}W_k - \sqrt{3}H_k \right) \right)^2, \\ Y_{k+1} &:= e^{-\frac{3-\sqrt{3}}{6}ah} Y_k^{(4)} + \tilde{b}(1 - e^{-\frac{3-\sqrt{3}}{6}ah}), \end{aligned}$$

since for the CIR model, the drift and diffusion ODEs admit closed-form solutions. The resulting numerical method (5.3) is then straightforward to implement and we might expect each step to be roughly twice as expensive as previous methodologies (since the above method requires generating two Gaussian random variables per step). We also note that the method (5.3), and each of its stages, preserves non-negativity. In addition, one can compute the mean and variance of both the SDE (5.2) and (5.3).

THEOREM 5.2. *The numerical solution given by (5.3) has the following moments:*

$$\begin{aligned}\mathbb{E}[Y_{k+1}|Y_k] &= e^{-ah}Y_k + b(1 - e^{-ah}) + R_k^E, \\ \text{Var}(Y_{k+1}|Y_k) &= \frac{\sigma^2}{a}(e^{-ah} - e^{-2ah})Y_k + \frac{b\sigma^2}{2a}(1 - e^{-ah})^2 + R_k^V,\end{aligned}$$

where the remainder terms R_k^E and R_k^V can be estimated as $O(h^5)$ in an $L^2(\mathbb{P})$ sense.

Proof. See the proof of Theorem C.1 in the appendix. \square

Remark 5.3. The associated mean and variance of the CIR model (5.2) are also known analytically [17] and given by the same formulae, but without the $O(h^5)$ terms.

$$\begin{aligned}\mathbb{E}[y_{t_{k+1}}|y_{t_k}] &= e^{-ah}y_{t_k} + b(1 - e^{-ah}), \\ \text{Var}(y_{t_{k+1}}|y_{t_k}) &= \frac{\sigma^2}{a}(e^{-ah} - e^{-2ah})y_{t_k} + \frac{b\sigma^2}{2a}(1 - e^{-ah})^2.\end{aligned}$$

Therefore, even though the primary focus of the paper is strong approximation, we see that the splitting (5.3) is also a high order weak approximation of the CIR model. Furthermore, due to the non-Lipschitz diffusion vector field in the CIR model, we can not directly apply our main result to establish the strong convergence of our method. We thus leave the error analysis of path-based splitting methods in the “non-smooth” setting as future work. Similar to [8], we expect results can be obtained in cases where the drift has polynomial growth and satisfies a (global) one-sided Lipschitz condition.

We will now present our experiment, comparing the strong convergence of the splitting (5.3) against several well-known methods. We use the following parameters:

$$a = 1, \quad b = 1, \quad \sigma = 1, \quad y_0 = 1, \quad T = 1.$$

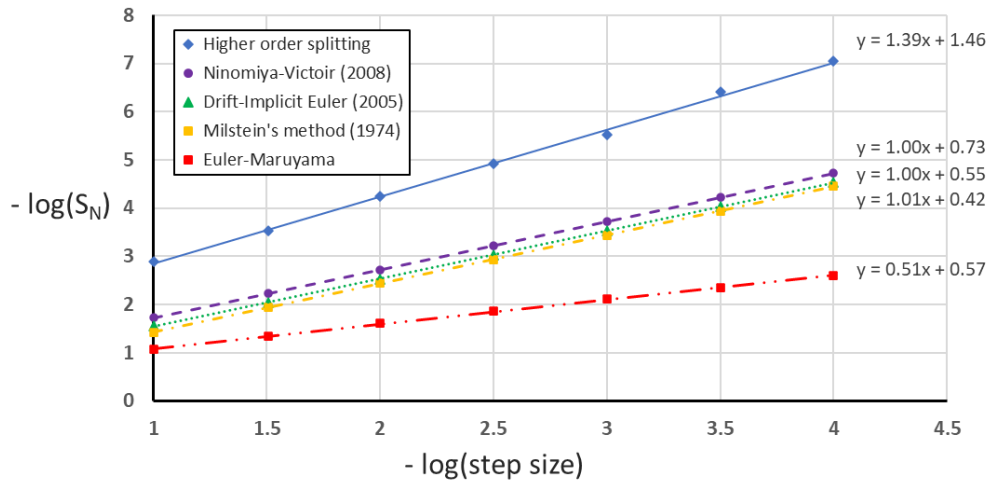


FIG. 4. S_N estimated for (5.2) with 100,000 sample paths as a function of step size $h = \frac{T}{N}$.

In the above graph, we see that the proposed splitting scheme achieves a high order convergence rate and better accuracy than other schemes (for a fixed step size). Moreover, we believe (5.3) is the first non-negative method for the CIR model to show high order strong convergence and to match the first two moments with $O(h^5)$ error. However, since the square root vector field is not globally Lipschitz continuous, our scheme converges slightly slower than the $O(h^{\frac{3}{2}})$ rate obtained in the “smooth” case.

As we discussed previously, each step of the splitting method (5.3) will be more computationally expensive than for low order schemes. This is quantified in Table 1.

TABLE 1
Computer time to simulate 100,000 sample paths of (5.2) in C++ with 100 steps (seconds)

Splitting (5.3)	Ninomiya-Victoir	Drift-Implicit Euler	Milstein	Euler
2.13	1.07	1.42	1.01	0.86

TABLE 2
Estimated time to produce 100,000 sample paths of (5.2) with an error of $S_N = 10^{-3}$ (seconds)

Splitting (5.3)	Ninomiya-Victoir	Drift-Implicit Euler	Milstein	Euler
0.27	1.99	4.17	3.69	490

We see that the high order splitting method (5.3) is roughly twice as expensive as the lower order schemes. Combining these times with Figure 4, we arrive at Table 2, which shows our method achieves a small error significantly faster than other schemes.

5.2. Additive noise SDEs, such as a stochastic anharmonic oscillator.

We first consider an arbitrary SDE with additive noise (that is, $g(\cdot)$ is a fixed matrix)

$$(5.4) \quad dy_t = f(y_t) dt + \sigma dW_t,$$

where $\sigma \in \mathbb{R}^{e \times d}$. As (5.4) has additive noise, it is in both Itô and Stratonovich form. Since each piece in γ yields an ODE, we would like to minimize the number of pieces. Moreover, it was shown in [26, p97 and Appendix A] that two-piece paths are unable to match the various iterated integrals of Brownian motion required in Theorem 3.12. Thus, in general, we propose driving (5.4) by a piecewise linear path with three pieces. So unless the SDE has special structure, such as underdamped Langevin dynamics, we recommend either the paths (4.7) or (4.8) to achieve 3/2 order strong convergence. In either case, we obtain a splitting method for the SDE (5.4) with the following form:

$$(5.5) \quad Y_{k+1} := \exp(f(\cdot)h + \sigma C_2)(Y_k + \sigma C_1) + \sigma C_3,$$

where the vectors $C_1, C_2, C_3 \in \mathbb{R}^d$ correspond to the increments of the driving path.

In this section, we will consider the general setting where the ODE governed by $f(\cdot)h + \sigma C_2$ in (5.5) does not admit a closed-form solution and must be discretised. Expanding terms in the Taylor expansion of this ODE, we see that (5.5) is equal to

$$\begin{aligned} & \left(I_d(\cdot) + f(\cdot)h + \sigma C_2 + \frac{1}{2}f'(\cdot)(f(\cdot)h + \sigma C_2)h + \frac{1}{6}f''(\cdot)(\sigma C_2)^{\otimes 2}h \right) (Y_k + \sigma C_1) + \sigma C_3 \\ &= Y_k + \sigma C_1 + \left(f(Y_k) + f'(Y_k)\sigma C_1 + \frac{1}{2}f''(Y_k)(\sigma C_1)^{\otimes 2} \right) h + \sigma C_2 + \frac{1}{2}f'(Y_k)f(Y_k)h^2 \\ & \quad + \frac{1}{2} \left(f'(Y_k)\sigma C_2 + f''(Y_k)((\sigma C_2) \otimes (\sigma C_1)) \right) h + \frac{1}{6}f''(Y_k)(\sigma C_2)^{\otimes 2}h + \sigma C_3 + \dots \end{aligned}$$

Rearranging these terms then gives the following expansion for the splitting method,

$$Y_{k+1} \approx Y_k + f(Y_k)h + \sigma(C_1 + C_2 + C_3) + \frac{1}{2}f'(Y_k)\left(\sigma C_1 + \frac{1}{2}\sigma C_2\right)h \\ + \frac{1}{2}f'(Y_k)f(Y_k)h^2 + \frac{1}{2}f''(Y_k)\left((\sigma C_1)^2 + (\sigma C_1) \otimes (\sigma C_2) + \frac{1}{3}(\sigma C_2)^2\right)h,$$

where the final line follows as the second derivative $f''(Y_k)$ is symmetric and bilinear.

Since we intend to discretise the ODE map $x \mapsto \exp(f(\cdot)h + \sigma C_2)x$, we would like the Taylor expansion of the numerical ODE solver to coincide with the above. For example, if we apply an explicit two-stage second order Runge-Kutta method (determined by a parameter α), then this will result in the following Taylor expansion:

$$x^{\text{RK}} = x + \left(1 - \frac{1}{2\alpha}\right)(f(x)h + \sigma C_2) + \frac{1}{2\alpha}\left(f(x + \alpha(f(x)h + \sigma C_2))h + \sigma C_2\right) \\ = x + f(x)h + \sigma C_2 + \frac{1}{2}f'(x)(f(x)h + \sigma C_2)h + \frac{1}{4}\alpha f''(x)(\sigma C_2)^{\otimes 2}h + \dots$$

Thus, the only explicit two-stage Runge-Kutta method matching the Taylor expansion of the splitting method (5.5) is Ralston's method [72] (which corresponds to $\alpha = \frac{2}{3}$). Hence, we propose the following numerical method for the additive noise SDE (5.4),

$$\begin{aligned} \tilde{Y}_k^{\text{SR}} &:= Y_k^{\text{SR}} + \sigma C_1, \\ \tilde{Y}_{k+\frac{2}{3}}^{\text{SR}} &:= \tilde{Y}_k^{\text{SR}} + \frac{2}{3}\left(f(\tilde{Y}_k^{\text{SR}})h + \sigma C_2\right), \\ (5.6) \quad Y_{k+1}^{\text{SR}} &:= Y_k^{\text{SR}} + \frac{1}{4}f(\tilde{Y}_k^{\text{SR}})h + \frac{3}{4}f(\tilde{Y}_{k+\frac{2}{3}}^{\text{SR}})h + \sigma W_k, \end{aligned}$$

where $C_1, C_2 \in \mathbb{R}^d$ are the first two increments of the driving piecewise linear path γ . Note that the final line is obtained by combining the second stage of Ralston's method with the terms coming from the last vertical piece of γ (assuming $W_k = C_1 + C_2 + C_3$).

Remark 5.4. We can extend this method to time-varying diffusions with $\sigma \equiv \sigma(t)$. For example, the terms $\sigma C_1, \sigma C_2$ and σW_k may be replaced by $\sigma(t_k)C_1, \sigma(t_k)C_2$ and

$$(5.7) \quad \int_{t_k}^{t_{k+1}} \sigma(r) dW_r = \frac{1}{2}(\sigma(t_k) + \sigma(t_{k+1}))W_k + (\sigma(t_{k+1}) - \sigma(t_k))H_k + O(h^{2.5}).$$

Although we shall not formally present an error analysis, it is clear from the above Taylor expansions that the method (5.6) achieves a 3/2 strong order convergence rate. Similarly, we consider the case where the splitting path (4.9) is applied to the additive noise SDE (5.4) and the resulting ODE is discretised using Euler's method. This gives

$$(5.8) \quad Y_{k+1}^{\text{SE}} := Y_k^{\text{SE}} + f\left(Y_k^{\text{SE}} + \sigma\left(\frac{1}{2}W_k + H_k\right)\right)h + \sigma W_k.$$

We refer to the numerical method (5.8) as the ‘‘Shifted Euler’’ discretisation of (5.4). Whilst the Shifted Euler method will have the same first order of convergence as the Euler-Maruyama method, we expect it to be more accurate (for sufficiently small h). This is due to the shifted Euler method (5.8) having the following Taylor expansion:

$$Y_{k+1}^{\text{SE}} = Y_k^{\text{SE}} + f(Y_k^{\text{SE}})h + \sigma W_k + f'(Y_k^{\text{SE}})\left(\underbrace{\sigma\left(\frac{1}{2}W_k + H_k\right)h}_{= \int_{t_k}^{t_{k+1}} W_{t_k, r} dr}\right) + O(h^2).$$

Thus, the Shifted Euler scheme has a local error of $O(h^2)$ whereas the Euler-Maruyama method produces a local error of $O(h^{\frac{3}{2}})$, which is due to the integral highlighted above.

Remark 5.5. The shifted Euler method can be extended to time-varying diffusion coefficients by replacing the terms σW_k and $\sigma \int_{t_k}^{t_{k+1}} W_{t_k,r} dr$ with $\int_{t_k}^{t_{k+1}} \sigma(r) dW_r$ and $\int_{t_k}^{t_{k+1}} \int_{t_k}^s \sigma(r) dW_r ds = \sigma(t_k) \int_{t_k}^{t_{k+1}} W_{t_k,r} dr + \frac{1}{6}(\sigma(t_{k+1}) - \sigma(t_k))W_k h^2 + O(h^{\frac{7}{2}})$.

Moreover, in applications where evaluating f is significantly faster than generating Gaussian random vectors, we can remove the space-time Lévy area H_k from (5.8). The resulting “increment-only” Shifted Euler method will then have the same cost per step as the traditional Euler-Maruyama method. However, for sufficiently small h , it will still be more accurate as it gives $\frac{1}{2}hW_k \approx \int_{t_k}^{t_{k+1}} W_{t_k,r} dr$ in its Taylor expansion.

We now present our numerical example; a scalar stochastic anharmonic oscillator.

$$(5.9) \quad dy_t = \sin(y_t) dt + dW_t, \quad (y_0 = 1, \quad T = 1)$$

We compare our approaches (high order method (5.6) and low order method (5.8)) against the 3/2 strong order SRA1 scheme in [73] and the Euler-Maruyama method:

$$Y_{k+1}^{A1} := Y_k^{A1} + \frac{1}{3}f(Y_k^{A1})h + \frac{2}{3}f\left(Y_k^{A1} + \frac{3}{4}\left(f(Y_k^{A1})h + \sigma(W_k + 2H_k)\right)\right)h + \sigma W_k,$$

$$Y_{k+1}^{EM} := Y_k^{EM} + f(Y_k^{EM})h + \sigma W_k.$$

We use the non-linear splitting path (4.8) to obtain the variables C_1, C_2 in (5.6).

As the Shifted Ralston and Euler methods have the same orders of convergence as the SRA1 and Euler-Maruyama methods, we estimate the ratios of their $L^2(\mathbb{P})$ errors. Our results are presented in the following graph, where we see the proposed methods achieve roughly a $3\times$ improvement in their accuracy for sufficiently small step sizes.

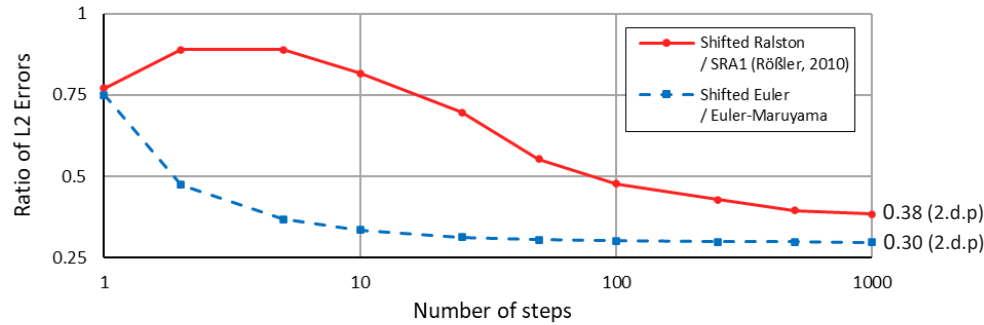


FIG. 5. S_N estimated for (5.9) with 1,000,000 sample paths, where N is the number of steps. To better illustrate differences in accuracy between methods, we plot the ratio $S_N^{(\text{Method 1})} / S_N^{(\text{Method 2})}$.

TABLE 3
Computer time to simulate 100,000 sample paths of (5.9) in C++ with 100 steps (seconds)

Shifted Ralston (5.6)	SRA1 scheme [73]	Shifted Euler (5.8)	Euler-Maruyama
3.16	2.29	1.91	1.09

TABLE 4

Estimated time to produce 100,000 sample paths of (5.9) with an error of $S_N = 10^{-4}$ (seconds)

Shifted Ralston (5.6)	SRA1 scheme [73]	Shifted Euler (5.8)	Euler-Maruyama
1.79	2.00	23.1	47.0

Taking the computational times into account, we see that the Shifted Ralston method gives very little improvement compared to the SRA1 scheme in this example. However, the Shifted Euler method clearly outperforms the Euler-Maruyama scheme.

As both the Shifted Ralston (5.6) and SRA1 [73] methods require two evaluations of the drift vector field per step, we expect them to have a similar computational cost in settings where drift evaluations are expensive (such as Langevin Monte Carlo [55]). However, if the noise is scalar, then the scheme based on the non-linear splitting path (4.8) has the potential to be almost three times more accurate, for sufficiently small h . We would like to highlight this ratio for small h as it can be explained theoretically. The shifted Ralston method uses the optimal approximation (B.1), which has an error:

$$\begin{aligned} & \mathbb{E} \left[\left(\frac{1}{2} \int_{t_k}^{t_{k+1}} W_{t_k, r}^2 dr - \mathbb{E} \left[\frac{1}{2} \int_{t_k}^{t_{k+1}} W_{t_k, r}^2 dr \mid W_k, H_k, n_k \right] \right)^2 \right]^{\frac{1}{2}} \\ &= \mathbb{E} \left[\frac{11}{25200} h^4 + \left(\frac{1}{720} - \frac{1}{384\pi} \right) h^3 W_k^2 + \frac{1}{700} h^3 H_k^2 - \frac{1}{320\sqrt{6\pi}} n_k h^{\frac{7}{2}} W_k \right]^{\frac{1}{2}} \\ &= \left(\frac{7}{3600} - \frac{1}{384\pi} \right)^{\frac{1}{2}} h^2, \end{aligned}$$

where the second line follows from the conditional variance (B.2). On the other hand, the Taylor expansion of the SRA1 scheme contains $\frac{3}{16}(W_k + 2H_k)^2$, and has the error:

$$\begin{aligned} & \mathbb{E} \left[\left(\frac{1}{2} \int_{t_k}^{t_{k+1}} W_{t_k, r}^2 dr - \frac{3}{16} (W_k + 2H_k)^2 \right)^2 \right]^{\frac{1}{2}} \\ &= \mathbb{E} \left[\left(\frac{1}{48} h W_k^2 + \frac{1}{4} h W_k H_k + \frac{3}{4} h H_k^2 - L_k \right)^2 \right]^{\frac{1}{2}} \\ &= \left(\mathbb{E} \left[\left(\frac{1}{48} h W_k^2 + \dots \right)^2 \right] - 2 \mathbb{E} \left[L_k \left(\frac{1}{48} h W_k^2 + \frac{1}{4} h W_k H_k + \frac{3}{4} h H_k^2 \right) \right] + \mathbb{E} [L_k^2] \right)^{\frac{1}{2}} \\ &= \left(\frac{1}{48} h^4 - 2 \mathbb{E} \left[\left(\frac{1}{30} h^2 + \frac{3}{5} h H_k^2 \right) \left(\frac{1}{48} h W_k^2 + \frac{1}{4} h W_k H_k + \frac{3}{4} h H_k^2 \right) \right] + \frac{1}{72} h^4 \right)^{\frac{1}{2}} \\ &= \left(\frac{1}{120} \right)^{\frac{1}{2}} h^2, \end{aligned}$$

where we used Theorems 3.9 and 3.10 from [29] to compute the above expectations.

Hence we can compute the ratio of these $L^2(\mathbb{P})$ errors as $\left(\frac{7}{30} - \frac{5}{16\pi} \right)^{\frac{1}{2}} = 0.37$ (2.d.p). Unsurprisingly, this is close to the error ratio of 0.38 that was seen in the experiment.

More generally, when the Brownian motion is multidimensional, the non-linear splitting approach is not able to accurately approximate the ‘‘cross’’ iterated integrals

$$(5.10) \quad \int_{\substack{r_3 < r_2 < r_1, \\ r_i \in [t_k, t_{k+1}]}} dW_{r_3}^i \circ dW_{r_2}^j dr_1 + \int_{\substack{r_3 < r_2 < r_1, \\ r_i \in [t_k, t_{k+1}]}} dW_{r_3}^j \circ dW_{r_2}^i dr_1 = \int_{t_k}^{t_{k+1}} W_{t_k, r}^i W_{t_k, r}^j dr,$$

where $i \neq j$. On the other hand, we can see that the linear splitting path (4.7) satisfies

$$\mathbb{E} \left[\int_{t_k}^{t_{k+1}} \gamma_{t_k,r}^i \gamma_{t_k,r}^j dr \middle| W_k \right] = \mathbb{E} \left[\int_{t_k}^{t_{k+1}} W_{t_k,r}^i W_{t_k,r}^j dr \middle| W_k \right] = \frac{1}{3} h W_k^i W_k^j + \frac{1}{6} h^2 \delta_{ij},$$

where the expectation is computable via standard properties of the Brownian bridge. Numerical schemes for commutative SDEs matching the above conditional expectation are known as ‘‘asymptotically efficient’’ (see [12, 15, 67] for examples of such methods).

An attractive feature of both the shifted Euler and Ralston approaches is that they are efficient in terms of drift evaluations per step, requiring one and two respectively. This is particularly appealing in applications where drift evaluations are expensive (such as in machine learning [46, 55]). We leave further investigations and the analysis of ‘‘Shifted’’ Runge-Kutta methods for additive noise SDEs as a topic of future work.

5.3. FitzHugh-Nagumo model. We consider a stochastic FitzHugh-Nagumo (FHN) model which has been used for describing the spike activity of neurons [8, 53]. The stochastic FHN model follows the two-dimensional additive noise SDE given by

$$(5.11) \quad d \begin{pmatrix} v_t \\ u_t \end{pmatrix} = \begin{pmatrix} \frac{1}{\epsilon} (v_t - v_t^3 - u_t) \\ \gamma v_t - u_t + \beta \end{pmatrix} dt + \begin{pmatrix} \sigma_1 & 0 \\ 0 & \sigma_2 \end{pmatrix} dW_t.$$

To discretise the stochastic FHN model, we apply the piecewise linear path (4.4) and, similar to [8], apply a Strang splitting to approximate the resulting drift ODE. Since $v' = \frac{1}{\epsilon}(v - v^3)$ admits a closed-form solution, this leads to the splitting method:

$$(5.12) \quad \begin{aligned} \begin{pmatrix} V_k^{(1)} \\ U_k^{(1)} \end{pmatrix} &:= \begin{pmatrix} V_k \\ U_k \end{pmatrix} + \begin{pmatrix} \sigma_1 & 0 \\ 0 & \sigma_2 \end{pmatrix} \begin{pmatrix} \frac{1}{2} W_k^1 + H_k^1 - \frac{1}{2} C_k^1 \\ \frac{1}{2} W_k^2 + H_k^2 - \frac{1}{2} C_k^2 \end{pmatrix}, \\ \begin{pmatrix} V_k^{(2)} \\ U_k^{(2)} \end{pmatrix} &:= \varphi_{\frac{1}{2}h}^{\text{Strang}} \begin{pmatrix} V_k^{(1)} \\ U_k^{(1)} \end{pmatrix} + \begin{pmatrix} \sigma_1 & 0 \\ 0 & \sigma_2 \end{pmatrix} \begin{pmatrix} C_k^1 \\ C_k^2 \end{pmatrix}, \\ \begin{pmatrix} V_{k+1} \\ U_{k+1} \end{pmatrix} &:= \varphi_{\frac{1}{2}h}^{\text{Strang}} \begin{pmatrix} V_k^{(2)} \\ U_k^{(2)} \end{pmatrix} + \begin{pmatrix} \sigma_1 & 0 \\ 0 & \sigma_2 \end{pmatrix} \begin{pmatrix} \frac{1}{2} W_k^1 - H_k^1 - \frac{1}{2} C_k^1 \\ \frac{1}{2} W_k^2 - H_k^2 - \frac{1}{2} C_k^2 \end{pmatrix}, \end{aligned}$$

where, for $u, v \in \mathbb{R}$, we define $\varphi_{\frac{1}{2}h}^{\text{Strang}} \begin{pmatrix} v \\ u \end{pmatrix}$ as

$$\varphi_{\frac{1}{2}h}^{\text{Strang}} \begin{pmatrix} v \\ u \end{pmatrix} := \begin{pmatrix} \tilde{v} \left(e^{-\frac{h}{2\epsilon}} + \tilde{v}^2 (1 - e^{-\frac{h}{2\epsilon}}) \right)^{-\frac{1}{2}} \\ \tilde{u} + \frac{1}{4} \beta h \end{pmatrix},$$

with \tilde{v} and \tilde{u} defined by

$$\begin{pmatrix} \tilde{v} \\ \tilde{u} \end{pmatrix} := \exp \left(\frac{1}{2} h \begin{pmatrix} 0 & -\frac{1}{\epsilon} \\ \gamma & -1 \end{pmatrix} \right) \begin{pmatrix} v \left(e^{-\frac{h}{2\epsilon}} + v^2 (1 - e^{-\frac{h}{2\epsilon}}) \right)^{-\frac{1}{2}} \\ u + \frac{1}{4} \beta h \end{pmatrix},$$

and the explicit formula for the above matrix exponential is given in [8, Section 6.2]. The random variables C_k^1 and C_k^2 are given by (4.5) and are generated independently.

We note that, similar to the CIR model, the stochastic FHN model is challenging to accurately simulate due to the vector field not being globally Lipschitz continuous. That said, as the drift does have polynomial growth and satisfies a one-sided Lipschitz condition, there are numerical methods for (5.11) with strong convergence guarantees. We will compare our scheme (5.12) against two such methods; the Strang splitting scheme proposed in [8] and the Tamed Euler-Maruyama method introduced in [40].

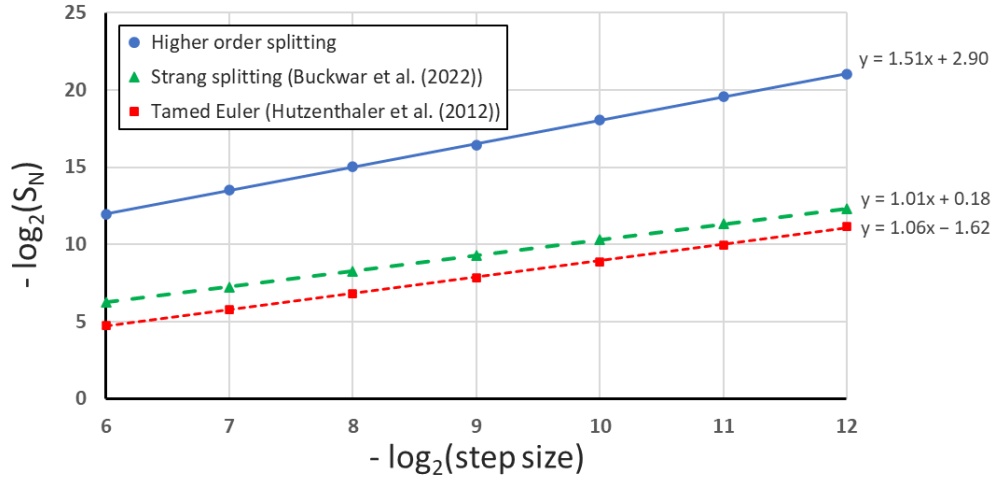


FIG. 6. S_N estimated for (5.11) using 1,000 sample paths as a function of step size $h = \frac{T}{N}$. The estimated strong errors for the Strang splitting and Tamed Euler schemes were taken from [8].

In this numerical experiment, we used the following parameters in the FHN model.

$$\epsilon = 1, \quad \gamma = 1, \quad \beta = 1, \quad \sigma_1 = 1, \quad \sigma_2 = 1, \quad (v_0, u_0) = (0, 0), \quad T = 5.$$

We see in Figure 6 that the proposed high order splitting exhibits an $3/2$ strong convergence rate and is significantly more accurate than other schemes (for fixed h). For example, our splitting approach achieves better accuracy in 320 steps than Strang splitting does in 10240 steps. As before, we present simulation times for each method.

TABLE 5
Computer time to simulate 1,000 sample paths of (5.11) in Python with 100 steps (seconds)

High order splitting (5.12)	Strang Splitting [8]	Tamed Euler-Maruyama [40]
8.15	2.66	1.71

TABLE 6
Estimated time to produce 1,000 sample paths of (5.11) with an error of $S_N = 10^{-3}$ (seconds)

High order splitting (5.12)	Strang Splitting [8]	Tamed Euler-Maruyama [40]
10.4	110	166

From Tables 5 and 6, we conclude that the proposed high order splitting method, which was derived using the path (4.4), gives the best performance for the FHN model.

5.4. Underdamped Langevin dynamics. Traditionally used as a molecular dynamics model [51, 52, 61], the underdamped Langevin diffusion (ULD) is given by

$$(5.13) \quad \begin{aligned} dx_t &= v_t dt, \\ dv_t &= -\gamma v_t dt - \nabla f(x_t) dt + \sqrt{2\gamma} dW_t, \end{aligned}$$

where $x, v \in \mathbb{R}^d$ are the position and momentum of a particle, $f : \mathbb{R}^d \rightarrow \mathbb{R}$ is a scalar potential, $\gamma > 0$ is a friction coefficient and W is a d -dimensional Brownian motion. Under mild conditions of f , the SDE (5.13) is known to admit a strong solution that is ergodic with stationary distribution $\pi(x, v) \propto e^{-f(x)} e^{-\frac{1}{2}\|v\|^2}$ [71, Proposition 6.1]. As a consequence, there has been recent interest in the application of (5.13) as an MCMC method for high-dimensional sampling [9, 10, 13, 14, 19, 30, 39, 63, 74, 75, 78].

In this section, we briefly summarise the results of [30], where the path (4.10) and a third order Runge-Kutta method are used to derive the following numerical scheme:

$$\begin{aligned} V_n^{(1)} &:= V_n + \sqrt{2\gamma} (H_n + 6K_n), \\ X_n^{(1)} &:= X_n + \left(\frac{1 - e^{-\frac{1}{2}\gamma h}}{\gamma} \right) V_n^{(1)} - \left(\frac{e^{-\frac{1}{2}\gamma h} + \frac{1}{2}\gamma h - 1}{\gamma^2} \right) \nabla f(X_n) \\ &\quad + \left(\frac{e^{-\frac{1}{2}\gamma h} + \frac{1}{2}\gamma h - 1}{\gamma^2 h} \right) \sqrt{2\gamma} (W_n - 12H_n), \\ X_{n+1} &:= X_n + \left(\frac{1 - e^{-\gamma h}}{\gamma} \right) V_n^{(1)} - \left(\frac{e^{-\gamma h} + \gamma h - 1}{\gamma^2} \right) \left(\frac{1}{3} \nabla f(X_n) + \frac{2}{3} \nabla f(X_n^{(1)}) \right) \\ &\quad + \left(\frac{e^{-\gamma h} + \gamma h - 1}{\gamma^2 h} \right) \sqrt{2\gamma} (W_n - 12H_n), \\ V_n^{(2)} &:= e^{-\gamma h} V_n^{(1)} - \frac{1}{6} e^{-\gamma h} \nabla f(X_n) h - \frac{2}{3} e^{-\frac{1}{2}\gamma h} \nabla f(X_n^{(1)}) h - \frac{1}{6} \nabla f(X_{n+1}) h \\ &\quad + \left(\frac{1 - e^{-\gamma h}}{\gamma} h \right) \sqrt{2\gamma} (W_n - 12H_n), \\ V_{n+1} &:= V_n^{(2)} - \sqrt{2\gamma} (H_n - 6K_n), \end{aligned}$$

which we refer to as the **SORT**¹ method. It is also worth noting that, since the final gradient evaluation $\nabla f(X_{n+1})$ can be used in the next step to compute (X_{n+2}, V_{n+2}) , the SORT method uses just two additional evaluations of the gradient ∇f per step. This is an example of the ‘‘First Same As Last’’ (FSAL) property in numerical analysis. Moreover, as evaluating ∇f is usually much more computationally expensive than generating d -dimensional Gaussian random variables in practice, it follows that the SORT method is about twice as expensive per step as the Euler-Maruyama method.

It was shown in [30] that under smoothness and convexity assumptions on f , the Shifted ODE approximation based on (4.10) can achieve third order convergence. However, this error analysis relies on properties of the ODE, and thus obtaining such convergence guarantees for the SORT method itself remains a topic of future research.

In the numerical experiment, we consider an application of ULD in data science, namely the simulation of ULD as an MCMC algorithm for Bayesian logistic regression. We use German credit data in [56], where each of the $m = 1000$ individuals has $d = 49$

¹Shifted ODE with Runge-Kutta Three

features $x_i \in \mathbb{R}^d$ and a label $y_i \in \{-1, 1\}$ indicating if they are creditworthy or not. The Bayesian logistic regression model states that $\mathbb{P}(Y_i = y_i | x_i) = (1 + e^{-y_i x_i^\top \theta})^{-1}$ where $\theta \in \mathbb{R}^d$ are parameters coming from the target density $\pi(\theta) \propto \exp(-f(\theta))$ with

$$f(\theta) = \delta \|\theta\|^2 + \sum_{i=1}^m \log(1 + \exp(-y_i x_i^\top \theta)).$$

In the experiment, the regularisation parameter is set to $\delta = 0.05$, the ULD friction coefficient is set to $\gamma = 2$ and the initial value θ_0 is sampled from a Gaussian prior as

$$\theta_0 \sim \mathcal{N}(0, 10I_d).$$

In addition, we use a fixed time horizon of $T = 1000$. The results are presented below:

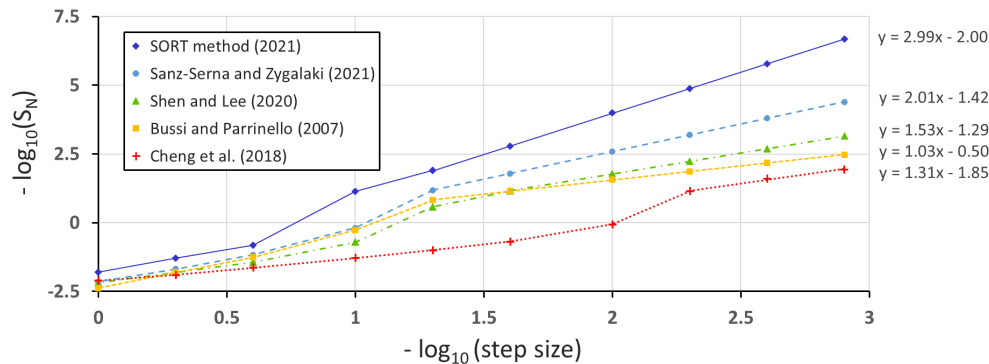


FIG. 7. S_N estimated for (5.13) with 1,000 sample paths as a function of step size $h = \frac{T}{N}$.

From the above graph, we see that the SORT method [30] and UBU splitting [74] (plotted as blue circles) are the best performing strong numerical schemes for ULD. We note that both the UBU [74] and Strang [9] splittings require a single additional gradient evaluation per step and achieve essentially the same accuracy in this example. Despite the SORT method having twice the computational cost as UBU/Strang per step, we see that it is the best performing method to achieve an accuracy of $S_N \leq 0.05$. Moreover, we believe that the SORT method is the first approximation of ULD to exhibit third order convergence whilst only requiring evaluations of the gradient ∇f .

6. Conclusion. In this paper, we have presented a new simple methodology for designing and analysing splitting methods for stochastic differential equations (SDEs). The key idea is to replace the system’s Brownian motion with a piecewise linear path, which results in a path-based splitting method that is straightforward to analyse using its “controlled” Taylor expansion (a well-known technique within rough path theory). Moreover, for SDEs that satisfy a commutativity condition, this led to several high order splitting methods which displayed state-of-the-art convergence in experiments. As part of this investigation, we also detailed how recently developed estimators for iterated integrals of Brownian motion can be directly incorporated into such methods. Since these estimators were simply obtained as the expectation of iterated integrals conditional on the generatable random variables, they are optimal in an $L^2(\mathbb{P})$ sense. The technical details underlying the integral estimators are presented in Appendix B.

Furthermore, the results in this paper may lead to several areas of future research:

- **Development and analysis of methods inspired by splitting paths**

For example, in the additive noise setting, the following Strong 1.5 Stochastic Runge-Kutta method is based on the splitting path (4.10), but with $K_{s,t} = 0$.

$$(6.1) \quad \begin{aligned} \tilde{Y}_k^{\text{SRK}} &:= Y_k^{\text{SRK}} + \sigma H_k, \\ \tilde{Y}_{k+\frac{5}{6}}^{\text{SRK}} &:= \tilde{Y}_k^{\text{SRK}} + \frac{5}{6} \left(f(\tilde{Y}_k^{\text{SRK}})h + \sigma W_k \right), \\ Y_{k+1}^{\text{SRK}} &:= Y_k^{\text{SRK}} + \frac{2}{5} f(\tilde{Y}_k^{\text{SRK}})h + \frac{3}{5} f(\tilde{Y}_{k+\frac{5}{6}}^{\text{SRK}})h + \sigma W_k. \end{aligned}$$

As (6.1) does not follow a high order splitting path or use Ralston's method, it was not included in Section 5.2 and thus we leave its analysis as future work. Similarly, conducting error analyses and further numerical investigations for the Shifted Euler and Runge-Kutta methods from Section 5 is a future topic.

- **Development of high order splitting methods for general SDEs**

For example, the below method is a combination of the Strang splitting (4.2) and the log-ODE method from rough path theory [65, Appendices A and B].

$$Y_{k+1} := \exp\left(\frac{1}{2}f(\cdot)h\right) \exp\left(g(\cdot)W_k + \sum_{i < j} [g_i, g_j](\cdot)A_k^{ij}\right) \exp\left(\frac{1}{2}f(\cdot)h\right)Y_k,$$

where $[g_i, g_j](\cdot) = g_j'(\cdot)g_i(\cdot) - g_i'(\cdot)g_j(\cdot)$ is the standard vector field Lie bracket and $A_k = \{A_k^{ij}\}_{1 \leq i, j \leq d}$ is the Lévy area of the Brownian motion over $[t_k, t_{k+1}]$.

If A_k is replaced by a random matrix \tilde{A}_k , with the same mean and covariance, we expect the resulting splitting method to achieve $O(h^2)$ weak convergence. Moreover, higher order convergence was observed in [42] where this splitting method was employed to test a deep-learning-based model for generating A_k .

Similarly, we expect that the Ninomiya-Ninomiya [68] and Ninomiya-Victoir [69] weak second order schemes can be reinterpreted as path-based splittings. Furthermore, combining the Strang and Ninomiya-Ninomiya splittings yields

$$Y_{k+1} := \exp\left(\frac{1}{2}f(\cdot)h\right) \exp\left(g(\cdot)\left(\frac{1}{2}W_k - \sqrt{2}B_k\right)\right) \exp\left(g(\cdot)\left(\frac{1}{2}W_k + \sqrt{2}B_k\right)\right) \exp\left(\frac{1}{2}f(\cdot)h\right)Y_k,$$

where $B_k = W_{t_k, t_k + \frac{1}{2}h} - \frac{1}{2}W_k \sim \mathcal{N}(0, \frac{h}{4}I_d)$ is the Brownian bridge's midpoint. Just like the Ninomiya-Ninomiya scheme, we expect this splitting method has second order weak convergence, but with the advantage that the drift ODEs can be “merged” between steps and solved using a second order ODE solver.

- **Extension of path-based framework to piecewise log-ODE methods**

When (1.2) holds, we could instead consider the “Strang-log-ODE” splitting,

$$Y_{k+1} := \exp\left(\frac{1}{2}f(\cdot)h\right) \exp\left(g(\cdot)W_k + [g, f](\cdot)hH_k\right) \exp\left(\frac{1}{2}f(\cdot)h\right)Y_k,$$

where $[g, f](\cdot)hH_k := \sum_{i=1}^d [g_i, f](\cdot)hH_k^i$ is the Lie bracket applied to hH_k . However, whilst we expect this method to achieve $O(h^{\frac{3}{2}})$ strong convergence, our path-based splitting framework is not applicable due to the Lie bracket. In particular, extending our theory to piecewise log-ODE methods would be helpful for SDEs where vector field derivatives can be computed or estimated.

- **Incorporating (W_k, H_k, n_k) -methods into Multilevel Monte Carlo**

Multilevel Monte Carlo (MLMC), introduced by Giles in [35], is a popular control variate strategy for achieving variance reduction in SDE simulation. Whilst the MLMC literature is extensive, we refer the reader to [1, 21, 34, 36] for details on some of the improvements to MLMC that have been proposed. The variance reduction obtained by MLMC is a consequence of the strong convergence properties of the SDE solver as sample paths are computed for each level using two step sizes (h and $\frac{1}{2}h$), but with the same Brownian paths. However, the majority of MLMC methods for SDE simulation use only the increments of the Brownian motion. Thus, we conjecture that further variance reduction can be achieved using high order (W_k, H_k, n_k) -based SDE solvers. This hypothesis is supported by the experiments detailed in [80, Section 6.3] (for a commutative SDE) and [42, Section 6] (for a non-commutative SDE). That said, in the extensive MLMC literature, the application of high order numerical methods for SDEs has seen relatively little attention [1, 21, 42, 80].

- **Incorporating adaptive step sizes into (W_k, H_k, n_k) -based methods**

Since it is possible to generate both $(W_{s,u}, H_{s,u}, n_{s,u})$ and $(W_{u,t}, H_{u,t}, n_{u,t})$ conditional on $(W_{s,t}, H_{s,t}, n_{s,t})$, where $u = s + \frac{1}{2}h$ is the midpoint of $[s, t]$, the proposed splitting methods can be applied using an adaptive step size. Such a methodology was detailed and initial investigated in [26, Chapter 6].

- **Application to high-dimensional SDEs in physics and data science**

High-dimensional SDEs have seen a variety of real-world applications, ranging from molecular dynamics [51, 61] to machine learning [45, 46, 54, 77, 82, 85]. Therefore, it would be interesting to investigate whether the splitting methods developed in this paper could improve algorithms used in these applications.

REFERENCES

- [1] A. AL GERBI, B. JOURDAIN, AND E. CLÉMENT, *Ninomiya–Victoir scheme: Strong convergence, antithetic version and application to multilevel estimators*, Monte Carlo Methods and Applications, 22 (2016), pp. 197–228.
- [2] A. ALFONSI, *On the discretization schemes for the CIR (and Bessel squared) processes*, Monte Carlo Methods and Applications, 11 (2005), pp. 355–384.
- [3] A. ALFONSI, *High order discretization schemes for the CIR process: Application to Affine Term Structure and Heston models*, Mathematics of Computation, 79 (2010), pp. 209–237.
- [4] A. ALFONSI, *Strong order one convergence of a drift implicit Euler scheme: Application to the CIR process*, Statistics & Probability Letters, 83 (2013), pp. 602–607.
- [5] C. BAYER, *The geometry of iterated stratonovich integrals*, preprint, (2006), https://www.wias-berlin.de/people/bayerc/files/strat_geom.pdf.
- [6] S. BISWAS, C. KUMAR, NEELIMA, G. D. REIS, AND C. REISINGER, *An explicit Milstein-type scheme for interacting particle systems and McKean–Vlasov SDEs with common noise and non-differentiable drift coefficients*, to appear in the Annals of Applied Probability (preprint available at <https://arxiv.org/2208.10052>), (2023).
- [7] D. BRIGO AND F. MERCURIO, *Interest Rate Models – Theory and Practice, second edition*, Springer, 2006.
- [8] E. BUCKWAR, A. SAMSON, M. TAMBORRINO, AND I. TUBIKANEC, *A splitting method for SDEs with locally Lipschitz drift: Illustration on the FitzHugh–Nagumo model*, Applied Numerical Mathematics, 179 (2022), pp. 191–220.
- [9] E. BUCKWAR, M. TAMBORRINO, AND I. TUBIKANEC, *Spectral density-based and measure-preserving ABC for partially observed diffusion processes. An illustration on Hamiltonian SDEs*, Statistics and Computing, 30 (2020), pp. 627–648.
- [10] G. BUSSI AND M. PARRINELLO, *Accurate sampling using Langevin dynamics*, Physical Review E, 75 (2007).

- [11] T. CASS AND P. FRIZ, *Densities for rough differential equations under Hörmander’s condition*, *Annals of mathematics*, (2010), pp. 2115–2141.
- [12] F. CASTELL AND J. GAINES, *The ordinary differential equation approach to asymptotically efficient schemes for solution of stochastic differential equations*, *Annales de l’Institut Henri Poincaré, Probabilités et Statistiques*, 32 (1996), pp. 231–250.
- [13] M. CHAK, N. KANTAS, T. LELIÈVRE, AND G. A. PAVLIOTIS, *Optimal friction matrix for underdamped Langevin sampling*, to appear in *ESAIM: Mathematical Modelling and Numerical Analysis* (preprint available at <https://arxiv.org/abs/2112.06844>), (2023).
- [14] X. CHENG, N. S. CHATTERJI, P. L. BARTLETT, AND M. I. JORDAN, *Underdamped Langevin MCMC: A non-asymptotic analysis*, *Proceedings of the 31st Conference On Learning Theory*, Volume 75 of *Proceedings of Machine Learning Research*, (2018).
- [15] J. M. C. CLARK, *An efficient approximation scheme for a class of stochastic differential equations*, in *Advances in Filtering and Optimal Stochastic Control*, Springer, 1982.
- [16] J. M. C. CLARK AND R. J. CAMERON, *The maximum rate of convergence of discrete approximations for stochastic differential equations*, in *Stochastic Differential Systems Filtering and Control*, ed. by Grigelionis (Springer, Berlin), 1980.
- [17] J. C. COX, J. E. INGERSOLL, AND S. A. ROSS, *A Theory of the Term Structure of Interest Rates*, *Econometrica*, 53 (1985), pp. 385–407.
- [18] A. COZMA AND C. REISINGER, *Strong order 1/2 convergence of full truncation Euler approximations to the Cox–Ingersoll–Ross process*, *IMA Journal of Numerical Analysis*, 40 (2020), pp. 358–376.
- [19] A. S. DALALYAN AND L. RIOU-DURAND, *On sampling from a log-concave density using kinetic Langevin diffusions*, *Bernoulli*, 26 (2020), pp. 1956–1988.
- [20] A. DAVIE, *KMT theory applied to approximations of SDE*, in *Stochastic Analysis and Applications*, vol. 100 of *Springer Proceedings in Mathematics and Statistics*, Springer, 2014, pp. 185–201.
- [21] K. DEBRABANT AND A. RÖSSLER, *On the Acceleration of the Multi-Level Monte Carlo Method*, *Journal of Applied Probability*, 52 (2018), pp. 307–322.
- [22] S. DEREICH, A. NEUENKIRCH, AND L. SZPRUCH, *An Euler-type method for the strong approximation of the Cox–Ingersoll–Ross process*, *Proceedings of the Royal Society A: Mathematical, Physical and Engineering Sciences*, 468 (2011), pp. 1105–1115.
- [23] A. S. DICKINSON, *Optimal Approximation of the Second Iterated Integral of Brownian Motion*, *Stochastic Analysis and Applications*, 25 (2007), pp. 1109–1128.
- [24] R. C. ELANDT, *The Folded Normal Distribution: Two Methods of Estimating Parameters from Moments*, *Technometrics*, 3 (1961), pp. 551–562.
- [25] W. FANG AND M. B. GILES, *Adaptive Euler–Maruyama method for SDEs with nonglobally Lipschitz drift*, *Annals of Applied Probability*, 30 (2020), pp. 526–560.
- [26] J. FOSTER, *Numerical approximations for stochastic differential equations*, PhD thesis, University of Oxford, 2020, <https://ora.ox.ac.uk/objects/uuid:775fc3f5-501c-425f-8b43-fc5a7b2e4310>.
- [27] J. FOSTER AND K. HABERMANN, *Brownian bridge expansions for Lévy area approximations and particular values of the Riemann zeta function*, *Combinatorics, Probability and Computing*, (2022).
- [28] J. FOSTER, T. LYONS, AND V. MARGARINT, *An asymptotic radius of convergence for the Loewner equation and simulation of SLE traces via splitting*, *Journal of Statistical Physics*, 189 (2022).
- [29] J. FOSTER, T. LYONS, AND H. OBERHAUSER, *An Optimal Polynomial Approximation of Brownian Motion*, *SIAM Journal on Numerical Analysis*, 58 (2020), pp. 1393–1421.
- [30] J. FOSTER, T. LYONS, AND H. OBERHAUSER, *The shifted ODE method for underdamped Langevin MCMC*, <https://arxiv.org/abs/2101.03446>, (2021).
- [31] P. K. FRIZ AND M. HAIRER, *A Course on Rough Paths: With an Introduction to Regularity Structures*, Springer, 2020.
- [32] P. K. FRIZ AND N. B. VICTOIR, *Multidimensional Stochastic Processes as Rough Paths: Theory and Applications*, vol. 120, Cambridge University Press, 2010.
- [33] J. G. GAINES AND T. LYONS, *Random Generation of Stochastic Area Integrals*, *SIAM Journal on Applied Mathematics*, 54 (1994), pp. 1132–1146.
- [34] M. B. GILES, *Improved multilevel Monte Carlo convergence using the Milstein scheme*, in *Monte Carlo and Quasi-Monte Carlo Methods*, ed. by Keller, Heinrich and Niederreiter (Springer, Berlin), 2008.
- [35] M. B. GILES, *Multilevel Monte Carlo path simulation*, *Operations Research*, 56 (2008), pp. 607–617.
- [36] M. B. GILES AND L. SZPRUCH, *Antithetic multilevel Monte Carlo estimation for multi-*

- dimensional SDEs without Lévy area simulation*, *Annals of Applied Probability*, 24 (2014), pp. 1585–1620.
- [37] M. HEFTER AND A. JENTZEN, *On arbitrarily slow convergence rates for strong numerical approximations of Cox–Ingersoll–Ross processes and squared Bessel processes*, *Finance and Stochastics*, 23 (2019), pp. 139–172.
- [38] S. L. HESTON, *A Closed-Form Solution for Options with Stochastic Volatility with Applications to Bond and Currency Options*, *The Review of Financial Studies*, 6 (1993), pp. 327–343.
- [39] Z. HU, F. HUANG, AND H. HUANG, *Optimal Underdamped Langevin MCMC Method*, *Advances in Neural Information Processing Systems*, (2021).
- [40] M. HUTZENTHALER, A. JENTZEN, AND P. E. KLOEDEN, *Strong convergence of an explicit numerical method for SDEs with nonglobally Lipschitz continuous coefficients*, *Annals of Applied Probability*, 22 (2012), pp. 1611–1641.
- [41] Y. IGUCHI AND T. YAMADA, *Operator splitting around Euler–Maruyama scheme and high order discretization of heat kernels*, *ESAIM: Mathematical Modelling and Numerical Analysis*, 55 (2021), pp. 323–367.
- [42] A. JELINČIČ, J. TAO, W. F. TURNER, T. CASS, J. FOSTER, AND H. NI, *Generative Modelling of Lévy Area for High Order SDE Simulation*, <https://arxiv.org/abs/2308.02452>, (2023).
- [43] C. KELLY, G. LORD, AND H. MAULANA, *The role of adaptivity in a numerical method for the Cox–Ingersoll–Ross model*, *Journal of Computational and Applied Mathematics*, 410 (2022).
- [44] P. KIDGER, *On Neural Differential Equations*, PhD thesis, University of Oxford, 2021, <https://ora.ox.ac.uk/objects/uuid:af32d844-df84-4fdc-824d-44bebc3d7aa9>.
- [45] P. KIDGER, J. FOSTER, X. LI, AND T. LYONS, *Efficient and Accurate Gradients for Neural SDEs*, *Advances in Neural Information Processing Systems*, (2021).
- [46] P. KIDGER, J. FOSTER, X. LI, H. OBERHAUSER, AND T. LYONS, *Neural SDEs as Infinite-Dimensional GANs*, *Proceedings of 38th International Conference on Machine Learning*, (2021).
- [47] P. KIDGER, J. MORRILL, J. FOSTER, AND T. LYONS, *Neural Controlled Differential Equations for Irregular Time Series*, *Advances in Neural Information Processing Systems*, (2020).
- [48] P. E. KLOEDEN AND E. PLATEN, *Numerical Solution of Stochastic Differential Equations*, Springer, Berlin, 1992.
- [49] R. KRUSE AND Y. WU, *A randomized and fully discrete Galerkin finite element method for semilinear stochastic evolution equations*, *Mathematics of Computation*, 88 (2019), pp. 2793–2825.
- [50] R. KRUSE AND Y. WU, *A randomized Milstein method for stochastic differential equations with non-differentiable drift coefficients*, *Discrete and Continuous Dynamical Systems. Series B. A Journal Bridging Mathematics and Sciences*, 24 (2019), pp. 3475–3502.
- [51] B. LEIMKUEHLER AND C. MATTHEWS, *Molecular Dynamics: With Deterministic and Stochastic Numerical Methods*, *Interdisciplinary Applied Mathematics*, Springer, 2015.
- [52] T. LELIÈVRE AND G. STOLTZ, *Partial differential equations and stochastic methods in molecular dynamics*, *Acta Numerica*, 25 (2016), pp. 681–880.
- [53] J. R. LEÓN AND A. SAMSON, *Hypoelliptic stochastic FitzHugh–Nagumo neuronal model: mixing, up-crossing and estimation of the spike rate*, *Annals of Applied Probability*, 28 (2018), pp. 2243–2274.
- [54] R. LI, H. ZHA, AND M. TAO, *Sqrt(d) dimension dependence of Langevin Monte Carlo*, *Proceedings of the 10th International Conference on Learning Representations*, (2022).
- [55] X. LI, D. WU, L. MACKEY, AND M. A. ERDOGDU, *Stochastic Runge–Kutta Accelerates Langevin Monte Carlo and Beyond*, *Advances in Neural Information Processing Systems*, (2019).
- [56] M. LICHMAN, *UCI machine learning repository*, <https://archive.ics.uci.edu/ml>, 2013.
- [57] T. LYONS, M. CARUANA, AND T. LÉVY, *Differential Equations Driven by Rough Paths*, vol. 1908 of *Lecture Notes in Mathematics.*, Springer, 2007.
- [58] T. LYONS AND N. VICTOIR, *Cubature on Wiener space*, *Proceedings of the Royal Society A: Mathematical, Physical and Engineering Sciences*, 460 (2004), pp. 169–198.
- [59] X. MAO, *Stochastic Differential Equations and Applications, second edition*, Elsevier, 2008.
- [60] G. N. MILSTEIN AND J. SCHOENMAKERS, *Uniform approximation of the Cox–Ingersoll–Ross process*, *Advances in Applied Probability*, 47 (2015), pp. 1132–1156.
- [61] G. N. MILSTEIN AND M. V. TRETYAKOV, *Stochastic Numerics for Mathematical Physics, second edition*, Springer, 2021.
- [62] T. MISAWA, *Numerical integration of stochastic differential equations by composition methods*, in *Dynamical systems and differential geometry (Japanese)*, no. 1180, 2000, pp. 166–190.
- [63] P. MONMARCHÉ, *High-dimensional MCMC with a standard splitting scheme for the underdamped Langevin diffusion*, *Electronic Journal of Statistics*, 15 (2021), pp. 4117–4166.

- [64] J. MORRILL, P. KIDGER, L. YANG, AND T. LYONS, *On the Choice of Interpolation Scheme for Neural CDEs*, Transactions on Machine Learning Research, (2022).
- [65] J. MORRILL, C. SALVI, P. KIDGER, J. FOSTER, AND T. LYONS, *Neural Rough Differential Equations for Long Time Series*, Proceedings of the 38th International Conference on Machine Learning, (2021).
- [66] J. MRONGOWIUS AND A. RÖSSLER, *On the approximation and simulation of iterated stochastic integrals and the corresponding Lévy areas in terms of a multidimensional Brownian motion*, Stochastic Analysis and Applications, 40 (2022), pp. 397–425.
- [67] N. J. NEWTON, *Asymptotically Efficient Runge-Kutta Methods for a Class of Itô and Stratonovich Equations*, SIAM Journal on Applied Mathematics, 51 (1991), pp. 303–604.
- [68] M. NINOMIYA AND S. NINOMIYA, *A new higher-order weak approximation scheme for stochastic differential equations and the Runge–Kutta method*, Finance and Stochastics, 13 (2009), pp. 415–443.
- [69] S. NINOMIYA AND N. VICTOIR, *Weak Approximation of Stochastic Differential Equations and Application to Derivative Pricing*, Applied Mathematical Finance, 15 (2008), pp. 107–121.
- [70] S. PATHIRAJA, *L2 convergence of smooth approximations of stochastic differential equations with unbounded coefficients*, Stochastic Analysis and Applications, (2023).
- [71] G. A. PAVLIOTIS, *Stochastic Processes and Applications*, Springer, New York, 2014.
- [72] A. RALSTON, *Runge-Kutta methods with minimum error bounds*, Mathematics of Computation, (1962), pp. 431–437.
- [73] A. RÖSSLER, *Runge–Kutta methods for the strong approximation of solutions of stochastic differential equations*, SIAM Journal on Numerical Analysis, 8 (2010), pp. 922–952.
- [74] J. M. SANZ-SERNA AND K. C. ZYGALAKIS, *Wasserstein distance estimates for the distributions of numerical approximations to ergodic stochastic differential equations*, Journal of Machine Learning Research, 22 (2021).
- [75] R. SHEN AND Y. T. LEE, *The Randomized Midpoint Method for Log-Concave Sampling*, Advances in Neural Information Processing Systems, (2019).
- [76] A. SHMATKOV, *Rate of Convergence of Wong-Zakai Approximations for SDEs and SPDEs*, PhD thesis, University of Edinburgh, 2005.
- [77] Y. SONG, J. SOHL-DICKSTEIN, D. P. KINGMA, A. KUMAR, S. ERMON, AND B. POOLE, *Score-Based Generative Modeling through Stochastic Differential Equations*, Proceedings of the International Conference on Learning Representations, (2021).
- [78] Z. SONG AND Z. TAN, *Hamiltonian-Assisted Metropolis Sampling*, Journal of the American Statistical Association, Theory and Methods, (2021).
- [79] G. STRANG, *On the construction and comparison of difference schemes*, SIAM Journal on Numerical Analysis, 5 (1968), pp. 506–517.
- [80] C. STRANGE, *Path-based splitting methods for SDEs and machine learning for battery lifetime prognostics*, PhD thesis, University of Edinburgh, 2023, era.ed.ac.uk/handle/1842/41025.
- [81] I. TUBIKANEC, M. TAMBORRINO, P. LANSKY, AND E. BUCKWAR, *Qualitative properties of different numerical methods for the inhomogeneous geometric Brownian motion*, Journal of Computational and Applied Mathematics, 406 (2022).
- [82] M. WELLING AND Y. W. TEH, *Bayesian Learning via Stochastic Gradient Langevin Dynamics*, Proceedings of the 28th International Conference on Machine Learning, (2011).
- [83] M. WIKTORSSON, *Joint characteristic function and simultaneous simulation of iterated Itô integrals for multiple independent Brownian motions*, Annals of Applied Probability, 11 (2001), pp. 470–487.
- [84] E. WONG AND M. ZAKAI, *On the Convergence of Ordinary Integrals to Stochastic Integrals*, Annals of Mathematical Statistics, 36 (1965), pp. 1560–1564.
- [85] Q. ZHANG AND Y. CHEN, *Path Integral Sampler: A Stochastic Control Approach For Sampling*, Proceedings of the International Conference on Learning Representations, (2022).

Appendix A. Cancellation of integrals under commutativity condition.

In this section, we present the calculations required to simplify the Taylor expansions of the SDE (1.1) and CDE (1.3) when the commutativity condition (1.2) is satisfied. To make these calculations easier, we identify iterated integrals with non-commutative polynomials and present the shuffle product, commonly used in rough path theory [57].

DEFINITION A.1. *Let \mathcal{A}_d denote the set of letters $\{0, 1, \dots, d\}$. We can identify linear combinations of iterated integrals with elements in $\mathbb{R}\langle \mathcal{A}_d \rangle$ by $I_e^W = I_e^\gamma = 1$ and*

$$i_1 \cdots i_m \leftrightarrow I_{i_1 \cdots i_m}^W := \int_s^t \int_s^{r_1} \cdots \int_s^{r_{m-1}} \circ dW_{r_n}^{i_1} \circ dW_{r_{m-1}}^{i_2} \cdots \circ dW_{r_2}^{i_{m-1}} \circ dW_{r_1}^{i_m},$$

$$i_1 \cdots i_m \leftrightarrow I_{i_1 \cdots i_m}^\gamma := \int_s^t \int_s^{r_1} \cdots \int_s^{r_{m-1}} d\gamma_{r_m}^{i_1} d\gamma_{r_{m-1}}^{i_2} \cdots d\gamma_{r_2}^{i_{m-1}} d\gamma_{r_1}^{i_m},$$

$$\lambda u + \mu v \leftrightarrow I_{\lambda u + \mu v} := \lambda I_u + \mu I_v,$$

for $m \geq 0$, $i_1, i_2, \dots, i_m \in \mathcal{A}_d$, $u, v \in \mathcal{A}_d^*$ and $\lambda, \mu \in \mathbb{R}$.

DEFINITION A.2. Suppose that \mathcal{A}_d is a set containing d letters and let $\mathbb{R}\langle \mathcal{A}_d \rangle$ be the corresponding space of non-commutative polynomials in \mathcal{A}_d with real coefficients. Then the **shuffle product** $\sqcup\sqcup : \mathbb{R}\langle \mathcal{A}_d \rangle \times \mathbb{R}\langle \mathcal{A}_d \rangle \rightarrow \mathbb{R}\langle \mathcal{A}_d \rangle$ is the unique bilinear map such that

$$ua \sqcup\sqcup vb = (u \sqcup\sqcup vb)a + (ua \sqcup\sqcup v)b,$$

$$u \sqcup\sqcup e = e \sqcup\sqcup u = u,$$

where e denotes the empty letter.

With this notation, we can link the shuffle project to the integration by parts formula. As a result, the shuffle project will allow us to expand products of iterated integrals.

THEOREM A.3 (Integration by parts formula for integrals). For all $u, v \in \mathbb{R}\langle \mathcal{A}_d \rangle$, we have

$$(A.1) \quad I_u \cdot I_v = I_{u \sqcup\sqcup v}$$

Proof. It is clear that the identity (A.1) holds when $u = e$ or $v = e$ since $I_e = 1$. Suppose that (A.1) holds for all words $u, v \in \mathcal{A}_d^*$ with a combined length less than m . Then for words $u, v \in \mathcal{A}_d^*$ and letters $a, b \in \mathcal{A}_d$ such that $|ua| + |vb| = m$, we have

$$\begin{aligned} I_{ua}^W \cdot I_{vb}^W &= \int_s^t I_u^W(r) \circ dW_r^a \int_s^t I_v^W(r) \circ dW_r^b \\ &= \int_s^t \left(\int_s^{r_1} I_u^W(r_2) \circ dW_{r_2}^a \right) \circ d \left(\int_s^{r_1} I_v^W(r_2) \circ dW_{r_2}^b \right) \\ &\quad + \int_s^t \left(\int_s^{r_1} I_v^W(r_2) \circ dW_{r_2}^b \right) \circ d \left(\int_s^{r_1} I_u^W(r_2) \circ dW_{r_2}^a \right) \\ &= \int_s^t I_{ua}^W(r_1) I_v^W(r_1) \circ dW_{r_1}^b + \int_s^t I_{vb}^W(r_1) I_u^W(r_1) \circ dW_{r_1}^a \\ &= I_{(ua \sqcup\sqcup v)b + (u \sqcup\sqcup vb)a}^W, \end{aligned}$$

where the second line uses integration by parts (which holds for Stratonovich integrals) and the last line uses the induction hypothesis. The result now follows by linearity. The same argument gives (A.1) for iterated integrals with respect to the path γ . \square

Using Theorem A.3, it will be straightforward to rewrite products of integrals as linear combinations of (high order) integrals. In addition, it shall enable us to establish decompositions of iterated integrals into symmetric and antisymmetric components.

THEOREM A.4 (Symmetric and antisymmetric components of iterated integrals).

Let the Lie bracket $[\cdot, \cdot] : \mathbb{R}\langle \mathcal{A}_d \rangle \times \mathbb{R}\langle \mathcal{A}_d \rangle \rightarrow \mathbb{R}\langle \mathcal{A}_d \rangle$ be the unique bilinear map with

$$(A.2) \quad [u, v] = uv - vu,$$

for words $u, v \in \mathcal{A}_d^*$. Then, adopting the notation of Definition A.1 and Theorem A.3, we have

$$(A.3) \quad I_{ij} = \frac{1}{2}I_i \cdot I_j + \frac{1}{2}I_{[i,j]},$$

$$(A.4) \quad I_{ijk} = \frac{1}{6}I_i \cdot I_j \cdot I_k + \frac{1}{4}I_i \cdot I_{[j,k]} + \frac{1}{4}I_{[i,j]} \cdot I_k + \frac{1}{6}I_{[[i,j],k]} + \frac{1}{6}I_{[i,[j,k]]},$$

$$(A.5) \quad \begin{aligned} I_{ijkl} &= \frac{1}{24}I_i \cdot I_j \cdot I_k \cdot I_l + \frac{1}{12}I_i \cdot I_{[j,[k,l]]} + \frac{1}{12}I_i \cdot I_{[[j,k],l]} + \frac{1}{12}I_{[i,[j,k]]} \cdot I_l \\ &\quad + \frac{1}{12}I_{[[i,j],k]} \cdot I_l + \frac{1}{12}I_i \cdot I_j \cdot I_{[k,l]} + \frac{1}{12}I_i \cdot I_{[j,k]} \cdot I_l + \frac{1}{12}I_{[i,j]} \cdot I_k \cdot I_l \\ &\quad + \frac{1}{8}I_{[i,j]} \cdot I_{[k,l]} + \frac{1}{12}I_{[i,[j,[k,l]]]} + \frac{1}{12}I_{[[i,[j,k]],l]} + \frac{1}{12}I_{[[[i,j],k],l]} \\ &\quad + \frac{1}{12}(I_{kjli} - I_{kjl i} + I_{lij k} - I_{iljk}) + \frac{1}{12}(I_{jilk} - I_{kilj} + I_{jlik} - I_{kl ij}), \end{aligned}$$

for $i, j, k, l \in \mathcal{A}_d$.

Proof. The results follow by expanding the Lie brackets $[\cdot, \cdot]$ in the right hand sides using (A.2) and applying the integration by parts formula via Theorem A.1. \square

Hence, in order to simplify the Taylor expansions of (1.1) and (1.3), we will need to find symmetries in the vector field derivatives that will cause the antisymmetric parts in the iterated integrals to cancel out. To this end, we give the following lemma, which will set up the notation used in the main result of the section (Theorem A.6).

LEMMA A.5 (Codomains of vector field derivatives). *Given a sufficiently smooth vector field $f : \mathbb{R}^e \rightarrow \mathbb{R}^e$, its Fréchet derivatives will map between the following spaces:*

$$\begin{aligned} f' &: \mathbb{R}^e \rightarrow L(\mathbb{R}^e, \mathbb{R}^e), \\ f'' &: \mathbb{R}^e \rightarrow L(\mathbb{R}^e, L(\mathbb{R}^e, \mathbb{R}^e)), \\ f''' &: \mathbb{R}^e \rightarrow L(\mathbb{R}^e, L(\mathbb{R}^e, L(\mathbb{R}^e, \mathbb{R}^e))), \end{aligned}$$

where $L(U, V)$ denotes the space of linear maps between the vector spaces U and V . Equivalently, we can view $f^{(k)}(y)$ as a k -linear map on \mathbb{R}^e for each $y \in \mathbb{R}^e$. That is,

$$\begin{aligned} f' &: \mathbb{R}^e \rightarrow L(\mathbb{R}^e, \mathbb{R}^e), \\ f'' &: \mathbb{R}^e \rightarrow L((\mathbb{R}^e)^{\otimes 2}, \mathbb{R}^e), \\ f''' &: \mathbb{R}^e \rightarrow L((\mathbb{R}^e)^{\otimes 3}, \mathbb{R}^e). \end{aligned}$$

Proof. The result follows immediately from the definition of Fréchet derivative. \square

We now turn to the main result of the section, which shows that certain terms in the Taylor expansions of (1.1) and (1.3) simplify under the commutativity condition. We note that the CDE (1.3) can be written in the equivalent form

$$dy_r^\gamma = f(y_r^\gamma) d\gamma^\tau(r) + \sum_{i=1}^d g_i(y_r^\gamma) d(\gamma^\omega(r))^i.$$

THEOREM A.6. *Suppose that the following commutativity condition holds*

$$(A.6) \quad g'_i(y)g_j(y) = g'_j(y)g_i(y), \quad \forall y \in \mathbb{R}^e,$$

for $i, j \in \{1, \dots, d\}$. Then, the terms in the SDE (or CDE) Taylor expansions become

$$(A.7) \quad \sum_{i,j=1}^d g'_i(y)g_j(y)I_{ji} = \frac{1}{2} \sum_{i,j=1}^d g'_i(y)g_j(y)(I_i \cdot I_j),$$

$$(A.8) \quad \sum_{i,j,k=1}^d (g''_i(y)(g_j(y), g_k(y)) + g'_i(y)g'_j(y)g_k(y))I_{kji} = \frac{1}{6} \sum_{i,j,k=1}^d (\dots)(I_i \cdot I_j \cdot I_k),$$

$$(A.9) \quad \sum_{i,j,k,l=1}^d \left(g'''_i(y)(g_j(y), g_k(y), g_l(y)) + g''_i(y)(g'_j(y)g_l(y), g_k(y)) \right. \\ \left. + g''_i(y)(g'_j(y)g_k(y), g_l(y)) + g''_i(y)(g_j(y), g'_k(y)g_l(y)) \right. \\ \left. + g'_i(y)g''_j(y)(g_k(y), g_l(y)) + g'_i(y)g'_j(y)g'_k(y)g_l(y) \right) I_{lkji} \\ = \frac{1}{24} \sum_{i,j,k=1}^d (\dots)(I_i \cdot I_j \cdot I_k \cdot I_l),$$

where (\dots) denote the same sum of vector field derivatives as in the left hand sides.

Proof. For any multi-index (i_1, \dots, i_n) with $n \geq 2$, we introduce the notation

$$g_{i_1, \dots, i_n}(y) := g'_{i_1, \dots, i_{n-1}}(y)g_{i_n}(y).$$

By the product rule, it is then straightforward to see that $g_{ij}(y)$, $g_{ijk}(y)$ and $g_{ijkl}(y)$ are precisely the vector field derivatives appearing in equations (A.7), (A.8) and (A.9).

We will first prove that g_{i_1, \dots, i_n} is unchanged if the indices i_1, \dots, i_n are permuted. This clearly follows by the commutativity condition (A.6) when $n = 2$ and is trivially the case when $n = 1$. To establish this invariance for $n \geq 3$, we proceed by induction:

For $k < n$, we assume g_{i_1, \dots, i_k} is unchanged when indices i_1, \dots, i_k are permuted. Then the same can be said for any derivative of g_{i_1, \dots, i_k} . By the definition of g_{i_1, \dots, i_n} ,

$$g_{i_1, \dots, i_n}(y) = \underbrace{g'_{i_1, \dots, i_{n-1}}(y)}_{\substack{\text{permutation} \\ \text{invariant}}} g_{i_n}(y).$$

From the induction hypothesis, it follows that g_{i_1, \dots, i_n} is invariant to permutations in i_1, \dots, i_{n-1} . Moreover, applying the definition of $g_{i_1, \dots, i_{n-1}}$ and product rule yields:

$$g_{i_1, \dots, i_n}(y) = g'_{i_1, \dots, i_{n-1}}(y)g_{i_n}(y) \\ = (g'_{i_1, \dots, i_{n-2}}(y)g_{i_{n-1}}(y))'(y)g_{i_n}(y) \\ = \underbrace{g''_{i_1, \dots, i_{n-2}}(y)(g_{i_{n-1}}(y), g_{i_n}(y))}_{\text{symmetric and bilinear}} + g'_{i_1, \dots, i_{n-2}}(y) \underbrace{g'_{i_{n-1}}(y)g_{i_n}(y)}_{=g'_{i_n}(y)g_{i_{n-1}}(y)}.$$

So by the symmetry of the bilinear map $g''_{i_1, \dots, i_{n-2}}(y)$ and the commutativity of g (as indicated above), we see that g_{i_1, \dots, i_n} is unchanged if i_{n-1} and i_n are swapped. Therefore, the permutations invariance of g_{i_1, \dots, i_n} for $n \geq 3$ now follows by induction.

In particular, the vector field terms in (A.7), (A.8) and (A.9) will have symmetries in their indices. As a consequence, all the antisymmetric terms in the decompositions of I_{ji} , I_{kji} and I_{lkji} (given by Theorem A.4) will cancel out in their respective sums. Thus, only ‘‘symmetric parts’’ of integrals contribute to the sums (A.7), (A.8), (A.9), and the result follows from the decompositions (A.3), (A.4), (A.5) in Theorem A.4. \square

Appendix B. Unbiased approximation of high order iterated integrals.

In this section, we derive estimators for certain iterated stochastic integrals using a polynomial expansion of Brownian motion [29]. We use this expansion since its first two coefficients give the path's increment and space-time Lévy area (Definition 1.1). Just as in [29], the integral that we would primarily like to approximate is the so-called “space-space-time” Lévy area, which we define below. We note that a preliminary version of the results in this section were first presented in the doctoral thesis [26].

DEFINITION B.1. *Over an interval $[s, t]$, the **space-space-time Lévy area** $L_{s,t}$ of a standard Brownian motion is defined as*

$$L_{s,t} := \frac{1}{6} \left(\int_s^t \int_s^u \int_s^v \circ dW_r \circ dW_v \circ dW_u - 2 \int_s^t \int_s^u \int_s^v \circ dW_r \circ dW_v \circ dW_u + \int_s^t \int_s^u \int_s^v dr \circ dW_v \circ dW_u \right).$$

Remark B.2. Along with the path increment $W_{s,t}$, the Lévy areas $H_{s,t}$ and $L_{s,t}$ are sufficient to construct the iterated integrals appearing in the stochastic Taylor expansion (3.2), up to order 2 for SDEs satisfying the commutativity condition (1.2).

The key difference between the integral estimators defined in this section and those derived in [29], is that we shall additionally use the following random variable.

DEFINITION B.3. *The **space-time Lévy swing**² of Brownian motion over $[s, t]$ is defined as*

$$n_{s,t} := \text{sgn}(H_{s,u} - H_{u,t}),$$

where $u := \frac{1}{2}(s + t)$ is the interval's midpoint.

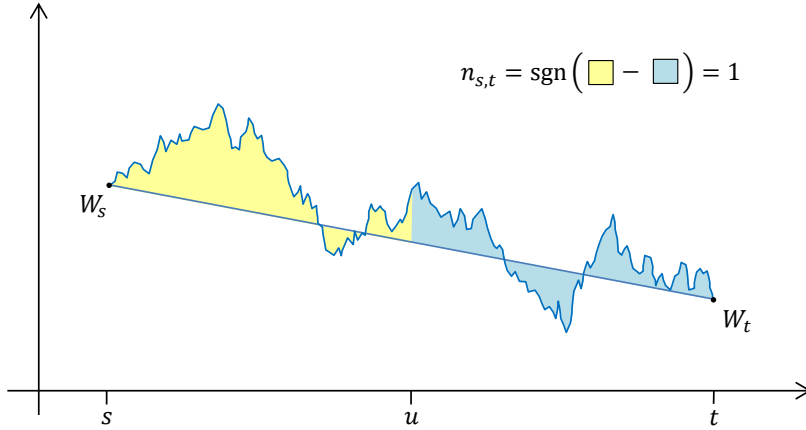


FIG. 8. *Space-time Lévy swing gives the side where the path has greater space-time Lévy area.*

Similar to [29], we propose approximating $L_{s,t}$ using its conditional expectation. That is, we would like to derive a closed-form expression for $\mathbb{E}[L_{s,t} | W_{s,t}, H_{s,t}, n_{s,t}]$. In addition, we shall derive the conditional variance of $L_{s,t}$ as it gives the $L^2(\mathbb{P})$ error.

²side with integral greater.

In this section, we focus on the case where Brownian motion is one-dimensional and leave the general case, a matrix of space-space-time Lévy areas, as future work. However, the off-diagonal terms in this matrix will have zero expectation due to the independence and symmetry of the d coordinate processes of the Brownian motion. Therefore, we may construct a high order multidimensional splitting path simply by taking independent copies of the paths detailed in Section 4. That said, as discussed in Section 5, we would lose optimality due to “cross” iterated integrals such as (5.10).

THEOREM B.4 (An optimal unbiased estimator of space-space-time Lévy area). *Let $H_{s,t}$ and $L_{s,t}$ be the previously defined Lévy areas of Brownian motion and time. Let $n_{s,t} := \text{sgn}(H_{s,u} - H_{u,t})$ denote the space-time Lévy swing given by definition B.3. Then the conditional mean and variance of $L_{s,t}$ given the information $(W, H, n)_{s,t}$ is*

$$(B.1) \quad \mathbb{E}[L_{s,t} | W_{s,t}, H_{s,t}, n_{s,t}] = \frac{1}{30}h^2 + \frac{3}{5}hH_{s,t}^2 - \frac{1}{8\sqrt{6\pi}}n_{s,t}h^{\frac{3}{2}}W_{s,t},$$

$$(B.2) \quad \text{Var}(L_{s,t} | W_{s,t}, H_{s,t}, n_{s,t}) = \frac{11}{25200}h^4 + \left(\frac{1}{720} - \frac{1}{384\pi}\right)h^3W_{s,t}^2 + \frac{1}{700}h^3H_{s,t}^2 \\ - \frac{1}{320\sqrt{6\pi}}n_{s,t}h^{\frac{7}{2}}W_{s,t}.$$

Proof. We first note by applying [29, Theorem 3.10] on $[s, u]$ and $[u, t]$, we have

$$\mathbb{E}[L_{s,u} | W_{s,u}, H_{s,u}] = \frac{1}{120}h^2 + \frac{3}{10}hH_{s,u}^2, \\ \text{Var}(L_{s,u} | W_{s,u}, H_{s,u}) = \frac{11}{403200}h^4 + h^3\left(\frac{1}{5760}W_{s,u}^2 + \frac{1}{5600}H_{s,u}^2\right), \\ \mathbb{E}[L_{u,t} | W_{u,t}, H_{u,t}] = \frac{1}{120}h^2 + \frac{3}{10}hH_{u,t}^2, \\ \text{Var}(L_{u,t} | W_{u,t}, H_{u,t}) = \frac{11}{403200}h^4 + h^3\left(\frac{1}{5760}W_{u,t}^2 + \frac{1}{5600}H_{u,t}^2\right).$$

To utilise the above expectations, we will “expand” the following integrals over $[s, t]$.

$$(B.3) \quad \int_s^t W_{s,r} dr = \int_s^u W_{s,r} dr + \int_u^t W_{s,r} dr \\ = \int_s^u W_{s,r} dr + \frac{1}{2}hW_{s,u} + \int_u^t W_{u,r} dr,$$

$$(B.4) \quad \int_s^t W_{s,r}^2 dr = \int_s^u W_{s,r}^2 dr + \int_u^t W_{s,r}^2 dr \\ = \int_s^u W_{s,r}^2 dr + \frac{1}{2}hW_{s,u}^2 + 2W_{s,u} \int_u^t W_{u,r} dr + \int_u^t W_{u,r}^2 dr.$$

By [29, Theorem 3.9], which follows from integration by parts, we have that, for $u \leq v$,

$$(B.5) \quad \int_u^v W_{v,r} dr = \frac{1}{2}(v-u)W_{u,v} + (v-u)H_{u,v},$$

$$(B.6) \quad \int_u^v W_{u,r}^2 dr = \frac{1}{3}(v-u)W_{u,v}^2 + (v-u)W_{u,v}H_{u,v} + 2L_{u,v}.$$

From the decomposition (B.3) and identity (B.5) on $[s, u]$ and $[u, t]$, it follows that

$$(B.7) \quad H_{s,t} = \frac{1}{4}(W_{s,u} - W_{u,t}) + \frac{1}{2}(H_{s,u} + H_{u,t}).$$

We now define the following random variables:

$$(B.8) \quad Z_{s,u} := \frac{1}{8}(W_{s,u} - W_{u,t}) - \frac{3}{4}(H_{s,u} + H_{u,t}),$$

$$(B.9) \quad N_{s,t} := H_{s,u} - H_{u,t}.$$

Since $W_{a,b} \sim \mathcal{N}(0, (b-a))$ and $H_{a,b} \sim \mathcal{N}(0, \frac{1}{12}(b-a))$ are independent, we see that $W_{s,t}, H_{s,t}, Z_{s,u}, N_{s,t}$ are jointly normal, uncorrelated and therefore also independent. From (B.8) and (B.9), it directly follows that $Z_{s,u} \sim \mathcal{N}(0, \frac{1}{16}h)$ and $N_{s,t} \sim \mathcal{N}(0, \frac{1}{12}h)$. In addition, by rearranging the above expressions for these random variables, we have

$$(B.10) \quad W_{s,u} = \frac{1}{2}W_{s,t} + \frac{3}{2}H_{s,t} + Z_{s,u},$$

$$(B.11) \quad W_{u,t} = \frac{1}{2}W_{s,t} - \frac{3}{2}H_{s,t} - Z_{s,u},$$

$$(B.12) \quad H_{s,u} = \frac{1}{4}H_{s,t} - \frac{1}{2}Z_{s,u} + \frac{1}{2}N_{s,t},$$

$$(B.13) \quad H_{u,t} = \frac{1}{4}H_{s,t} - \frac{1}{2}Z_{s,u} - \frac{1}{2}N_{s,t}.$$

Putting all of this together, and using the independence of Brownian increments, gives

$$\begin{aligned} & \mathbb{E} \left[\int_s^t W_{s,r}^2 dr \mid W_{s,u}, H_{s,u}, W_{u,t}, H_{u,t} \right] \\ &= \mathbb{E} \left[\int_s^u W_{s,r}^2 dr \mid W_{s,u}, H_{s,u} \right] + \frac{1}{2}hW_{s,u}^2 + 2W_{s,u} \int_u^t W_{u,r} dr \\ & \quad + \mathbb{E} \left[\int_u^t W_{u,r}^2 dr \mid W_{u,t}, H_{u,t} \right] \\ &= \frac{1}{6}hW_{s,u}^2 + \frac{1}{2}hW_{s,u}H_{s,u} + 2\mathbb{E}[L_{s,u} \mid W_{s,u}, H_{s,u}] + \frac{1}{2}hW_{s,u}^2 + \frac{1}{2}hW_{s,u}W_{u,t} \\ & \quad + hW_{s,u}H_{u,t} + \frac{1}{6}hW_{u,t}^2 + \frac{1}{2}hW_{u,t}H_{u,t} + 2\mathbb{E}[L_{u,t} \mid W_{u,t}, H_{u,t}] \\ &= \frac{1}{6}hW_{s,u}^2 + \frac{1}{2}hW_{s,u}H_{s,u} + \frac{3}{5}hH_{s,u}^2 + \frac{1}{60}h^2 + \frac{1}{2}hW_{s,u}^2 + \frac{1}{2}hW_{s,u}W_{u,t} \\ & \quad + hW_{s,u}H_{u,t} + \frac{1}{6}hW_{u,t}^2 + \frac{1}{2}hW_{u,t}H_{u,t} + \frac{3}{5}hH_{u,t}^2 + \frac{1}{60}h^2 \\ &= \frac{1}{3}hW_{s,t}^2 + hW_{s,t}H_{s,t} + \frac{6}{5}hH_{s,t}^2 + \frac{1}{30}h^2 \\ & \quad + \frac{1}{5}hH_{s,t}Z_{s,u} - \frac{1}{4}hW_{s,t}N_{s,t} + \frac{2}{15}hZ_{s,u}^2 + \frac{3}{10}hN_{s,t}^2, \end{aligned}$$

where the last line was obtained by substituting (B.10)–(B.13) into the previous line. Since $n_{s,t} := \text{sgn}(N_{s,t})$ and $N_{s,t} \sim \mathcal{N}(0, \frac{1}{12}h)$, it follows that $|N_{s,t}|$ has a half-normal distribution and is independent of $n_{s,t}$. Moreover, this implies that its moments are

$$(B.14) \quad \mathbb{E}[N_{s,t} \mid n_{s,t}] = \frac{1}{\sqrt{6\pi}}n_{s,t}h^{\frac{1}{2}}, \quad \mathbb{E}[N_{s,t}^3 \mid n_{s,t}] = \frac{1}{6\sqrt{6\pi}}n_{s,t}h^{\frac{3}{2}},$$

$$(B.15) \quad \mathbb{E}[N_{s,t}^2 \mid n_{s,t}] = \frac{1}{12}h, \quad \mathbb{E}[N_{s,t}^4 \mid n_{s,t}] = \frac{1}{48}h^2.$$

Explicit formulae for the first four central moments of the half-normal distribution are given in [24, Equation (16)]. Since $W_{s,t}, H_{s,t}, Z_{s,u}, N_{s,t}$ are independent, we have

$$\begin{aligned} & \mathbb{E} \left[\int_s^t W_{s,r}^2 dr \mid W_{s,t}, H_{s,t}, n_{s,t} \right] \\ &= \mathbb{E} \left[\mathbb{E} \left[\int_s^t W_{s,r}^2 dr \mid W_{s,t}, H_{s,t}, Z_{s,u}, N_{s,t} \right] \mid W_{s,t}, H_{s,t}, n_{s,t} \right]. \end{aligned}$$

As $(W_{s,t}, H_{s,t}, Z_{s,u}, N_{s,t})$ and $(W_{s,u}, H_{s,u}, W_{u,t}, H_{u,t})$ encode the same information, we have

$$\begin{aligned} & \mathbb{E} \left[\int_s^t W_{s,r}^2 dr \mid W_{s,t}, H_{s,t}, n_{s,t} \right] \\ &= \frac{1}{3} h W_{s,t}^2 + h W_{s,t} H_{s,t} + \frac{6}{5} h H_{s,t}^2 + \frac{1}{30} h^2 \\ & \quad + \frac{1}{5} h H_{s,t} \mathbb{E}[Z_{s,u}] - \frac{1}{4} h W_{s,t} \mathbb{E}[N_{s,t} | n_{s,t}] + \frac{2}{15} h \mathbb{E}[Z_{s,u}^2] + \frac{3}{10} h \mathbb{E}[N_{s,t}^2 | n_{s,t}] \\ &= \frac{1}{3} h W_{s,t}^2 + h W_{s,t} H_{s,t} + \frac{1}{15} h^2 + \frac{6}{5} h H_{s,t}^2 - \frac{1}{4\sqrt{6\pi}} n_{s,t} h^{\frac{3}{2}} W_{s,t}, \end{aligned}$$

where we used the moments $\mathbb{E}[Z_{s,u}] = 0$, $\mathbb{E}[Z_{s,u}^2] = \frac{1}{16} h$ as well as (B.14) and (B.15). The condition expectation (B.1) now follows by applying equation (B.6) to the above.

We employ a similar strategy to compute the conditional variance (B.2) of $L_{s,t}$. Using the decomposition (B.4) and independence of $(W_{s,u}, H_{s,u}, W_{u,t}, H_{u,t})$, we have

$$\begin{aligned} & \text{Var} \left(\int_s^t W_{s,r}^2 dr \mid W_{s,u}, W_{u,t}, H_{s,u}, H_{u,t} \right) \\ &= \text{Var} \left(\int_s^u W_{s,r}^2 dr + \frac{1}{2} h W_{s,u}^2 \right. \\ & \quad \left. + 2 W_{s,u} \int_u^t W_{u,r} dr + \int_u^t W_{u,r}^2 dr \mid W_{s,u}, W_{u,t}, H_{s,u}, H_{u,t} \right) \\ &= \text{Var} \left(\int_s^u W_{s,r}^2 dr \mid W_{s,u}, H_{s,u} \right) + \text{Var} \left(\int_u^t W_{u,r}^2 dr \mid W_{u,t}, H_{u,t} \right). \end{aligned}$$

Therefore, by (B.6) and the formulae for the condition variances of $L_{s,u}$ and $L_{u,t}$,

$$\begin{aligned} & \text{Var} \left(\int_s^t W_{s,r}^2 dr \mid W_{s,u}, W_{u,t}, H_{s,u}, H_{u,t} \right) \\ &= \frac{11}{50400} h^4 + h^3 \left(\frac{1}{1440} W_{s,u}^2 + \frac{1}{1440} W_{u,t}^2 + \frac{1}{1400} H_{s,u}^2 + \frac{1}{1400} H_{u,t}^2 \right). \end{aligned}$$

By plugging in (B.10) – (B.13), we can rewrite this in terms of $W_{s,t}, H_{s,t}, Z_{s,u}, N_{s,t}$.

$$\begin{aligned} & \text{Var} \left(\int_s^t W_{s,r}^2 dr \mid W_{s,u}, W_{u,t}, H_{s,u}, H_{u,t} \right) \\ &= \frac{11}{50400} h^4 + h^3 \left(\frac{1}{1440} W_{s,u}^2 + \frac{1}{1440} W_{u,t}^2 + \frac{1}{1400} H_{s,u}^2 + \frac{1}{1400} H_{u,t}^2 \right) \\ &= \frac{11}{50400} h^4 + h^3 \left(\frac{1}{2880} W_{s,t}^2 + \frac{9}{2800} H_{s,t}^2 + \frac{2}{525} H_{s,t} Z_{s,u} + \frac{11}{6300} Z_{s,u}^2 + \frac{1}{2800} N_{s,t}^2 \right). \end{aligned}$$

The second conditional moment of the iterated integral can be directly calculated as

$$\begin{aligned} & \mathbb{E} \left[\left(\int_s^t W_{s,r}^2 dr \right)^2 \middle| W_{s,u}, W_{u,t}, H_{s,u}, H_{u,t} \right] \\ &= \mathbb{E} \left[\int_s^t W_{s,r}^2 dr \middle| W_{s,u}, W_{u,t}, H_{s,u}, H_{u,t} \right]^2 + \text{Var} \left(\int_s^t W_{s,r}^2 dr \middle| W_{s,u}, W_{u,t}, H_{s,u}, H_{u,t} \right). \end{aligned}$$

Therefore, by substituting the expressions for the above conditional moments, we have

$$\begin{aligned} & \mathbb{E} \left[\left(\int_s^t W_{s,r}^2 dr \right)^2 \middle| W_{s,u}, W_{u,t}, H_{s,u}, H_{u,t} \right] \\ &= \left(\frac{1}{3} h W_{s,t}^2 + h W_{s,t} H_{s,t} + \frac{6}{5} h H_{s,t}^2 + \frac{1}{30} h^2 \right. \\ &\quad \left. + \frac{1}{5} h H_{s,t} Z_{s,u} - \frac{1}{4} h W_{s,t} N_{s,t} + \frac{2}{15} h Z_{s,u}^2 + \frac{3}{10} h N_{s,t}^2 \right)^2 + \frac{11}{50400} h^4 \\ &\quad \left. + h^3 \left(\frac{1}{2880} W_{s,t}^2 + \frac{9}{2800} H_{s,t}^2 + \frac{2}{525} H_{s,t} Z_{s,u} + \frac{11}{6300} Z_{s,u}^2 + \frac{1}{2800} N_{s,t}^2 \right). \right. \end{aligned}$$

Expanding the bracket and collecting terms yields

$$\begin{aligned} & \mathbb{E} \left[\left(\int_s^t W_{s,r}^2 dr \right)^2 \middle| W_{s,u}, W_{u,t}, H_{s,u}, H_{u,t} \right] \\ &= \frac{67}{50400} h^4 + \frac{1}{9} h^2 W_{s,t}^4 + \frac{36}{25} h^2 H_{s,t}^4 + \frac{4}{225} h^2 Z_{s,u}^4 + \frac{9}{100} h^2 N_{s,t}^4 + \frac{9}{5} h^2 W_{s,t}^2 H_{s,t}^2 \\ &\quad + \frac{4}{45} h^2 W_{s,t}^2 Z_{s,u}^2 + \frac{21}{80} h^2 W_{s,t}^2 N_{s,t}^2 + \frac{9}{25} h^2 H_{s,t}^2 Z_{s,u}^2 + \frac{18}{25} h^2 H_{s,t}^2 N_{s,t}^2 + \frac{2}{25} h^2 Z_{s,u}^2 N_{s,t}^2 \\ &\quad + \frac{13}{576} h^3 W_{s,t}^3 + \frac{233}{2800} h^3 H_{s,t}^3 + \frac{67}{6300} h^3 Z_{s,u}^3 + \frac{57}{2800} h^3 N_{s,t}^3 + \frac{1}{15} h^3 W_{s,t} H_{s,t} \\ &\quad - \frac{1}{60} h^3 W_{s,t} N_{s,t} + \frac{3}{175} h^3 H_{s,t} Z_{s,u} + \frac{2}{3} h^2 W_{s,t}^3 H_{s,t} - \frac{1}{10} h^2 W_{s,t} H_{s,t} Z_{s,u} N_{s,t} \\ &\quad - \frac{1}{6} h^2 W_{s,t}^3 N_{s,t} + \frac{12}{5} h^2 W_{s,t} H_{s,t}^3 - \frac{3}{20} h^2 W_{s,t} N_{s,t}^3 + \frac{12}{25} h^2 H_{s,t}^3 Z_{s,u} + \frac{4}{75} h^2 H_{s,t} Z_{s,u}^3 \\ &\quad + \frac{2}{15} h^2 W_{s,t}^2 H_{s,t} Z_{s,u} - \frac{1}{2} h^2 W_{s,t}^2 H_{s,t} N_{s,t} + \frac{2}{5} h^2 W_{s,t} H_{s,t}^2 Z_{s,u} + \frac{4}{15} h^2 W_{s,t} H_{s,t} Z_{s,u}^2 \\ &\quad + \frac{3}{5} h^2 W_{s,t} H_{s,t} N_{s,t}^2 - \frac{3}{5} h^2 W_{s,t} H_{s,t}^2 N_{s,t} - \frac{1}{15} h^2 W_{s,t} Z_{s,u}^2 N_{s,t} + \frac{3}{25} h^2 H_{s,t} Z_{s,u} N_{s,t}^2. \end{aligned}$$

By taking the expectation of the above terms conditional on $(W_{s,t}, H_{s,t}, n_{s,t})$ and substituting in the moments of $N_{s,t} | n_{s,t}$ given by (B.14) and (B.15), it follows that

$$\begin{aligned} & \mathbb{E} \left[\left(\int_s^t W_{s,r}^2 dr \right)^2 \middle| W_{s,t}, H_{s,t}, n_{s,t} \right] \\ &= \mathbb{E} \left[\mathbb{E} \left[\left(\int_s^t W_{s,r}^2 dr \right)^2 \middle| W_{s,u}, W_{u,t}, H_{s,u}, H_{u,t} \right] \middle| W_{s,t}, H_{s,t}, n_{s,t} \right] \\ &= \frac{13}{2100} h^4 + \frac{1}{9} h^2 W_{s,t}^4 + \frac{36}{25} h^2 H_{s,t}^4 + \frac{9}{5} h^2 W_{s,t}^2 H_{s,t}^2 + \frac{1}{20} h^3 W_{s,t}^3 + \frac{29}{175} h^3 H_{s,t}^3 \\ &\quad + \frac{2}{15} h^3 W_{s,t} H_{s,t} + \frac{12}{5} h^2 W_{s,t} H_{s,t}^3 + \frac{2}{3} h^2 W_{s,t}^3 H_{s,t} \\ &\quad - \frac{1}{\sqrt{6\pi}} n_{s,t} h^{\frac{5}{2}} \left(\frac{1}{6} W_{s,t}^3 + \frac{11}{240} h W_{s,t} + \frac{1}{2} W_{s,t}^2 H_{s,t} + \frac{3}{5} W_{s,t} H_{s,t}^2 \right). \end{aligned}$$

Thus, we can compute the required conditional variance using the following identity:

$$\begin{aligned} & \text{Var} \left(\int_s^t W_{s,r}^2 dr \mid W_{s,t}, H_{s,t}, n_{s,t} \right) \\ &= \mathbb{E} \left[\left(\int_s^t W_{s,r}^2 dr \right)^2 \mid W_{s,t}, H_{s,t}, n_{s,t} \right] - \left(\mathbb{E} \left[\int_s^t W_{s,r}^2 dr \mid W_{s,t}, H_{s,t}, n_{s,t} \right] \right)^2. \end{aligned}$$

Plugging in the expressions for these conditional moments and simplifying terms gives

$$\begin{aligned} & \text{Var} \left(\int_s^t W_{s,r}^2 dr \mid W_{s,t}, H_{s,t}, n_{s,t} \right) \\ &= \frac{13}{2100} h^4 + \frac{1}{9} h^2 W_{s,t}^4 + \frac{36}{25} h^2 H_{s,t}^4 + \frac{9}{5} h^2 W_{s,t}^2 H_{s,t}^2 + \frac{1}{20} h^3 W_{s,t}^2 + \frac{29}{175} h^3 H_{s,t}^2 \\ & \quad + \frac{2}{15} h^3 W_{s,t} H_{s,t} + \frac{12}{5} h^2 W_{s,t} H_{s,t}^3 + \frac{2}{3} h^2 W_{s,t}^3 H_{s,t} \\ & \quad - \frac{1}{\sqrt{6\pi}} n_{s,t} h^{\frac{5}{2}} \left(\frac{1}{6} W_{s,t}^3 + \frac{11}{240} h W_{s,t} + \frac{1}{2} W_{s,t}^2 H_{s,t} + \frac{3}{5} W_{s,t} H_{s,t}^2 \right) \\ & \quad - \left(\frac{1}{3} h W_{s,t} + h W_{s,t} H_{s,t} + \frac{1}{15} h^2 + \frac{6}{5} h H_{s,t}^2 - \frac{1}{4\sqrt{6\pi}} n_{s,t} h^{\frac{3}{2}} W_{s,t} \right)^2 \\ &= \frac{11}{6300} h^4 + \left(\frac{1}{180} - \frac{1}{96\pi} \right) h^3 W_{s,t}^2 + \frac{1}{175} h^3 H_{s,t}^2 - \frac{1}{80\sqrt{6\pi}} n_{s,t} h^{\frac{7}{2}} W_{s,t}. \end{aligned}$$

The result now follows as, by (B.6), the above is the conditional variance of $2L_{s,t}$. \square

In the construction of the piecewise linear paths defined by (4.4) and (4.8), there are two distinct solutions which result in paths with the required iterated integrals. To decide on the solution, we consider the ‘‘space-time-time’’ Lévy area of the path. Whilst this quantity is Gaussian for Brownian motion and can be exactly generated, it is asymptotically smaller than space-space-time Lévy area, and so less impactful. Therefore, we propose using the expectation of space-time-time Lévy area conditional on $(W_{s,t}, H_{s,t}, n_{s,t})$ and choosing the path γ which best matches this approximation.

DEFINITION B.5. *The rescaled **space-time-time Lévy area** of Brownian motion over an interval $[s, t]$ is defined as*

$$K_{s,t} := \frac{1}{h^2} \int_s^t \left(W_{s,u} - \frac{u-s}{h} W_{s,t} \right) \left(\frac{1}{2} h - (u-s) \right) du.$$

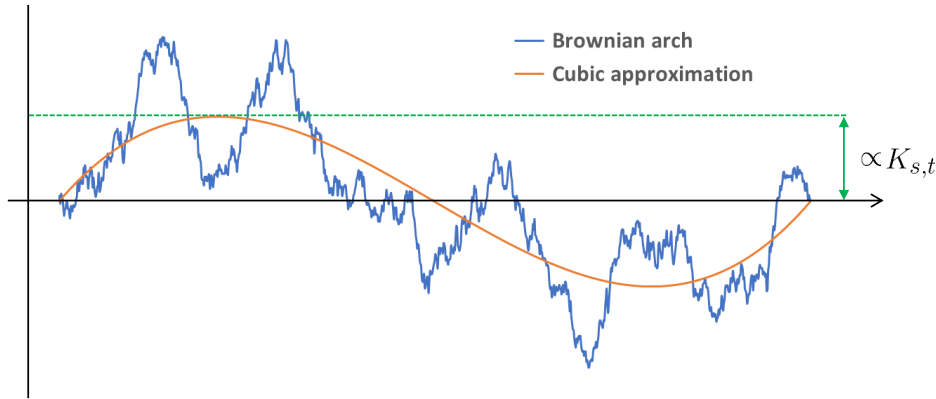


FIG. 9. Space-time-time Lévy area corresponds to a cubic approximation of the Brownian arch (which is a Brownian motion conditioned on having zero increment and space-time Lévy area [29]).

Since $W_{s,t}$, $H_{s,t}$ and $K_{s,t}$ can be identified with coefficients from a polynomial expansion of Brownian motion, it is straightforward to establish their independence. However, $K_{s,t}$ is not independent of $n_{s,t}$ and we can compute the following moments:

THEOREM B.6. *The space-time-time Lévy area $K_{s,t}$ is independent of $(W_{s,t}, H_{s,t})$ and has the following distribution and conditional moments,*

$$(B.16) \quad K_{s,t} \sim \mathcal{N}\left(0, \frac{1}{720}h\right),$$

$$(B.17) \quad \mathbb{E}[K_{s,t} | n_{s,t}] = \frac{1}{8\sqrt{6\pi}} n_{s,t} h^{\frac{1}{2}},$$

$$(B.18) \quad \mathbb{E}[K_{s,t}^2 | n_{s,t}] = \frac{1}{720}h.$$

Proof. It was shown in [29, Theorem 2.2], that for a Brownian bridge B on $[0, 1]$ and certain orthogonal polynomials e_1 and e_2 , we have

$$I_1 := \int_0^1 B_t \cdot \frac{e_1(t)}{t(1-t)} dt \quad \text{and} \quad I_2 := \int_0^1 B_t \cdot \frac{e_2(t)}{t(1-t)} dt$$

are independent random variables with $I_1 \sim \mathcal{N}(0, \frac{1}{2})$ and $I_2 \sim \mathcal{N}(0, \frac{1}{6})$. Moreover, by Theorems 2.7 and 2.8 in [29], the orthogonal polynomials e_1 and e_2 are given by

$$e_1(t) = \sqrt{6}t(t-1),$$

$$e_2(t) = \sqrt{30}t(t-1)(2t-1).$$

Thus $I_1 = \sqrt{6} \int_0^1 B_t dt$ and $I_2 = 2\sqrt{30} \int_0^1 B_t(t - \frac{1}{2}) dt$. It therefore follows that

$$\int_0^1 B_t dt \sim \mathcal{N}\left(0, \frac{1}{12}\right) \quad \text{and} \quad \int_0^1 B_t\left(\frac{1}{2} - t\right) dt \sim \mathcal{N}\left(0, \frac{1}{720}\right)$$

are independent. By the standard Brownian scaling, this implies $H_{s,t} \sim \mathcal{N}(0, \frac{1}{12}h)$ and $K_{s,t} \sim \mathcal{N}(0, \frac{1}{720}h)$ are independent. Moreover, since $H_{s,t}$ and $K_{s,t}$ are functions of the Brownian bridge $\{W_{s,u} - \frac{u-s}{h}W_{s,t}\}_{u \in [s,t]}$, they are also independent of $W_{s,t}$. We will now compute the expectation of $K_{s,t}$ conditional on $(W_{s,u}, W_{u,t}, H_{s,u}, H_{u,t})$.

$$\begin{aligned} & h^2 \mathbb{E}\left[K_{s,t} \mid W_{s,u}, W_{u,t}, H_{s,u}, H_{u,t}\right] \\ &= \mathbb{E}\left[\int_s^t \left(W_{s,r} - \frac{r-s}{h}W_{s,t}\right) \left(\frac{1}{2}h - (r-s)\right) dr \mid W_{s,u}, W_{u,t}, H_{s,u}, H_{u,t}\right] \\ &= \frac{1}{2}h \int_s^t W_{s,r} dr - \mathbb{E}\left[\int_s^t W_{s,r}(r-s) dr \mid W_{s,u}, W_{u,t}, H_{s,u}, H_{u,t}\right] + \frac{1}{12}h^2 W_{s,t} \\ &= \frac{1}{3}h^2 W_{s,t} + \frac{1}{2}h^2 H_{s,t} - \mathbb{E}\left[\int_s^u W_{s,r}(r-s) dr \mid W_{s,u}, H_{s,u}\right] - W_{s,u} \int_u^t (r-s) dr \\ &\quad - \mathbb{E}\left[\int_u^t W_{u,r}(r-s) dr \mid W_{u,t}, H_{u,t}\right] \\ &= \frac{1}{3}h^2 W_{s,t} + \frac{1}{2}h^2 H_{s,t} - \int_s^u \mathbb{E}[W_{s,r} \mid W_{s,u}, H_{s,u}](r-s) dr - \frac{3}{8}h^2 W_{s,u} \\ &\quad - \int_u^t \mathbb{E}[W_{u,r} \mid W_{u,t}, H_{u,t}](r-u) dr - \int_u^t W_{u,r}(u-s) dr. \end{aligned}$$

In [29], it was shown that $\mathbb{E}[W_{s,r} | W_{s,t}, H_{s,t}] = \frac{r-s}{t-s} W_{s,t} + \frac{6(r-s)(t-r)}{(t-s)^2} H_{s,t}$ for $r \in [s, t]$. Therefore, plugging this into the previous equation gives

$$\begin{aligned} & h^2 \mathbb{E}\left[K_{s,t} \mid W_{s,u}, W_{u,t}, H_{s,u}, H_{u,t}\right] \\ &= \frac{1}{3}h^2 W_{s,t} + \frac{1}{2}h^2 H_{s,t} - \frac{1}{12}h^2 W_{s,u} - \frac{1}{8}h^2 H_{s,u} - \frac{3}{8}h^2 W_{s,u} \\ &\quad - \frac{1}{12}h^2 W_{u,t} - \frac{1}{8}h^2 H_{u,t} - \frac{1}{2}h \left(\frac{1}{4}h W_{u,t} + \frac{1}{2}h H_{u,t} \right) \\ &= \frac{1}{2}h^2 H_{s,t} - \left(\frac{1}{4}h^2 H_{s,u} + \frac{1}{4}h^2 H_{u,t} + \frac{1}{8}h^2 W_{u,t} - \frac{1}{8}h^2 W_{s,u} \right) + \frac{1}{8}h^2 H_{s,u} - \frac{1}{8}h^2 H_{u,t}. \end{aligned}$$

By equation (B.7) in the previous proof, we see that the first two terms cancel. Thus

$$\mathbb{E}[K_{s,t} \mid W_{s,u}, W_{u,t}, H_{s,u}, H_{u,t}] = \frac{1}{8}N_{s,t},$$

and so the desired result (B.17) now follows as

$$\begin{aligned} \mathbb{E}[K_{s,t} \mid W_{s,t}, H_{s,t}, n_{s,t}] &= \mathbb{E}[\mathbb{E}[K_{s,t} \mid W_{s,u}, W_{u,t}, H_{s,u}, H_{u,t}] \mid W_{s,t}, H_{s,t}, n_{s,t}] \\ &= \frac{1}{8} \mathbb{E}[N_{s,t} \mid W_{s,t}, H_{s,t}, n_{s,t}] \\ &= \frac{1}{8\sqrt{6\pi}} n_{s,t} h^{\frac{1}{2}}, \end{aligned}$$

by the independence of $(W_{s,t}, H_{s,t}, N_{s,t})$ and equation (B.14), which were established in the proof of Theorem B.4. Finally, we note that $K_{s,t}^2$ does not change if W is replaced by $-W$, whereas $n_{s,t}$ changes sign when the Brownian motion is “flipped”. So by the symmetry of W , the random variables $K_{s,t}^2$ and $n_{s,t}$ are uncorrelated. Thus

$$\begin{aligned} \underbrace{\mathbb{E}[K_{s,t}^2 n_{s,t}]}_{=0} &= \frac{1}{2} \mathbb{E}[K_{s,t}^2 | n_{s,t} = 1] + \frac{1}{2} \mathbb{E}[-K_{s,t}^2 | n_{s,t} = -1], \\ \underbrace{\mathbb{E}[K_{s,t}^2]}_{=\frac{1}{\sqrt{20}}h} &= \frac{1}{2} \mathbb{E}[K_{s,t}^2 | n_{s,t} = 1] + \frac{1}{2} \mathbb{E}[K_{s,t}^2 | n_{s,t} = -1], \end{aligned}$$

gives the desired conditional moment (B.18). \square

Finally, using these optimal estimators for $L_{s,t}$ and $K_{s,t}$, we give the theoretical justification for the choices of piecewise linear paths previously used in (4.4) and (4.8). These paths match $\mathbb{E}[L_{s,t} | W_{s,t}, H_{s,t}, n_{s,t}]$ and correlate with $\mathbb{E}[K_{s,t} | W_{s,t}, H_{s,t}, n_{s,t}]$.

THEOREM B.7. *Consider the $(W_{s,t}, H_{s,t}, n_{s,t})$ -measurable piecewise linear paths $\gamma = (\gamma^\tau, \gamma^\omega) : [0, 1] \rightarrow \mathbb{R}^2$, $\tilde{\gamma} = (\tilde{\gamma}^\tau, \tilde{\gamma}^\omega) : [0, 1] \rightarrow \mathbb{R}^2$ given by $\gamma_0 = \tilde{\gamma}_0 = (s, W_s)$ and*

$$(B.19) \quad \gamma_{r_i, r_{i+1}} := \begin{cases} (0, A_{s,t}), & \text{if } i = 0 \\ (h, B_{s,t}), & \text{if } i = 1 \\ (0, W_{s,t} - A_{s,t} - B_{s,t}), & \text{if } i = 2, \end{cases}$$

$$(B.20) \quad \tilde{\gamma}_{r_i, r_{i+1}} := \begin{cases} (0, C_{s,t}), & \text{if } i = 0 \\ (\frac{1}{2}h, 0), & \text{if } i = 1 \\ (0, D_{s,t}), & \text{if } i = 2 \\ (\frac{1}{2}h, 0), & \text{if } i = 3 \\ (0, W_{s,t} - C_{s,t} - D_{s,t}), & \text{if } i = 4, \end{cases}$$

where $h = t - s$ and

$$\begin{aligned} & (A_{s,t}, B_{s,t}) \\ &= \arg \min_{\substack{(A,B) \in \mathbb{R}^2 \text{ s.t. constraints} \\ (B.21), (B.22), (B.23) \text{ hold}}} \left| \int_0^1 \gamma_{0,r}^\tau \gamma_{0,r}^\omega d\gamma_r^\tau - \mathbb{E} \left[\int_s^t (u-s) W_{s,u} du \mid W_{s,t}, H_{s,t}, n_{s,t} \right] \right|, \\ & (C_{s,t}, D_{s,t}) \\ &= \arg \min_{\substack{(C,D) \in \mathbb{R}^2 \text{ s.t. constraints} \\ (B.21), (B.22), (B.23) \text{ hold}}} \left| \int_0^1 \tilde{\gamma}_{0,r}^\tau \tilde{\gamma}_{0,r}^\omega d\tilde{\gamma}_r^\tau - \mathbb{E} \left[\int_s^t (u-s) W_{s,u} du \mid W_{s,t}, H_{s,t}, n_{s,t} \right] \right|. \end{aligned}$$

with the constraints (B.21), (B.22) and (B.23) for the paths γ and $\tilde{\gamma}$ given by

$$(B.21) \quad \gamma_1^\omega - \gamma_0^\omega = \tilde{\gamma}_1^\omega - \tilde{\gamma}_0^\omega = W_{s,t},$$

$$(B.22) \quad \int_0^1 (\gamma_r^\omega - \gamma_0^\omega) d\gamma_r^\tau = \int_0^1 (\tilde{\gamma}_r^\omega - \tilde{\gamma}_0^\omega) d\tilde{\gamma}_r^\tau = \int_s^t W_{s,u} du,$$

$$(B.23) \quad \int_0^1 (\gamma_r^\omega - \gamma_0^\omega)^2 d\gamma_r^\tau = \int_0^1 (\tilde{\gamma}_r^\omega - \tilde{\gamma}_0^\omega)^2 d\tilde{\gamma}_r^\tau = \mathbb{E} \left[\int_s^t W_{s,u}^2 du \mid W_{s,t}, H_{s,t}, n_{s,t} \right].$$

Then the first increments, $A_{s,t}$ and $C_{s,t}$, of the piecewise linear paths γ and $\tilde{\gamma}$ are

$$\begin{aligned} A_{s,t} &:= \frac{1}{2}W_{s,t} + H_{s,t} - \frac{1}{2}B_{s,t}, \\ C_{s,t} &:= \frac{1}{2}W_{s,t} + H_{s,t} - \frac{1}{2}D_{s,t}, \end{aligned}$$

where the second increments, $B_{s,t}$ and $D_{s,t}$, of the paths are given by the formulae

$$\begin{aligned} B_{s,t} &:= \epsilon_{s,t} \left(W_{s,t}^2 + \frac{12}{5}H_{s,t}^2 + \frac{4}{5}h - \frac{3}{\sqrt{6\pi}}h^{\frac{1}{2}}n_{s,t}W_{s,t} \right)^{\frac{1}{2}}, \\ D_{s,t} &:= \epsilon_{s,t} \left(\frac{1}{3}W_{s,t}^2 + \frac{4}{5}H_{s,t}^2 + \frac{4}{15}h - \frac{1}{\sqrt{6\pi}}n_{s,t}h^{\frac{1}{2}}W_{s,t} \right)^{\frac{1}{2}}, \\ \epsilon_{s,t} &:= \operatorname{sgn} \left(W_{s,t} - \frac{3}{\sqrt{24\pi}}h^{\frac{1}{2}}n_{s,t} \right). \end{aligned}$$

Proof. Since γ and $\tilde{\gamma}$ are piecewise linear, it is simple to compute the integrals

$$\begin{aligned} \int_0^1 (\gamma_r^\omega - \gamma_0^\omega) d\gamma_r^\tau &= h \left(A_{s,t} + \frac{1}{2} B_{s,t} \right), \\ \int_0^1 (\gamma_r^\omega - \gamma_0^\omega)^2 d\gamma_r^\tau &= h \left(A_{s,t}^2 + A_{s,t} B_{s,t} + \frac{1}{3} B_{s,t}^2 \right), \\ \int_0^1 (\tilde{\gamma}_r^\omega - \tilde{\gamma}_0^\omega) d\tilde{\gamma}_r^\tau &= h \left(C_{s,t} + \frac{1}{2} D_{s,t} \right), \\ \int_0^1 (\tilde{\gamma}_r^\omega - \tilde{\gamma}_0^\omega)^2 d\tilde{\gamma}_r^\tau &= h \left(C_{s,t}^2 + C_{s,t} D_{s,t} + \frac{1}{2} D_{s,t}^2 \right). \end{aligned}$$

It follows from the constraints (B.22) and (B.23) with equations (B.5) and (B.6) that

$$\begin{aligned} h \left(A_{s,t} + \frac{1}{2} B_{s,t} \right) &= \frac{1}{2} h W_{s,t} + h H_{s,t}, \\ h \left(A_{s,t}^2 + A_{s,t} B_{s,t} + \frac{1}{3} B_{s,t}^2 \right) &= \frac{1}{3} h W_{s,t}^2 + h W_{s,t} H_{s,t} + 2\mathbb{E}[L_{s,t} \mid W_{s,t}, H_{s,t}, n_{s,t}], \\ h \left(C_{s,t} + \frac{1}{2} D_{s,t} \right) &= \frac{1}{2} h W_{s,t} + h H_{s,t}, \\ h \left(C_{s,t}^2 + C_{s,t} D_{s,t} + \frac{1}{2} D_{s,t}^2 \right) &= \frac{1}{3} h W_{s,t}^2 + h W_{s,t} H_{s,t} + 2\mathbb{E}[L_{s,t} \mid W_{s,t}, H_{s,t}, n_{s,t}], \end{aligned}$$

So by Theorem B.4, substituting in the formula for the conditional expectation yields

$$\begin{aligned} A_{s,t} + \frac{1}{2} B_{s,t} &= \frac{1}{2} W_{s,t} + H_{s,t}, \\ A_{s,t}^2 + A_{s,t} B_{s,t} + \frac{1}{3} B_{s,t}^2 &= \frac{1}{3} W_{s,t}^2 + W_{s,t} H_{s,t} + \frac{1}{15} h + \frac{6}{5} H_{s,t}^2 - \frac{1}{4\sqrt{6\pi}} n_{s,t} h^{\frac{1}{2}} W_{s,t}, \\ C_{s,t} + \frac{1}{2} D_{s,t} &= \frac{1}{2} W_{s,t} + H_{s,t}, \\ C_{s,t}^2 + C_{s,t} D_{s,t} + \frac{1}{2} D_{s,t}^2 &= \frac{1}{3} W_{s,t}^2 + W_{s,t} H_{s,t} + \frac{1}{15} h + \frac{6}{5} H_{s,t}^2 - \frac{1}{4\sqrt{6\pi}} n_{s,t} h^{\frac{1}{2}} W_{s,t}, \end{aligned}$$

Since $a^2 + ab + \frac{1}{3}b^2 = (a + \frac{1}{2}b)^2 + \frac{1}{12}b^2$ and $c^2 + cd + \frac{1}{3}d^2 = (c + \frac{1}{2}d)^2 + \frac{1}{4}d^2$, this gives

$$\begin{aligned} \frac{1}{12} B_{s,t}^2 &= \frac{1}{3} W_{s,t}^2 + W_{s,t} H_{s,t} + \frac{1}{15} h + \frac{6}{5} H_{s,t}^2 - \frac{1}{4\sqrt{6\pi}} n_{s,t} h^{\frac{1}{2}} W_{s,t} - \left(\frac{1}{2} W_{s,t} + H_{s,t} \right)^2, \\ \frac{1}{4} D_{s,t}^2 &= \frac{1}{3} W_{s,t}^2 + W_{s,t} H_{s,t} + \frac{1}{15} h + \frac{6}{5} H_{s,t}^2 - \frac{1}{4\sqrt{6\pi}} n_{s,t} h^{\frac{1}{2}} W_{s,t} - \left(\frac{1}{2} W_{s,t} + H_{s,t} \right)^2, \end{aligned}$$

and so there are two possible values of $B_{s,t}$ and $D_{s,t}$ where (B.22) and (B.23) hold,

$$\begin{aligned} B_{s,t} &= \pm \sqrt{W_{s,t}^2 + \frac{12}{5} H_{s,t}^2 + \frac{4}{5} h - \frac{3}{\sqrt{6\pi}} n_{s,t} h^{\frac{1}{2}} W_{s,t}}, \\ D_{s,t} &= \pm \sqrt{\frac{1}{3} W_{s,t}^2 + \frac{4}{5} H_{s,t}^2 + \frac{4}{15} h - \frac{1}{\sqrt{6\pi}} n_{s,t} h^{\frac{1}{2}} W_{s,t}}. \end{aligned}$$

Thus, if equations (B.22) and (B.23) are satisfied, we have

$$\begin{aligned} \int_0^1 (\gamma_r^\tau - \gamma_0^\tau)(\gamma_r^\omega - \gamma_0^\omega) d\gamma_r^\tau &= \frac{1}{2}h^2 A_{s,t} + \frac{1}{3}h^2 B_{s,t} \\ &= \frac{1}{4}h^2 W_{s,t} + \frac{1}{2}h^2 H_{s,t} \pm \frac{1}{12}h^2 \sqrt{W_{s,t}^2 + \frac{12}{5}H_{s,t}^2 + \frac{4}{5}h - \frac{3}{\sqrt{6\pi}}n_{s,t}h^{\frac{1}{2}}W_{s,t}}, \\ \int_0^1 (\tilde{\gamma}_r^\tau - \tilde{\gamma}_0^\tau)(\tilde{\gamma}_r^\omega - \tilde{\gamma}_0^\omega) d\tilde{\gamma}_r^\tau &= \frac{1}{2}h^2 C_{s,t} + \frac{3}{8}h^2 D_{s,t} \\ &= \frac{1}{4}h^2 W_{s,t} + \frac{1}{2}h^2 H_{s,t} \pm \frac{1}{8}h^2 \sqrt{\frac{1}{3}W_{s,t}^2 + \frac{4}{5}H_{s,t}^2 + \frac{4}{15}h - \frac{1}{\sqrt{6\pi}}n_{s,t}h^{\frac{1}{2}}W_{s,t}}. \end{aligned}$$

Using Theorem B.6, we can estimate the corresponding integral of Brownian motion.

$$\begin{aligned} &\mathbb{E} \left[\int_s^t (u-s) W_{s,u} du \mid W_{s,t}, H_{s,t}, n_{s,t} \right] \\ &= \mathbb{E} \left[\frac{1}{2}h \int_s^t W_{s,u} du - \int_s^t \frac{u-s}{h} W_{s,t} \left(\frac{1}{2}h - (u-s) \right) du \mid W_{s,t}, H_{s,t}, n_{s,t} \right] \\ &\quad - \mathbb{E} \left[\int_s^t \left(W_{s,u} - \frac{u-s}{h} W_{s,t} \right) \left(\frac{1}{2}h - (u-s) \right) du \mid W_{s,t}, H_{s,t}, n_{s,t} \right] \\ &= \frac{1}{3}h^2 W_{s,t} + \frac{1}{2}h^2 H_{s,t} - h^2 \mathbb{E}[K_{s,t} \mid n_{s,t}] \\ &= \frac{1}{3}h^2 W_{s,t} + \frac{1}{2}h^2 H_{s,t} - \frac{1}{8\sqrt{6\pi}}n_{s,t}h^{\frac{5}{2}}. \end{aligned}$$

Taking the difference between these integrals gives

$$\begin{aligned} &\left| \int_0^1 (\gamma_r^\tau - \gamma_0^\tau)(\gamma_r^\omega - \gamma_0^\omega) d\gamma_r^\tau - \mathbb{E} \left[\int_s^t (u-s) W_{s,u} du \mid W_{s,t}, H_{s,t}, n_{s,t} \right] \right| \\ &= \left| -\frac{1}{12}h^2 W_{s,t} + \frac{1}{8\sqrt{6\pi}}n_{s,t}h^{\frac{5}{2}} \pm \frac{1}{12}h^2 \sqrt{W_{s,t}^2 + \frac{12}{5}H_{s,t}^2 + \frac{4}{5}h - \frac{3}{\sqrt{6\pi}}n_{s,t}h^{\frac{1}{2}}W_{s,t}} \right|, \end{aligned}$$

and

$$\begin{aligned} &\left| \int_0^1 (\tilde{\gamma}_r^\tau - \tilde{\gamma}_0^\tau)(\tilde{\gamma}_r^\omega - \tilde{\gamma}_0^\omega) d\tilde{\gamma}_r^\tau - \mathbb{E} \left[\int_s^t (u-s) W_{s,u} du \mid W_{s,t}, H_{s,t}, n_{s,t} \right] \right| \\ &= \left| -\frac{1}{12}h^2 W_{s,t} + \frac{1}{8\sqrt{6\pi}}n_{s,t}h^{\frac{5}{2}} \pm \frac{1}{8}h^2 \sqrt{\frac{1}{3}W_{s,t}^2 + \frac{4}{5}H_{s,t}^2 + \frac{4}{15}h - \frac{1}{\sqrt{6\pi}}n_{s,t}h^{\frac{1}{2}}W_{s,t}} \right|. \end{aligned}$$

Since we would like the path γ to minimise this quantity, the optimal choice of sign for the square root term is $\epsilon_{s,t} := \text{sgn}(W_{s,t} - \frac{3}{\sqrt{24\pi}}h^{\frac{1}{2}}n_{s,t})$, and the result follows. \square

Appendix C. Conditional moments of proposed CIR splitting method.

In this section, we will compute the conditional mean and variance of the proposed splitting method (5.3) for the CIR model (5.2). Recall that this method is given by

$$\begin{aligned}
Y_k^{(1)} &:= e^{-\frac{3-\sqrt{3}}{6}ah}Y_k + \tilde{b}(1 - e^{-\frac{3-\sqrt{3}}{6}ah}), \\
Y_k^{(2)} &:= \left(\sqrt{Y_k^{(1)}} + \frac{\sigma}{2} \left(\frac{1}{2}W_k + \sqrt{3}H_k \right) \right)^2, \\
Y_k^{(3)} &:= e^{-\frac{\sqrt{3}}{3}ah}Y_k^{(2)} + \tilde{b}(1 - e^{-\frac{\sqrt{3}}{3}ah}), \\
Y_k^{(4)} &:= \left(\sqrt{Y_k^{(3)}} + \frac{\sigma}{2} \left(\frac{1}{2}W_k - \sqrt{3}H_k \right) \right)^2, \\
(C.1) \quad Y_{k+1} &:= e^{-\frac{3-\sqrt{3}}{6}ah}Y_k^{(4)} + \tilde{b}(1 - e^{-\frac{3-\sqrt{3}}{6}ah}).
\end{aligned}$$

THEOREM C.1. *The numerical solution given by (C.1) has the following moments:*

$$(C.2) \quad \mathbb{E}[Y_{k+1}|Y_k] = e^{-ah}Y_k + b(1 - e^{-ah}) + R_k^E,$$

$$(C.3) \quad \text{Var}(Y_{k+1}|Y_k) = \frac{\sigma^2}{a}(e^{-ah} - e^{-2ah})Y_k + \frac{b\sigma^2}{2a}(1 - e^{-ah})^2 + R_k^V,$$

where the remainder terms R_k^E and R_k^V are given by

$$\begin{aligned}
R_k^E &:= \frac{1}{4}\sigma^2 \left(\frac{1}{2}(e^{-\frac{3+\sqrt{3}}{6}ah} + e^{-\frac{3-\sqrt{3}}{6}ah})h - \frac{1 - e^{-ah}}{a} \right), \\
R_k^V &:= \sigma^2 \left(\frac{1}{2}(e^{-\frac{9+\sqrt{3}}{6}ah} + e^{-\frac{9-\sqrt{3}}{6}ah})h - \frac{1}{a}(e^{-ah} - e^{-2ah}) \right) Y_k \\
&\quad + \frac{1}{2}\tilde{b}\sigma^2 \left((e^{-\frac{3+\sqrt{3}}{3}ah} + e^{-\frac{3-\sqrt{3}}{3}ah} - e^{-\frac{9+\sqrt{3}}{6}ah} - e^{-\frac{9-\sqrt{3}}{6}ah})h - \frac{1}{a}(1 - e^{-ah})^2 \right) \\
&\quad + \frac{1}{8}\sigma^4 \left(\frac{1}{2}(e^{-ah} + \frac{1}{2}(e^{-\frac{3+\sqrt{3}}{3}ah} + e^{-\frac{3-\sqrt{3}}{3}ah}))h^2 - \frac{1}{a^2}(1 - e^{-ah})^2 \right),
\end{aligned}$$

which can be estimated as $\|R_k^E\|_{L^2(\mathbb{P})}, \|R_k^V\|_{L^2(\mathbb{P})} \sim O(h^5)$ for sufficiently small h .

Proof. We first note that $\frac{1}{2}W_k + \sqrt{3}H_k$ and $\frac{1}{2}W_k - \sqrt{3}H_k$ are jointly normal and

$$\mathbb{E} \left[\left(\frac{1}{2}W_k + \sqrt{3}H_k \right) \left(\frac{1}{2}W_k - \sqrt{3}H_k \right) \right] = \frac{1}{4} \cdot h - 3 \cdot \frac{1}{12}h = 0.$$

It thus follows that $\frac{1}{2}W_k + \sqrt{3}H_k$ and $\frac{1}{2}W_k - \sqrt{3}H_k$ are independent random variables. Therefore, we see that in (C.1), the term $Y_k^{(3)}$ is independent of $\frac{1}{2}W_k - \sqrt{3}H_k$ and so

$$\begin{aligned}
\mathbb{E}[Y_k^{(4)}|Y_k] &= \mathbb{E}[Y_k^{(3)}|Y_k] + \sigma \mathbb{E} \left[(Y_k^{(3)})^{\frac{1}{2}} | Y_k \right] \mathbb{E} \left[\frac{1}{2}W_k - \sqrt{3}H_k | Y_k \right] + \frac{1}{8}\sigma^2 h \\
&= \mathbb{E}[Y_k^{(3)}|Y_k] + \frac{1}{8}\sigma^2 h, \\
\mathbb{E} \left[(Y_k^{(4)})^2 | Y_k \right] &= \mathbb{E} \left[(Y_k^{(3)})^2 | Y_k \right] + \frac{3}{64}\sigma^4 h^2 + 2\sigma \mathbb{E} \left[(Y_k^{(3)})^{\frac{3}{2}} | Y_k \right] \mathbb{E} \left[\frac{1}{2}W_k - \sqrt{3}H_k \right] \\
&\quad + \frac{3}{4}\sigma^2 h \mathbb{E}[Y_k^{(3)}|Y_k] + \frac{1}{2}\sigma^3 \mathbb{E} \left[(Y_k^{(3)})^{\frac{1}{2}} | Y_k \right] \mathbb{E} \left[\left(\frac{1}{2}W_k - \sqrt{3}H_k \right)^3 \right] \\
&= \mathbb{E} \left[(Y_k^{(3)})^2 | Y_k \right] + \frac{3}{4}\sigma^2 h \mathbb{E}[Y_k^{(3)}|Y_k] + \frac{3}{64}\sigma^4 h^2.
\end{aligned}$$

Using $\text{Var}(Y_k^{(4)} | Y_k) = \mathbb{E}[(Y_k^{(4)})^2 | Y_k] - (\mathbb{E}[Y_k^{(4)} | Y_k])^2$, the conditional variance is

$$\text{Var}(Y_k^{(4)} | Y_k) = \text{Var}(Y_k^{(3)} | Y_k) + \frac{1}{2}\sigma^2 h \mathbb{E}[Y_k^{(3)} | Y_k] + \frac{1}{32}\sigma^4 h^2.$$

Similarly, by the same calculation, we also have that

$$\mathbb{E}[Y_k^{(2)} | Y_k] = \mathbb{E}[Y_k^{(1)} | Y_k] + \frac{1}{8}\sigma^2 h,$$

$$\text{Var}(Y_k^{(2)} | Y_k) = \text{Var}(Y_k^{(1)} | Y_k) + \frac{1}{2}\sigma^2 h \mathbb{E}[Y_k^{(1)} | Y_k] + \frac{1}{32}\sigma^4 h^2.$$

Using the above, it is straightforward to compute the conditional expectation of Y_{k+1} .

$$\begin{aligned} \mathbb{E}[Y_{k+1} | Y_k] &= e^{-\frac{3-\sqrt{3}}{6}ah} \mathbb{E}[Y_k^{(4)} | Y_k] + \tilde{b}(1 - e^{-\frac{3-\sqrt{3}}{6}ah}) \\ &= e^{-\frac{3-\sqrt{3}}{6}ah} \mathbb{E}[Y_k^{(3)} | Y_k] + \frac{1}{8}\sigma^2 e^{-\frac{3-\sqrt{3}}{6}ah} + \tilde{b}(1 - e^{-\frac{3-\sqrt{3}}{6}ah}) \\ &= e^{-\frac{3+\sqrt{3}}{6}ah} \mathbb{E}[Y_k^{(2)} | Y_k] + \tilde{b}(1 - e^{-\frac{3+\sqrt{3}}{6}ah}) + \frac{1}{8}\sigma^2 h e^{-\frac{3-\sqrt{3}}{6}ah} \\ &= e^{-\frac{3+\sqrt{3}}{6}ah} \mathbb{E}[Y_k^{(1)} | Y_k] + \tilde{b}(1 - e^{-\frac{3+\sqrt{3}}{6}ah}) + \frac{1}{8}\sigma^2 h (e^{-\frac{3+\sqrt{3}}{6}ah} + e^{-\frac{3-\sqrt{3}}{6}ah}) \\ &= e^{-ah} Y_k + \tilde{b}(1 - e^{-ah}) + \frac{1}{8}\sigma^2 h e^{-\frac{3+\sqrt{3}}{6}ah} + \frac{1}{8}\sigma^2 h e^{-\frac{3-\sqrt{3}}{6}ah}. \end{aligned}$$

Thus we obtain equation (C.2) as $\tilde{b} = b - \frac{\sigma^2}{4a}$. Taylor expanding the above terms gives

$$\begin{aligned} &\frac{1}{2}(e^{-\frac{3+\sqrt{3}}{6}ah} + e^{-\frac{3-\sqrt{3}}{6}ah})h \\ &= \frac{1}{2}\left(1 - \frac{3+\sqrt{3}}{6}ah + \frac{2+\sqrt{3}}{12}(ah)^2 - \frac{9+5\sqrt{3}}{216}(ah)^3 + O(h^4)\right)h \\ &\quad + \frac{1}{2}\left(1 - \frac{3-\sqrt{3}}{6}ah + \frac{2-\sqrt{3}}{12}(ah)^2 - \frac{9-5\sqrt{3}}{216}(ah)^3 + O(h^4)\right)h \\ &= h - \frac{1}{2}ah^2 + \frac{1}{6}a^2h^3 - \frac{1}{24}a^3h^4 + O(h^5) \\ &= \frac{1 - e^{-ah}}{a} + O(h^5), \end{aligned}$$

which is the required estimate for R_k^E . Similarly, we compute the variance of Y_{k+1} as

$$\begin{aligned} &\text{Var}(Y_{k+1} | Y_k) \\ &= e^{-\frac{3-\sqrt{3}}{3}ah} \text{Var}(Y_k^{(4)} | Y_k) \\ &= e^{-\frac{3-\sqrt{3}}{3}ah} \text{Var}(Y_k^{(3)} | Y_k) + \frac{1}{2}\sigma^2 e^{-\frac{3-\sqrt{3}}{3}ah} h \mathbb{E}[Y_k^{(3)} | Y_k] + \frac{1}{32}\sigma^4 h^2 e^{-\frac{3-\sqrt{3}}{3}ah} \\ &= e^{-\frac{3+\sqrt{3}}{3}ah} \text{Var}(Y_k^{(2)} | Y_k) + \frac{1}{2}\sigma^2 h e^{-ah} \mathbb{E}[Y_k^{(2)} | Y_k] + \frac{1}{2}\tilde{b}\sigma^2 h (e^{-\frac{3-\sqrt{3}}{3}ah} - e^{-ah}) \\ &\quad + \frac{1}{32}\sigma^4 h^2 e^{-\frac{3-\sqrt{3}}{3}ah} \\ &= e^{-\frac{3+\sqrt{3}}{3}ah} \text{Var}(Y_k^{(1)} | Y_k) + \frac{1}{2}\sigma^2 h e^{-\frac{3+\sqrt{3}}{3}ah} \mathbb{E}[Y_k^{(1)} | Y_k] + \frac{1}{32}\sigma^4 h^2 e^{-\frac{3+\sqrt{3}}{3}ah} \\ &\quad + \frac{1}{2}\sigma^2 h e^{-ah} \mathbb{E}[Y_k^{(1)} | Y_k] + \frac{1}{16}\sigma^4 h^2 e^{-ah} + \frac{1}{2}\tilde{b}\sigma^2 h (e^{-\frac{3-\sqrt{3}}{3}ah} - e^{-ah}) \\ &\quad + \frac{1}{32}\sigma^4 h^2 e^{-\frac{3-\sqrt{3}}{3}ah}, \end{aligned}$$

and therefore

$$\begin{aligned}\text{Var}(Y_{k+1} | Y_k) &= \frac{1}{2}\sigma^2 h(e^{-\frac{9+\sqrt{3}}{6}ah} + e^{-\frac{9-\sqrt{3}}{6}ah})Y_k \\ &\quad + \frac{1}{2}\tilde{b}\sigma^2 h(e^{-\frac{3+\sqrt{3}}{3}ah} + e^{-\frac{3-\sqrt{3}}{3}ah} - e^{-\frac{9+\sqrt{3}}{6}ah} - e^{-\frac{9-\sqrt{3}}{6}ah}) \\ &\quad + \frac{1}{16}\sigma^4 h^2(e^{-ah} + \frac{1}{2}(e^{-\frac{3+\sqrt{3}}{3}ah} + e^{-\frac{3-\sqrt{3}}{3}ah})).\end{aligned}$$

Just as for $e^{-\frac{3+\sqrt{3}}{6}ah} + e^{-\frac{3-\sqrt{3}}{6}ah}$, we will consider Taylor expansions of these terms.

$$\begin{aligned}\frac{1}{2}(e^{-\frac{3+\sqrt{3}}{3}ah} + e^{-\frac{3-\sqrt{3}}{3}ah})h &= \frac{1 - e^{-2ah}}{2a} + O(h^5), \\ \frac{1}{2}(e^{-\frac{9+\sqrt{3}}{6}ah} + e^{-\frac{9-\sqrt{3}}{6}ah})h &= e^{-ah}\left(\frac{1 - e^{-ah}}{a}\right) + O(h^5) \\ &= \frac{1}{a}(e^{-ah} - e^{-2ah}) + O(h^5), \\ \frac{1}{2}(e^{-ah} + \frac{1}{2}(e^{-\frac{3+\sqrt{3}}{3}ah} + e^{-\frac{3-\sqrt{3}}{3}ah}))h^2 &= \frac{1}{2}\left(1 - ah + \frac{1}{2}(ah)^2 + O(h^3)\right)h^2 \\ &\quad + \frac{1}{2}\left(1 - ah + \frac{2}{3}(ah)^2 + O(h^3)\right)h^2 \\ &= h^2 - ah^3 + \frac{7}{12}a^2h^4 + O(h^5) \\ &= \frac{1}{a^2}(1 - e^{-ah})^2 + O(h^5), \\ \frac{1}{2}(e^{-\frac{3+\sqrt{3}}{3}ah} + e^{-\frac{3-\sqrt{3}}{3}ah} - e^{-\frac{9+\sqrt{3}}{6}ah} - e^{-\frac{9-\sqrt{3}}{6}ah})h &= \frac{1 - e^{-2ah}}{2a} - e^{-ah}\left(\frac{1 - e^{-ah}}{a}\right) + O(h^5) \\ &= \frac{1}{2a}(1 - e^{-ah})^2 + O(h^5).\end{aligned}$$

The result (C.3) follows from the above along with the finite second moment of Y_k . \square